

AD-767614

AFFDL-TR-73-42

# DEVELOPMENT AND EVALUATION OF METHODS OF PLANE STRESS FRACTURE ANALYSIS

REVIEW AND EVALUATION OF STRUCTURAL  
RESIDUAL STRENGTH PREDICTION TECHNIQUES

*R. M. VERETTE AND D. P. WILHEM*  
*NORTHROP CORPORATION*  
*AIRCRAFT DIVISION*

TECHNICAL REPORT AFFDL-TR-73-42

MAY 1973

Approved for public release; distribution unlimited.

AIR FORCE FLIGHT DYNAMICS LABORATORY  
AIR FORCE SYSTEMS COMMAND  
WRIGHT-PATTERSON AIR FORCE BASE, OHIO 45433

20070924043

## NOTICE

When Government drawings, specification, or other data are used for any purpose other than in connection with a definitely related Government procurement operation, the United States Government thereby incurs no responsibility nor any obligation whatsoever; and the fact that the government may have formulated, furnished, or in any way supplied the said drawings, specification, or other data, is not to be regarded by implication or otherwise as in any manner licensing the holder or any other person or corporation, or conveying any rights or permission to manufacture, use, or sell any patented invention that may in any way be related thereto.

Copies of this report should not be returned unless return is required by security considerations, contractual obligations, or notice on a specific document.

AFFDL-TR-73-42

# **DEVELOPMENT AND EVALUATION OF METHODS OF PLANE STRESS FRACTURE ANALYSIS**

## **REVIEW AND EVALUATION OF STRUCTURAL RESIDUAL STRENGTH PREDICTION TECHNIQUES**

*R. M. VERETTE AND D. P. WILHEM*

*NORTHROP CORPORATION*

*AIRCRAFT DIVISION*

TECHNICAL REPORT AFFDL-TR-73-42

MAY 1973

Approved for public release; distribution unlimited.

**AIR FORCE FLIGHT DYNAMICS LABORATORY  
AIR FORCE SYSTEMS COMMAND  
WRIGHT-PATTERSON AIR FORCE BASE, OHIO 45433**



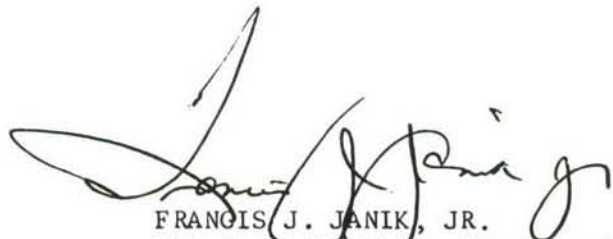
## FOREWORD

This report was prepared by Northrop Corporation, Aircraft Division, Hawthorne, California, under Air Force Contract F33615-72-C-1796. The project was initiated under Project Number 486U, "Advanced Metallic Structures," Advanced Development Program. The work reported herein was administered under the direction of the Air Force Flight Dynamics Laboratory, Air Force Systems Command, Wright-Patterson Air Force Base, Ohio, by Captain George F. Zielsdorff, FBR, project engineer.

The research was conducted between July 1972 and December 1972 as a conclusion to Phase I. This report was submitted by the authors R. M. Verette and D. P. Wilhem, March 1973, for AFFDL review. The report has been assigned NOR 73-32 for internal control at Northrop Corporation.

The authors wish to acknowledge the constructive discussion and comments regarding this study by the program consultant, Professor George C. Sih (Lehigh University). The secretarial assistance of Lessie Speciale is also acknowledged. The aforementioned program was under the technical direction of C. Rosenkranz of the Structures Research and Technology Department.

This technical report has been reviewed and is approved.



FRANCIS J. JANIK, JR.  
Chief, Solid Mechanics Branch  
Structures Division  
Air Force Flight Dynamics Laboratory



## ABSTRACT

The treatment of residual strength prediction for aircraft structures having through flaws is considered in this report. A discussion of the circumstances which normally give rise to plane stress or mixed mode fracture is presented along with a summary of those elements which would constitute an "ideal" residual strength method. This method would be capable of prescribing the remaining strength possessed by a broad variety of flawed aircraft structures under actual service environments. Currently available prediction techniques fall considerably short of the desired goal, and the strong and weak points of existing methods, as well as comparisons with test results, are presented. A recommended technique is described for residual strength prediction which bridges the gap between the existing methods and the ideal. The recommended approach will account for slow crack growth and plasticity. It appears that the approach will utilize the J integral in combination with a modified form of the crack growth resistance curve in making residual strength predictions.

## CONTENTS

SECTION		PAGE
I	INTRODUCTION.....	1
II	PLANE STRESS AND MIXED MODE FRACTURE CRITICAL AIRCRAFT STRUCTURE.....	4
	2.1 DEFINITION OF TERMS RELATING TO THIN SECTION FRACTURE.....	4
	2.2 IDENTIFICATION OF FRACTURE CRITICAL AIRCRAFT STRUCTURE AND ASSOCIATED CRACK GEOMETRIES.....	6
	2.3 LOADING CONDITIONS APPLICABLE TO FRACTURE CRITICAL STRUCTURE.....	10
III	THE "IDEAL" RESIDUAL STRENGTH PREDICTION TECHNIQUE.....	11
	3.0 INTRODUCTION TO THE "IDEAL" TECHNIQUE.....	11
	3.1 PARAMETERS AFFECTING RESIDUAL STRENGTH.....	11
	3.2 RELATING THE MATERIAL PROPERTIES, ANALYSIS METHOD, AND FRACTURE CRITERION.....	13
	3.2.1 Determining Material Properties.....	15
	3.2.2 Performing Required Analyses.....	16
	3.2.3 Applying the Fracture Criterion.....	18
IV	REVIEW OF CURRENTLY AVAILABLE RESIDUAL STRENGTH PREDICTION TECHNIQUES.....	20
	4.1 NOTCH STRENGTH OR CRACK STRENGTH ANALYSIS METHOD....	20
	4.1.1 Historical Development of Notch (Crack) Analysis (NSA-CSA) Method.....	20
	4.1.2 Theory of NSA and CSA Method.....	21
	4.1.3 Computational Procedure.....	26
	4.1.4 Capability, Limitations and Possible Poten- tial for the NSA (CSA) Method in Struct- ural Residual Strength Determination....	27
	4.2 EFFECTIVE WIDTH ANALYSIS METHOD.....	27

## CONTENTS (CONTINUED)

SECTION	PAGE
4.2.1 Historical Development of Effective Width Analysis Method.....	27
4.2.2 Theory of Effective Width Method.....	27
4.2.3 Computational Procedure.....	31
4.2.4 Capability, Limitations and Possible Poten- tial for the Effective Width Method in Structural Residual Strength Determina- tion.....	31
4.3 LINEAR ELASTIC FRACTURE MECHANICS METHODS.....	32
4.3.1 Theory and Historical Development of Fracture Mechanics Methods.....	32
4.3.2 Capability, Limitations and Possible Poten- tial for the Linear Elastic Fracture Mechanics Method in Structural Residual Strength Determination.....	32
4.4 SUMMARY.....	33
4.4.1 Applicability of Existing Methods.....	33
4.4.2 Treatment of Material Parameters.....	34
V DEMONSTRATION OF CAPABILITIES FOR RESIDUAL STRENGTH PREDICTION.....	35
5.1 SIMPLE UNREINFORCED PANELS.....	36
5.1.1 Fracture Strength Repeatability.....	36
5.1.2 Impact of Material Fracture Variability on Selected Criterion and Analysis Method..	38
5.2 SIMPLE REINFORCED PANELS.....	40
5.2.1 Residual Strength Repeatability.....	40
5.3 RESIDUAL STRENGTH PREDICTIONS FOR SIMPLE REINFORCED PANELS.....	44



## CONTENTS (CONTINUED)

SECTION	PAGE
5.3.1 Poe's Method with $K_c$ of LEFM as a Failure Criterion.....	44
5.3.1.1 Assumptions.....	44
5.3.1.2 Procedure.....	45
5.3.2 Kuhn Method with NSA as a Failure Criterion..	46
5.3.2.1 Assumptions.....	48
5.3.2.2 Procedure.....	48
5.4 RESIDUAL STRENGTH PREDICTIONS FOR PANELS OF COMPLEX GEOMETRY.....	50
5.5 PARAMETRIC INFLUENCES AND THEIR EFFECT ON RESIDUAL STRENGTH PREDICTION.....	51
5.5.1 Crack Growth Resistance Concept and Its Use as a Failure Criterion.....	51
5.5.2 Crack Tip Buckling.....	53
5.5.3 Strain Rate.....	54
5.5.4 Specimen Dependency and Anisotropic Behavior.	54
5.5.5 Value of Continued Development of Existing Methods.....	55
VI PLANNED DEVELOPMENT OF RESIDUAL STRENGTH PREDICTION TECHNIQUE.....	56
6.1 CANDIDATE ANALYSIS METHODS.....	56
6.1.1 Treatment of Structures Made of Prandtl-Reuss Materials.....	59
6.1.1.1 Example Problem.....	62
6.1.2 Treatment of Structures Made of Materials Displaying Dugdale-Type Plastic Zones...	72
6.1.2.1 Example Problem.....	76

## CONTENTS (CONTINUED)

SECTION	PAGE
6.1.3 Indicated Direction of Analytical Approach - Planned Residual Strength Prediction Technique.....	81
6.2 CANDIDATE FAILURE CRITERION.....	84
6.2.1 Basis for the $J_{cr}$ Failure Criterion.....	85
6.3 MATERIAL PROPERTY DATA REQUIREMENTS.....	88
REFERENCES .....	90

## FIGURES

FIGURE		PAGE
1	TYPICAL VARIATION IN CRITICAL STRESS INTENSITY WITH THICKNESS FOR PLANE STRESS-STRAIN AND MIXED MODE....	5
2	FLAW GEOMETRIES FOR LOADED SKIN/STRINGER CONSTRUCTION....	7
3	TYPICAL MULTI-BAY CRACKS IN TENSION STRUCTURE.....	8
4	TYPICAL CRACK SITUATIONS IN PRESSURIZED FUSELAGE SHELL...	9
5	FLOW DIAGRAM SHOWING MAJOR STEPS IN PERFORMING A RESIDUAL STRENGTH PREDICTION.....	14
6	EFFECT OF SEVERAL MATERIAL PROPERTIES ON FRACTURE STRENGTH.....	17
7	SPECIMEN WITH THROUGH-THE-THICKNESS FLAW.....	22
8	GEOMETRY FOR EFFECTIVE WIDTH ANALYSIS METHOD.....	28
9	SCHEMATIC OF THE FRACTURE PROCESS IN PLANE STRESS WITH ACCOMPANYING SLOW TEAR.....	37
10(a)	REFERENCE 32 FRACTURE DATA - STRESS AT INITIATION OF SLOW TEAR VERSUS INITIAL CRACK SIZE.....	39
10(b)	REFERENCE 32 FRACTURE DATA - CRITICAL STRESS VERSUS INITIAL CRACK SIZE.....	39
11	SCHEMATIC OF FRACTURE PROCESS FOR SIMPLE REINFORCED PANELS	41
12	REFERENCE 32 FRACTURE DATA-STRESS AT INITIATION OF SLOW TEAR VERSUS INITIAL CRACK SIZE.....	43
13(a)	RESIDUAL STRENGTH FOR REFERENCE 32 DATA USING REFERENCE 31 METHOD OF ANALYSIS AND $K_c$ FRACTURE CRITERION.....	47
13(b)	RESIDUAL STRENGTH FOR REFERENCE 32 DATA USING REFERENCE 31 METHOD OF ANALYSIS AND $K_c$ FRACTURE CRITERION.....	47
14	KUHN ANALYSIS METHOD USING NSA FRACTURE CRITERION COMPARED TO LEFM METHODS AND $K_c$ CRITERION - CASE 2 PANELS.....	49
15	COMPARISON OF $K_R$ CURVES FOR VARIOUS SPECIMEN TYPES.....	52
16	RECTANGULAR PATH FOR J CALCULATION.....	58



# FIGURES (CONTINUED)

FIGURE		PAGE
17	CRACKED STIFFENED SHEET.....	63
18	GRID SYSTEM AND $\Gamma$ CONTOUR FOR J CALCULATION.....	64
19	UNIAXIAL STRESS-STRAIN CURVE.....	65
20	NODES INVOLVED IN J CALCULATION.....	68
21	J VS. APPLIED STRESS FOR A STRAP-STIFFENED SHEET CONTAIN- ING A CRACK WITH $a = 2$ INCHES.....	70
22	NEAR-LINEAR RELATIONSHIP BETWEEN $\sqrt{J}$ AND APPLIED STRESS FOR CRACKED STIFFENED SHEET.....	71
23	PLASTIC ZONES ARISING DUE TO APPLIED STRESS OF 3300, 5400, AND 7300 PSI.....	73
24	$\Gamma$ CONTOUR USED IN J CALCULATION FOR DUGDALE-TYPE MATERIALS.....	75
25	CRACKED STIFFENED SHEET.....	77
26	APPLIED TENSILE STRESS-PLASTIC ZONE LENGTH RELATIONSHIP..	82
27	CRACK OPENING DISPLACEMENT - PLASTIC ZONE SIZE RELATION- SHIP.....	83
28	RESIDUAL STRENGTH TANGENCY CONDITIONS SHOWING CRITICAL STRESS $\sigma_{cr}$ AND CRITICAL CRACK HALF LENGTH $a_{cr}$ AT FRACTURE INSTABILITY.....	87

# TABLES

TABLE		PAGE
I	PARAMETERS TO BE ACCOUNTED FOR IN AN "IDEAL" RESIDUAL STRENGTH PREDICTION TECHNIQUE.....	12
II	TERMS USED IN J INTEGRAL DETERMINATION.....	60
III	STRESS INCREMENTS - ELASTIC-PLASTIC ANALYSIS.....	66
IV	CALCULATIONS FOR DUGDALE PROBLEM.....	78

# SYMBOLS AND NORMAL UNITS\*

Symbol		Units
$A_e$	Area of stiffened element	inches <sup>2</sup>
$a$	Half crack length—for center cracked panels	inches
$a_o$	Initial half crack length—for center cracked panels	inches
$a_c$	Critical half crack length— for center cracked panels	inches
$\Delta a$	Crack extension	inches
$B$	Material thickness	inches
$C_m$	Materials "constant" in basic CSA method	$\sqrt{\text{inches}}$
$C_m'$	Materials "constant" in modified CSA method	$\sqrt{\text{inches}}$
$c$	Crack half length (Dugdale approach)	inches
$E$	Young's Modulus	psi or ksi x 10 <sup>3</sup>
$E_n$	Secant modulus of elasticity (@ point where $\sigma_{\max}$ is measured)	psi or ksi x 10 <sup>3</sup>
$E_N$	Secant modulus (@ $\sigma_N$ )	psi or ksi x 10 <sup>3</sup>
$E_s$	Secant modulus for average stress (away from the notch)	psi or ksi x 10 <sup>3</sup>
$E_u$	Modulus @ ultimate strength	psi or ksi x 10 <sup>3</sup>
$e$	Elongation	
$F_{ty}$	Tensile yield stress (.2% offset)	psi or ksi

---

\*Except where noted in text.



# SYMBOLS (CONTINUED)

Symbol		Units
$\bar{F}_{ty}$	Average .2% tensile yield stress	psi or ksi
$F_{tp}$	Tensile proportional limit stress	psi or ksi
$F_{tu}$	Ultimate tensile stress	psi or ksi
$G$	Strain energy release rate	inch-lbs/inch <sup>2</sup>
$G_c$	Critical strain energy release rate	inch-lbs/inch <sup>2</sup>
$\hat{i}, \hat{j}$	Unit vectors	
$J$	Contour integral	lb./in.
$K$	Stress intensity factor	ksi $\sqrt{\text{inch}}$
$K_{Ic}$	Plane strain fracture toughness	ksi $\sqrt{\text{inch}}$
$K_c$	Critical value of stress intensity factor	ksi $\sqrt{\text{inch}}$
$K_N$	"Practical" stress concentration factor	
$K_R$	Crack growth resistance	ksi $\sqrt{\text{inch}}$
$K_u$	Stress concentration factor (@ maximum load)	
$K_t$	Stress concentration factor	
$k$	Constant	
$n$	Strain hardening exponent	
$n_1, n_2$	Components of unit outward normal vector	
$P$	Load	lbs.
$R$	Crack growth resistance curve	
$s$	Spacing between reinforcements	inches
$T$	Temperature	°F
$\vec{T}$	Traction vector	psi

# SYMBOLS (CONTINUED)

Symbol		Units
$t_s$	Thickness of reinforcement	inches
$U$	Strain energy	$\frac{\text{in.-lb.}}{\text{in.}}$
$u, v$	Displacements	inches
$W$	Width or, Strain energy density	inches psi
$W_e$	Material constant in effective width method	inches
$W_o$	Effective width for infinite width panel	inches
$W_l$	Empirically developed characteristic length	inches
$w$	Width of reinforcement	inches
$x, y$	Coordinates	
$\sigma$	Nominal stress	psi or ksi
$\dot{\sigma}$	Stress rate	psi/sec. or ksi/sec.
$\sigma_{bc}$	Critical buckling stress	psi or ksi
$\sigma_c$	Critical (gross area) fracture stress	psi or ksi
$\bar{\sigma}$	Equivalent stress	psi
$\sigma_g$	Gross area tensile stress	psi or ksi
$\sigma_i$	Initial value of stress (gross area) or Stress to initiate slow tear	psi or ksi
$\sigma_{\max}$	Maximum stress at notch $\sigma_{\max} = K_t \sigma_N$	psi or ksi
$\sigma_N$	Net area stress	psi or ksi

# SYMBOLS (CONTINUED)

Symbol		Units
$\sigma_x', \sigma_y', \sigma_z'$	Deviatoric stress components	psi
$\sigma_x, \sigma_y, \sigma_{xy}$	In-plane stresses	psi or ksi
$\dot{\epsilon}$	Strain rate	micro inches/inch/sec.
$\epsilon_x, \epsilon_y, \gamma_{xy}$	In-plane strains	
$\bar{\epsilon}_p$	Equivalent plastic strain	
$\Gamma$	Contour used in J calculation	
$\delta$	Crack opening displacement (distance between crack faces at some point)	inches
$\lambda_w$	Finite geometry correction	
$\omega_e$	Effective flank angle	radians
$\rho$	Notch root radius	inches
$\rho'$	Neuber constant	inches
$\nu$	Poisson's ratio	



## I INTRODUCTION

This report describes the research conducted during Phase I of a three phase investigation into the development of an improved method of thin section residual strength prediction for cracked (where conditions of plane stress or mixed mode fracture prevails) aircraft structure. Phases II and III, which will detail the development of, and provide experimental substantiation for the method, will be reported on in subsequent documents.

The purpose of this Phase I study is to objectively examine the currently available methods of thin section residual strength prediction. In the evaluation, the focus has been on:

- (a) the potential of the existing methods as the basis of a more comprehensive prediction technique,
- (b) the manner in which the parameters which are known to influence residual strength are incorporated in existing techniques, and
- (c) the fracture criteria which are used in the existing residual strength prediction techniques.

It has been found that certain elements of a sound residual strength prediction technique exist, but in fragmented, disjointed form. Hence a systematic review of the current literature is required in order to recommend a course of action for residual strength methodology development in subsequent research activity.

It is highly desirable to clearly differentiate between what is meant by the terms "fracture strength" and "residual strength."

First, consider the term "fracture strength." If a material contains no interruptions or discontinuities in geometry, it can be loaded statically (say in uniaxial tension) until its ultimate strength  $F_{tu}$  is reached, at which time failure occurs. If, instead of being geometrically perfect, the material contains a discontinuity (in the form of a crack), it can normally no longer be loaded up to its ultimate strength. Some reduction in strength may arise because of the crack, and the material can only be loaded up to its fracture strength ( $\sigma_c$ ). A study of the numerous influencing material properties which affect the fracture strength of a material (e.g., yield strength, alloy type, etc.) constitutes a significant part of fracture strength analysis. In treating this problem, it has been found helpful to try to relate some characteristic of the environment around the crack tip to the fracture strength. The selection of a specific characteristic and the attainment of a "critical" value of this characteristic when the material reaches its fracture strength is also a significant part of fracture strength analysis. The characteristic or "fracture criterion" has been the subject of study for some years in the field of fracture mechanics.

In establishing a material fracture strength criterion or criteria, there are normally strict controls placed on the direction, rate, and type of loading as well as narrow limits on range of applicability. Structural members containing cracks in most cases experience more complex stress states (e.g., stress gradients, biaxial loading, etc.) than are common in a controlled laboratory material fracture strength test. Also present in structure are geometrical and material discontinuities in the form of splices, fasteners, curvature, supporting structure, etc., which are not a part of a material fracture strength test. For these cases component tests of both fatigue and fracture critical elements of any primary structure are normally required. However, it is not uncommon to have performed elaborate element (subcomponent) tests only to find that unexpected in-service failures take place because the local stress states occurring in-service were inadequately investigated on the element level. In these cases, a laboratory based material fracture criterion was initially operative but was altered by changes in structural environment (i.e., stress state, discontinuities, etc.). Therein lies the basic difference between what is called fracture strength and residual strength; the former is governed by a material fracture criterion whereas "residual strength" implies alteration to the criterion due to a structurally controlled environment.

In this report the emphasis has been placed on those techniques applicable to the prediction of residual strength of through-cracked, thin section structure. In most cases alterations to the material fracture criterion will have to be made to account for some of the influencing parameters such as temperature, strain rate, etc.

In thin section fracture of tough materials, considerable amounts of slow stable tear and accompanying crack tip plasticity limit the applicability of an elastically based failure criterion. Also problems of non-linear material behavior in the supporting structure and attachments and the resulting stress redistribution must be addressed in the overall residual strength analysis method.

To assist in the solution of these problems, the use of high speed computer analyses (for stresses and displacements) permits a more accurate picture of the local stress states in complex structural elements to be obtained than are possible using closed form solutions. The task remains to include the effects of plasticity, load rate, temperature, and other crack tip environmental parameters into a viable fracture strength criterion, and to include these parameters into a workable residual strength analysis method. Possible avenues of approach leading to the more refined and accurate prediction of residual strength are presented in this report.



The report has been organized in such a way that the emphasis on structural (as opposed to material) considerations has been maintained throughout, yet those material properties which are believed to play an important role in the required fracture criterion have received equal emphasis and recognition. Section II defines those ranges of material variables for which fracture in a plane stress or mixed mode is likely and details typical crack sites in aircraft structures which must be treated in the developed method.

In Section III, a long range view toward the residual strength problem is adopted by citing the attributes of an "ideal" residual strength prediction method. This section sets the ultimate goals (as presently conceived) of a "complete" residual strength prediction technique.

The gap which exists between the "ideal" method described in Section III and the methods currently available is presented in Sections IV and V. In Section IV, several existing residual strength methods are discussed in the following manner; background, simplifications, computational procedure and potential for each method. Necessary empirical constants for use in applying each method are indicated. On the basis of the goals of the "ideal" method a linear elastic fracture mechanics approach is suggested as being the most promising of the existing methods for small scale yielding problems.

A discussion of data scatter is presented in Section V. In particular, the problem considered is that of a center cracked sheet with Z section stringers, where the crack is both between and underneath the stringers. Experimental results are compared to results from several of the prediction techniques cited in Section IV. Section V concludes with a discussion of several of the parametric influences known to affect residual strength (e.g., strain rate, crack tip buckling, environment, etc.) which are not presently accounted for in residual strength methods.

Section VI presents the ingredients of the residual strength prediction method which will be developed and applied to realistic aircraft structural configurations in subsequent phases. It must be acknowledged that the method of Section VI falls short of the "ideal" method of Section III. Nevertheless, the improved method is conceived of as being a good deal more satisfactory than other methods in that influencing parameters are more realistically treated. Specifically, it is planned to use the J integral as the parameter with which to characterize the crack tip environment. Also, it is felt that a generalization of the crack growth resistance curve can be used in conjunction with results of J integral calculations to yield estimates of residual strength.

The degree to which the residual strength prediction method agrees with experimental results, and hence the confidence which can be placed in the use of the method, will be established in subsequent Phases.

## II PLANE STRESS AND MIXED MODE FRACTURE CRITICAL AIRCRAFT STRUCTURE

### 2.1 DEFINITION OF TERMS RELATING TO THIN SECTION FRACTURE

For fracture to occur in the plane stress or mixed mode (i.e., in a manner intermediate between plane stress and plane strain), nominal material thicknesses ( $B$ ) will generally be in sheet or thin plate gages. The "true" plane stress mode of fracture, by definition, implies material thickness on the order of foil gages since "through the thickness" variations in stresses are assumed to be nonexistent. Therefore, the term "generalized plane stress" would be more descriptive for the fracture mode of metallic materials for gages in use in typical aircraft skin construction. In elasticity terminology, "generalized plane stress" implies that even though "through the thickness" variations in stresses and displacements are permitted, averaged values of stresses and displacements can be used with negligible error in a two-dimensional formulation.

In the normal fracture mechanics approach (using the notion of critical stress intensity factor,  $K$ ), the definition of the domains in which plane stress, mixed mode, and plane strain fractures may be expected follows trends which can be illustrated as in Figure 1. For each material the shape of this curve is unique but in general the shaded area encompasses thicknesses normally encountered in typical aircraft skin. The mixed mode region requires knowledge of the three dimensional elastic-plastic stress state near the crack tip for exact solution. Such solutions are not currently available. However, fracture criteria may be established and attempts can be made to approximate solutions for this class of problems (see Section IV). The area of "true" plane stress with associated foil thicknesses is of academic interest; however, the terminology "plane stress fracture" is generally prevalent in the literature and has been used in this report to indicate fracture of thin section material. It is to the problem of residual strength prediction under generalized plane stress conditions that this program has been addressed.



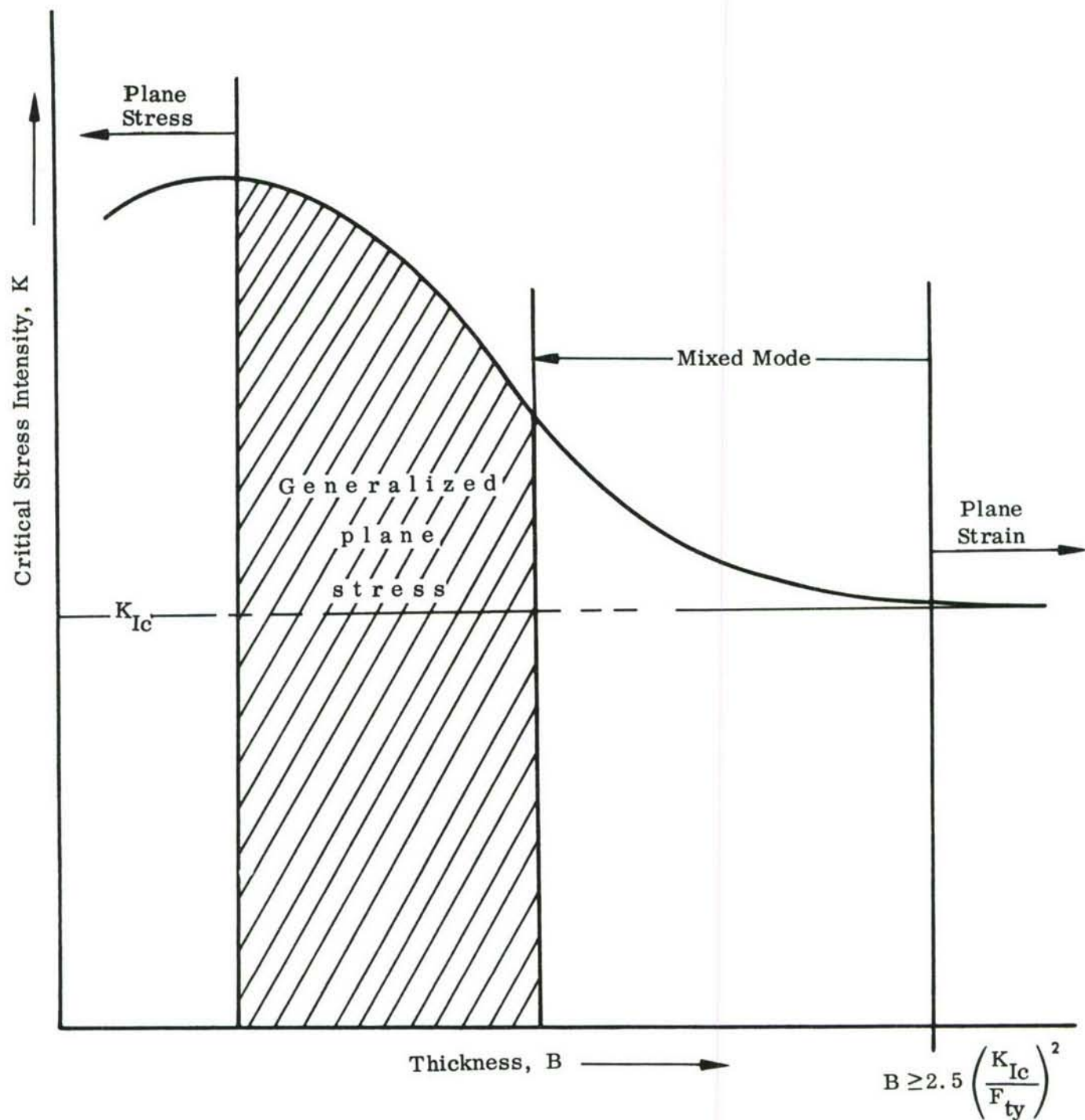


FIGURE 1 TYPICAL VARIATION IN CRITICAL STRESS INTENSITY WITH THICKNESS FOR PLANE STRESS-STRAIN AND MIXED MODE

## 2.2 IDENTIFICATION OF FRACTURE CRITICAL AIRCRAFT STRUCTURE AND ASSOCIATED CRACK GEOMETRIES

Several surveys have been conducted by the Air Force to identify the causes, locations, and numbers of structural failures in aircraft systems. A recent comprehensive survey (Reference 1) categorized early life structural failures in both military and commercial aircraft. This survey indicated that primary airframe structural failure could be grossly classified for all systems as to location in the following manner: aft fuselage frames (~15%), outboard and inboard wing skins (~10% to 13%), wing inboard main frames (~10%). It was pointed out in Reference 1 that since the areas listed above represent a large portion of the total airframe it stands to reason that, due to the number of fasteners normally associated with these areas, fatigue crack initiation sites were in abundance\*. In the aft fuselage and outer wing structure the skin material is normally in the thinner gages. This is particularly true for larger aircraft and clearly indicates the tendency for the development of generalized plane stress and mixed mode conditions at the crack tip. Due to the thinner material gages prevalent in the locations of interest, the problem of through the thickness cracks is considered to be the most likely crack geometry requiring investigation. Therefore, through cracks are the prime candidate crack geometries considered in this program.

Candidate structure and crack geometries have been chosen and will represent the general classes of residual strength problems which the to-be-developed prediction method should be capable of solving. These general classes of problems are shown in Figures 2 through 4. Particular attention will be devoted to damage tolerant wing and fuselage structure being designed and fabricated under AMS/ADP programs so that these structures may be a part of the selected structural geometry for Phase III evaluation. In all cases the emphasis has been placed on flaw orientation, location, and relevant loading direction rather than on specific hardware (e.g., spar, frame, longeron/attachment, etc.). This approach has been taken due to the possibility of having several different sub-assemblies fastened with a number of methods of attachment (bolts, rivets, interference fasteners, etc.). For the structure of Figures 2, 3, and 4, through-the-thickness cracks occur in either the skin or the support structure or both. In most cases a crack originating at one edge of a fastener hole will propagate from both sides after an initial "shake-down" period of fatigue crack growth. Therefore the condition shown in A of Figures 2 and 3 would be less likely to occur than those of B and C of Figure 2 and B of Figure 3.

---

\* The majority of the cracks reported in these structural areas were not necessarily critical. This was the case with the remaining 65% to 70% of observed non-primary structural cracks. However, the propensity toward cracking was in the areas listed.

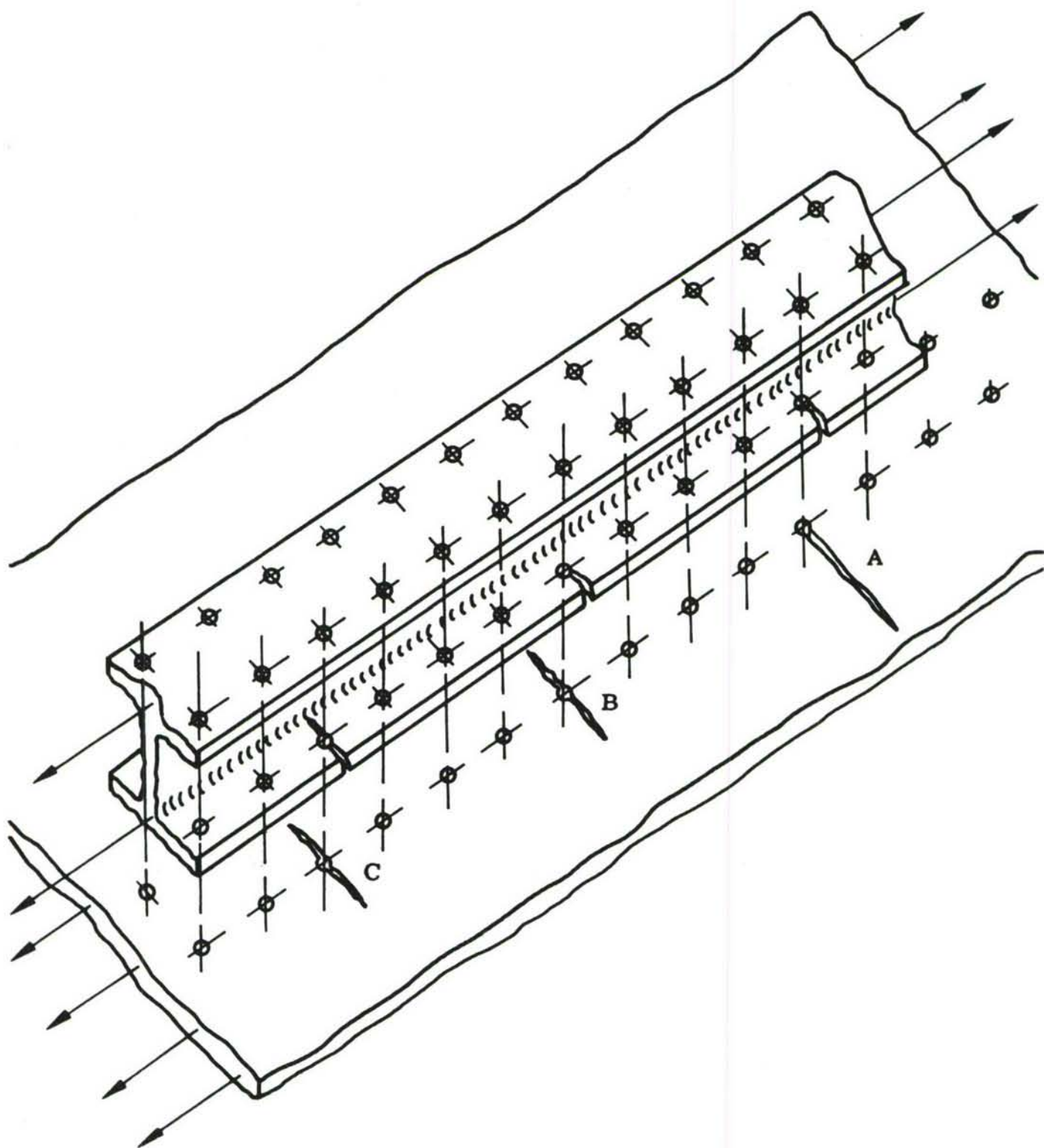


FIGURE 2. FLAW GEOMETRIES FOR LOADED SKIN/STRINGER CONSTRUCTION.



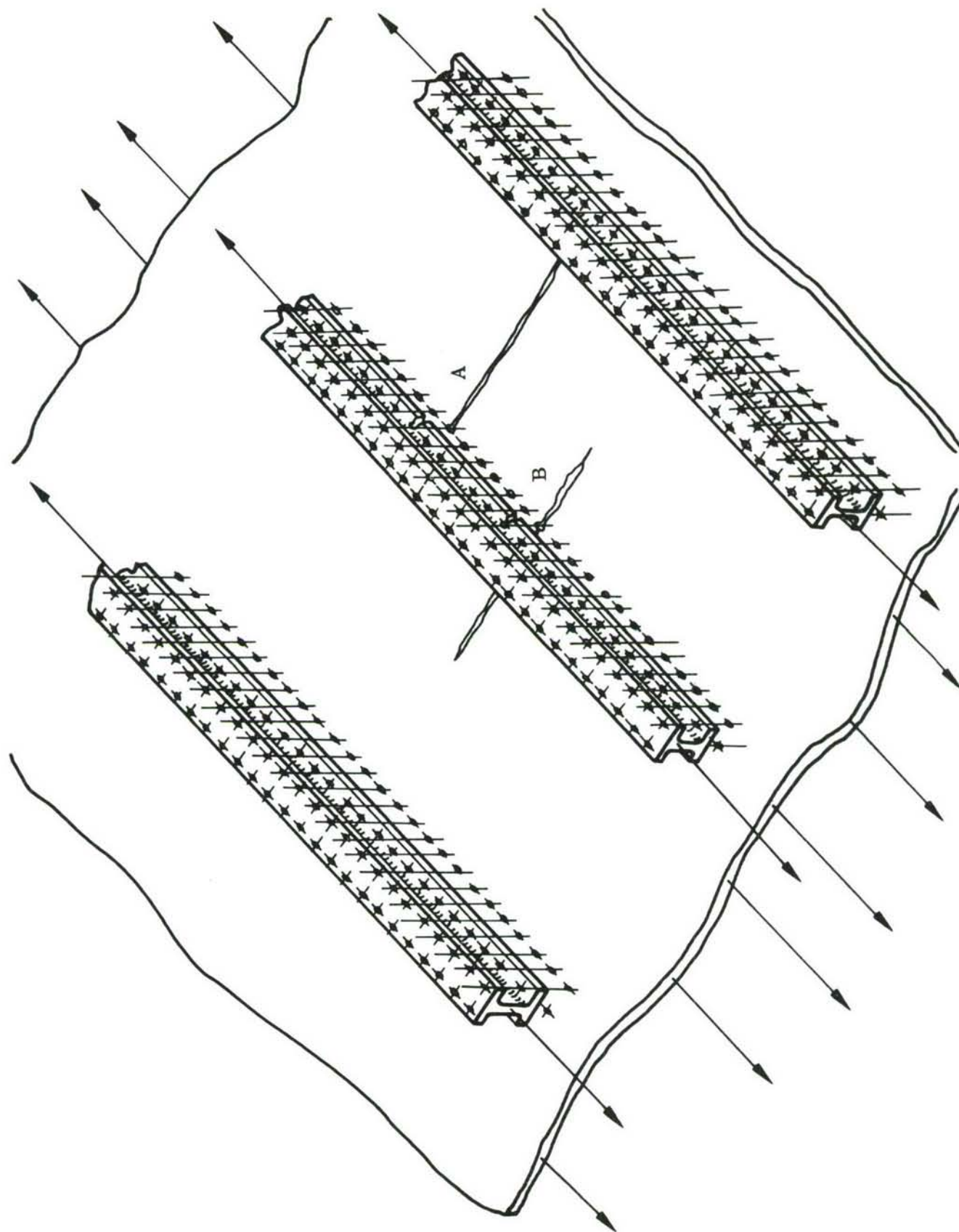


FIGURE 3. TYPICAL MULTI-BAY CRACKS IN TENSION STRUCTURE



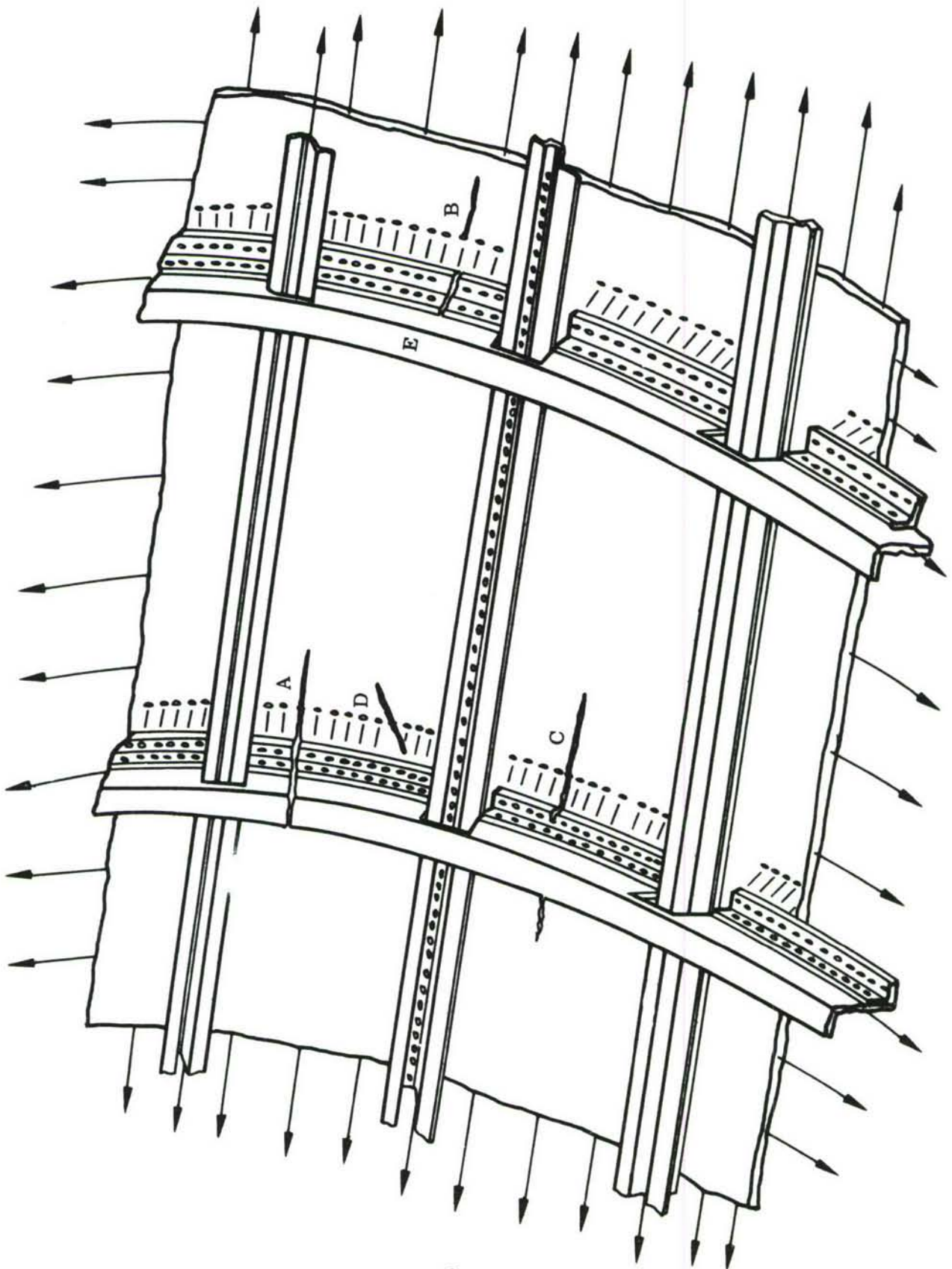


FIGURE 4. TYPICAL CRACK SITUATIONS IN PRESSURIZED FUSELAGE SHELL

In many cases, due to the existence of complex stress states, the crack can initiate and grow at angles to the principal loading direction (Figure 4, D). Although it is known that eventually these angled cracks will grow (by repeated loading) in the direction normal to the principal stress direction, fracture can occur with angled cracks for nonperpendicular loading and should be accounted for in an advanced residual strength analysis method.

In many cases the supporting structure can fail during fatigue crack propagation with or without detection of crack growth in the skin panel (e.g., Figure 4, crack in frame at location E) or in the skin and frame, Figure 4 A and B. These substructural crack situations (with accompanying load transfer to the skin) should also be included in an advanced residual strength analysis method.

### 2.3 LOADING CONDITIONS APPLICABLE TO FRACTURE CRITICAL STRUCTURE

Indicated in Figures 2, 3, and 4, are the global loading conditions which would represent loads encountered in service for representative structure of a lower wing skin (inboard and outboard) and aft fuselage. Biaxial loading and/or biaxial loading plus shear is an integral part of the stress condition for certain structural arrangements, e.g., Figure 4.

Thus an advanced residual strength method should be able to analyze structures and crack geometries of the complexity of Figures 2, 3, and 4. It must also contain elements of a fracture criterion which are capable of evaluating material factors such as anisotropy, for example, or complex loading situations such as D of Figure 4. In this case any preferred rolling or metalurgical anomalies would result in directional dependence of fracture strength.

Loading conditions which should be considered are those resulting from wing bending due to maneuver and gust (for lower wing structure) and those resulting from fuselage bending and pressurization for representative fuselage structure. Precrack orientations which will be considered are those which are normal to the largest principal stress since it is known that any subsequent slow tear will take place along those paths. Others to be considered are angled cracks such as shown on Figure 4.



### III THE "IDEAL" RESIDUAL STRENGTH PREDICTION TECHNIQUE

#### 3.0 INTRODUCTION TO THE "IDEAL" TECHNIQUE

In this section the subject of residual strength prediction is discussed from the viewpoint of a user of a prediction technique. A user is primarily interested in whether or not a given technique can be applied to his particular problem. The details of how the prediction is made (i.e., whether numerical methods, nonlinear strain-displacement relations, etc., are used in arriving at the prediction) are of only secondary interest to a user. To be of value to the widest possible group of users, a predicting technique must possess considerably more capability than the methods presently available. This section is devoted to a discussion of what characteristics the "ideal" residual strength prediction technique should possess.

#### 3.1 PARAMETERS AFFECTING RESIDUAL STRENGTH

A residual strength method should be able to predict remaining strength of cracked, structural elements. This implies that all "environmental" factors which can influence residual strength must be accounted for. Also, in order to be an effective technique applicable to true-to-life situations, a residual strength method must be capable of treating both simple and complex geometries, and plane stress, mixed mode or plane strain crack conditions for a broad spectrum of materials and loading conditions. Also, surface flaws, embedded flaws and through flaws must be capable of treatment.

In general, the parameters which affect the residual strength of aircraft structures can be grouped into three main categories. They are:

- (1) structural,
- (2) loading, and
- (3) material parameters.

The number of structural parameters exceeds those of the other two types, as shown in Table I. The structural parameters listed are those which exist at the "element" level rather than at the "subcomponent" level. That is, the residual strength method would be applied to a stiffened tension cover, for example, rather than to an entire wing box. This is the case since simplifying assumptions (e.g., plane stress conditions) can be most conveniently made at the element level. Also, numerical methods (e.g., finite element techniques) can be most efficiently utilized at this level. Although Table I lists the most important parameters which would be included in a residual strength prediction method, it is by no means complete. For example, the presence of cap strips made of unidirectional composite material on the outstanding flanges of stiffeners can add significantly to panel stiffness, and thus may be used increasingly in the future. The method should treat single or multiple cracks of arbitrary length and having arbitrary locations and orientations with respect to the stiffening and loading present.

TABLE I PARAMETERS TO BE ACCOUNTED FOR IN AN "IDEAL" RESIDUAL STRENGTH PREDICTION TECHNIQUE

<u>STRUCTURAL PARAMETERS</u>	<u>LOADING PARAMETERS</u>	<u>MATERIAL PARAMETERS</u>
<ul style="list-style-type: none"> <li>Overall structural arrangement</li> <li>Type of Construction                             <ul style="list-style-type: none"> <li>Skin stiffened (e.g., stringers, longerons, etc.)</li> <li>Monolithic (thick skin/unreinforced)</li> <li>Layered - (e.g., core stabilized honeycomb)</li> <li>Planked</li> <li>Integrally stiffened (e.g., waffle pattern)</li> </ul> </li> <li>Panel Geometry                             <ul style="list-style-type: none"> <li>Planform shape (e.g., rectangular, trapezoidal, etc.)</li> <li>Panel curvature</li> <li>Boundary conditions - (e.g., attachment to spars, ribs, frames, etc.)</li> <li>Orientation of stiffening with respect to panel boundaries and stiffener spacing</li> </ul> </li> </ul>	<ul style="list-style-type: none"> <li>Uniaxial Tension</li> <li>Biaxial</li> <li>Biaxial + Shear</li> </ul>	<ul style="list-style-type: none"> <li>Crack Tip Plasticity (not necessarily small with respect to crack length)</li> <li>Slow Tear (i.e., stable crack extension)</li> <li>Crack Tip Buckling</li> <li>Load/Strain Rate Sensitivity</li> <li>Thermal Effects</li> <li>Environmental Effects</li> <li>Thickness/Property Variation</li> <li>Anisotropy</li> <li>Stiffener Yielding</li> <li>Strain Hardening</li> </ul>
Detailed structural considerations		
<ul style="list-style-type: none"> <li>Skin thickness changes (e.g., taper or abrupt)</li> <li>Reinforcement geometry (e.g., rectangular, hat section, channel, Z, etc.)</li> <li>Attachment details (e.g., bolted, riveted, screwed, bonded, welded, etc.)</li> <li>Fastener Flexibility</li> <li>Eccentricity</li> </ul>		



From a stress analyst's point of view, once a given structure has been sized based on static and/or fatigue strength considerations, the question of flaw tolerance must be considered. Assuming that the best material choice (or choices) based on fatigue, crack propagation and toughness requirements has (or have) been made for the structure in question, the residual strength for anticipated in-service cracks and loading conditions must be determined.

Ultimately it would be desirable to optimize the structure for damage tolerance simultaneously along with other design requirements commonly considered in design optimization studies. Thus a design having desired weight, strength, stiffness, and damage tolerant characteristics would be obtained. The optimization could take place by using an existing redundant analysis technique in an iterative fashion (i.e., some sort of structural synthesis could be accomplished) with the residual strength prediction method embedded into the synthesis as a damage tolerant algorithm. To some extent, this has been the procedure followed at one large aircraft company (e.g., see Reference 2). Although the procedure outlined in Reference 2 lacks the degree of generality indicated in Table I, it does incorporate some of the basic procedures which a residual strength prediction method should possess, e.g., the ability to analyze in-service loading conditions.

### 3.2 RELATING THE MATERIAL PROPERTIES, ANALYSIS METHOD, AND FRACTURE CRITERION

In the determination of the residual strength of a cracked structure, the interchange between material properties, fracture criterion (or criteria) and analysis method can be somewhat confusing in view of the close interrelation which exists between the various activities. To assist in visualizing this interrelationship, a flow diagram of the major steps in performing a residual strength prediction is shown in Figure 5. The procedure is envisioned as being a six step operation. Step (1) constitutes a statement of the problem to be solved. Of the many structural and loading parameters which the method is to be capable of treating and which have been delineated in Table I, the particular parameters germane to the problem at hand are earmarked in step (1) and supplied to step (3). In addition, a specification of the candidate material or materials of interest is made in step (2) and also supplied to step (3). The material identification (step 2) is required only to select the appropriate fracture criterion in step (3) and involves only the most cursory materials information.

Step (3) of the procedure consists of the "executive" functions to be performed. Utilizing the output of steps (1) and (2) the appropriate fracture criterion is selected in step (3) and direction is supplied to the subsequent activities of steps (4), (5), and (6).

Although the bulk of the work required to make a residual strength prediction is accomplished in steps (4), (5), and (6), the determination of precisely what is to be done (i.e., the steering of the detailed activities) is accomplished in step (3). The generality which the procedure must possess necessitates having a versatile "executive" step capable of directing which material properties are required, what analyses should be performed, and what criterion (or criteria) should be applied. Steps (4), (5), and (6) of the technique are discussed separately in the following sections.



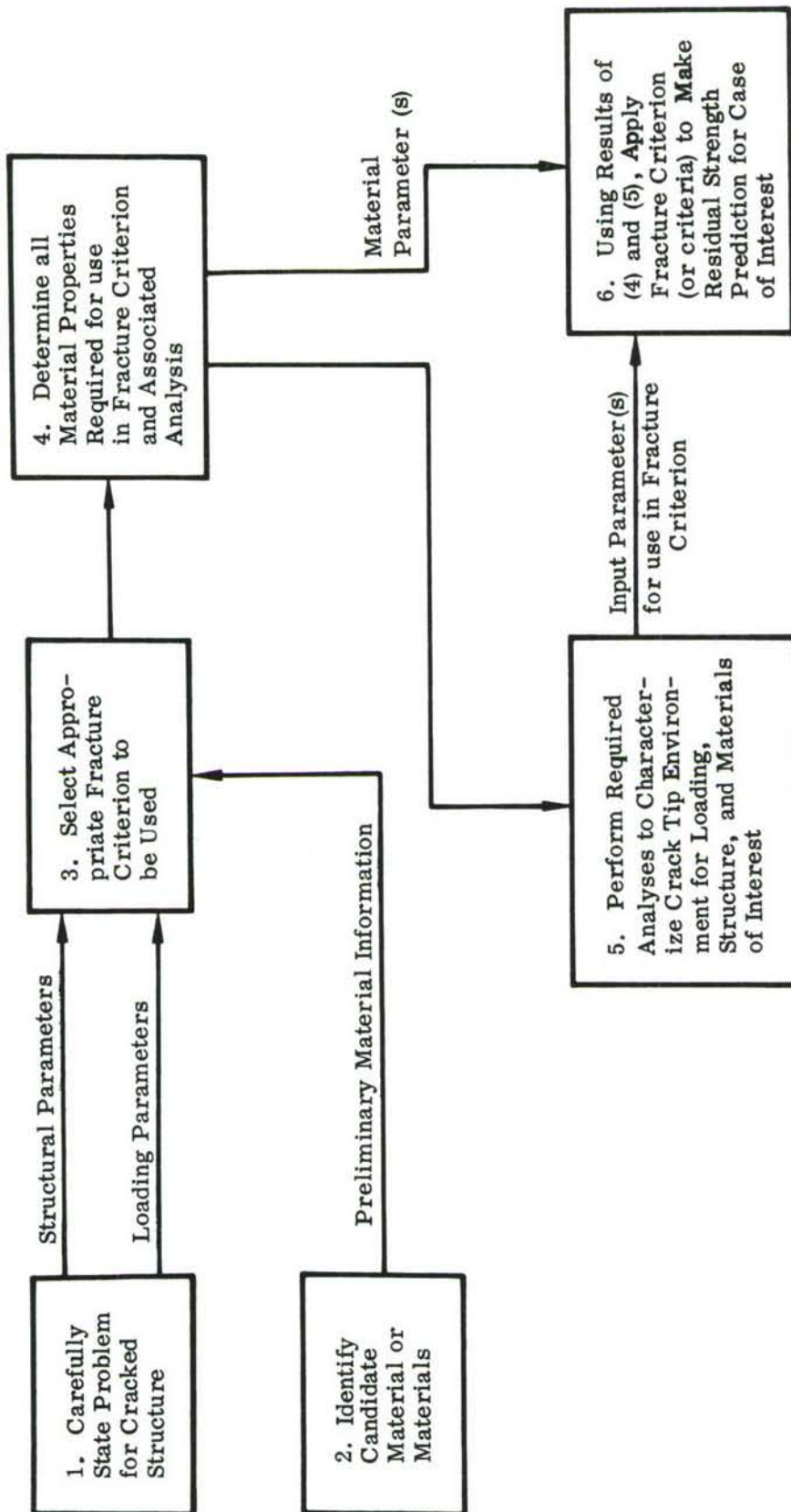


FIGURE 5. FLOW DIAGRAM SHOWING MAJOR STEPS IN PERFORMING A RESIDUAL STRENGTH PREDICTION

### 3.2.1 Determining Material Properties

In the present context, material properties assume importance only as they have an impact on the fracture criterion selected in step (3). Thus, rather than amassing large quantities of materials data for possible inclusion in a fracture criterion, only those data specifically required as dictated in step (3) will be determined.

It is envisioned that, regardless of the precise form of the fracture criterion ultimately used, material stress-strain behavior, as obtained from conventional uniaxial tests, will be required. For plane strain fracture, the influence of material stress-strain behavior (i.e., the stress-strain curves displayed by steel, aluminum, titanium, etc) on toughness ( $K_{Ic}$ ) has been well documented as shown in Reference 3. Basic relationships have been proposed between toughness, strain hardening, and other material properties as indicated in Reference 4. For material which exhibits brittle or semi-brittle fracture, crack tip plasticity exerts a minor influence and is confined to zones which are small compared to the crack length and specimen dimensions. In this case,  $K_{Ic}$  approaches a basic material property. For a structure whose thickness gives rise to plane stress or mixed mode fracture conditions, (see Section II, Figure 1) the plastically deformed material is no longer bounded by elastic material (in the through-the-thickness direction) and large plastic zones (zone size  $\geq$  crack length) develop. In this case linear elastic fracture mechanics is inappropriate and  $K_{Ic}$  loses its meaning as a material property. Some modification to or generalization of a critical K must be considered or a new nonlinear criterion developed.

For the method indicated in Figure 5, those material properties which are considered to play a major role in influencing nonlinear elastic-plastic fracture behavior will be obtained in step (4) for use in the analytical activities of step (5) and for inclusion in the failure criterion to be applied in step (6). Material properties include the following as candidates:

- . Yield Surfaces (Tresca versus Von Mises)
- . Yield Strength
- . Strain Hardening Exponent
- . Secant Moduli
- . Stress/Strain Curves to Large Strains
- . Elastic Strain
- . Plastic Strain
- . Directional Properties
- . Thermal Properties (e.g., creep rate, coefficient of thermal expansion)
- . Stress/Strain Rate ( $\dot{\epsilon}$ ,  $\dot{\sigma}$ )
- . Presence of Upper and Lower Yield Points.

This listing of material properties is not complete, nor are all the elements mutually exclusive. Nevertheless, it represents the basic ingredients for the material property contribution to any hypothetical residual strength analysis procedure. On the basis of examining representative load/stress versus crack length curves to fracture, the effect of some of these parameters on material fracture strength can be indicated schematically as in



Figures 6 (a, b, and c). Taken separately the effect of any material property on fracture strength could be examined empirically. However, these parameters should enter as part of the fracture criterion indicated as step (6) in Figure 5 as either separate or compound factors. That is, a suitable combination of several of the factors on the list may be most appropriate for use in step (6) of Figure 5. Ideally all of the parameters listed should be treated in analytical form. That is, it should be possible to incorporate the numerical values determined in step (4) into appropriate analytical expressions which could be succinctly capsulized in step (5) into a small number of problem "descriptors." These "descriptors" could then be compared to the fracture "descriptors" to ascertain residual strength in step (6). Since analytical relationships have not been derived between all of the parameters listed and fracture strength, it will only be possible to analytically process some of the material parameters, and the remaining will enter step (6) directly. Those parameters most susceptible to analytical treatment are indicated in Section 3.2.2.

In addition to the material parameters listed, material behavior on the micromechanistic scale (e.g., dislocation mechanisms) is known to affect fracture, although the exact influence is subject to considerable debate. It is not the intent of this study to include micro-aspects into a failure criterion, but the "ideal" procedure would include such micro-effects.

Although there is a tendency to think of obtaining material properties as being an experimental activity, this should be viewed, in the context of Figure 5, as only an interim situation. Ultimately all the materials data required to execute the analyses indicated in step (5) and apply the criteria in step (6) will have been experimentally determined. At that point, the prediction technique shown in Figure 5 will be completely analytical. It will be possible to make residual strength predictions for cracked aircraft structure without the necessity of having to perform supplemental material tests. The method could ultimately utilize the step (4) data which had been accessed from a computer data tape. As an illustration of this method of utilizing materials data, all necessary MIL-HDBK-5 materials data has been placed on a tape for use (at Wright-Patterson Air Force Base) with a large Air Force developed finite element program.

### 3.2.2 Performing Required Analyses

As shown in Figure 5, materials data will flow from step (4) to both steps (5) and (6). Taking a familiar example in the case of an unflawed structural member, the pertinent materials data might reduce to  $E$ ,  $\nu$ , and  $F_{ty}$ .  $E$  and  $\nu$  established in step (4) are supplied to step (5), where a structural analysis is performed to determine stresses throughout the body. The stresses from step (5) and  $F_{ty}$  from step (4) are supplied to step (6) where structural adequacy is assessed.

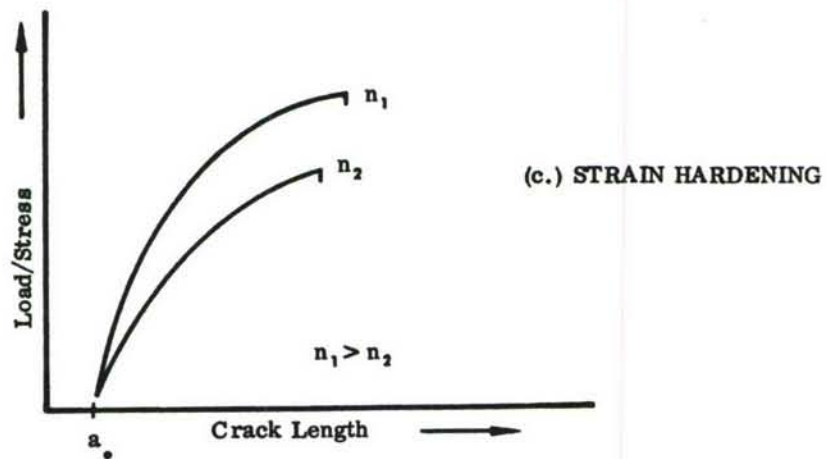
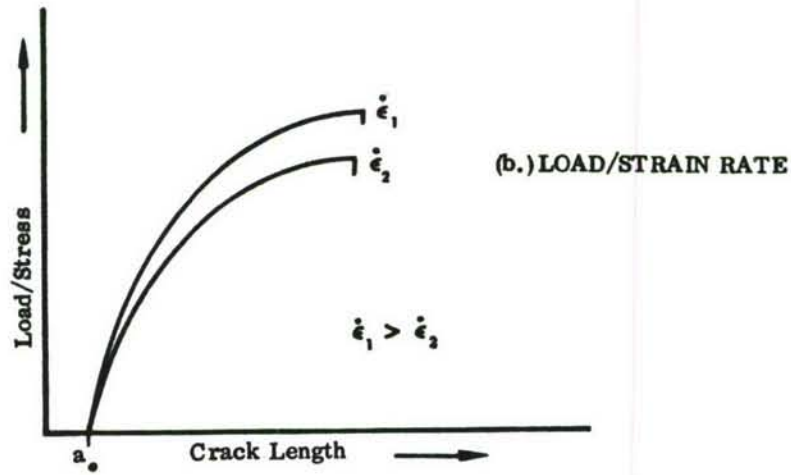
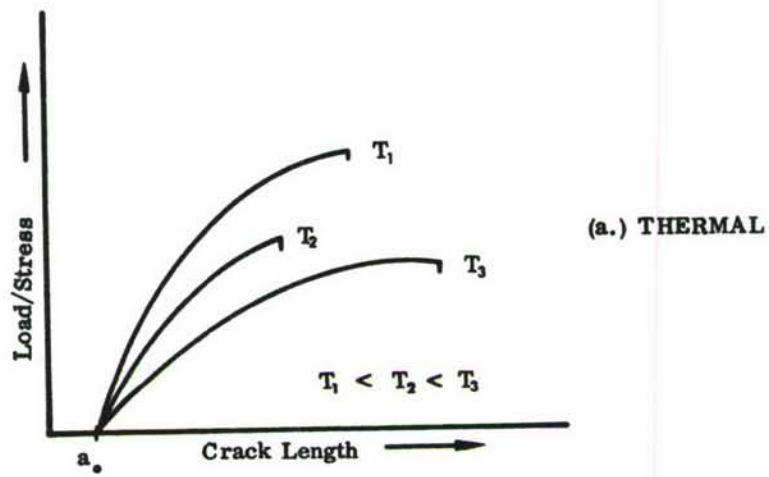


FIGURE 6 EFFECT OF SEVERAL MATERIAL PROPERTIES ON FRACTURE STRENGTH



In the case of residual strength prediction, it is almost certain that a finite element program will be used in step (5) to perform the required detailed structural analysis calculations. The desirability of having a finite element program available is much more pronounced for aircraft structural use than if the problem were restricted to simple unreinforced plates, for example. The almost limitless combinations of possible structural, loading, and material parameters makes the use of a finite element program necessary.

The combination of number of parameters and accuracy required in order to obtain useful information dictates that high speed digital computers be used in step (5). Since treatment of elastic-plastic behavior has been found to necessitate large region sizes for efficient solution, the requirement for large computers is apparent.

It is envisaged that many of the time saving devices which have been recently introduced in the use of finite elements would be incorporated. Among these desired capabilities are automatic mesh generation (for crack configurations), band width minimization techniques, simplified data input, optimized computer logic for treating extending cracks, and the use of "active column" logic to efficiently perform matrix decomposition.

Rather than requiring a priori assumptions as to the shape and extent of plastic zones the method should automatically determine the plastic zones as a part of the problem solution. Materials displaying any sort of stress-strain curve should be amenable to solution without having to make drastically simplifying assumptions. Also, the method should incorporate incremental theory plasticity rather than the theoretically unsound deformation theory plasticity.

In step (5), analyses will be conducted which will characterize the crack tip environment for used in step (6). In addition to minimizing work involved in data input excessive manipulation and interpretation of the output data in order to apply the fracture criterion should not be required. This would encourage more widespread use and will also eliminate a common source of error. The step (5) activity is visualized as the development and application of analyses techniques in which existing finite element programs are used as a part of the analysis procedure.

### 3.2.3 Applying the Fracture Criterion

The fracture criterion (or perhaps criteria) to be used should encompass all aspects of the affecting parameters listed in Section 3.2.1 and in Table I, and should apply to any crack geometry.

It is also important to note that a skin fracture critical and reinforcement fracture critical criterion may be required. In the case of brittle or semi-brittle skin material where small scale yielding prevails, an elastic or slightly modified elastic criterion such as plane strain fracture toughness will work adequately for the skin critical case. However,



when large amounts of crack tip plasticity are present and slow tear becomes a major portion of the load versus crack length curve, an elastic fracture criterion becomes inadequate. Both plasticity (as discussed in Reference 5) and slow tear need to be treated explicitly. It appears that the crack growth resistance curve (Reference 6) or some generalization of it may be embedded into the fracture criterion to account for slow tear. The use of the J integral (see e.g., References 7 through 10) may also play an important role as a fracture criterion even though mixed mode fracture and slow tear currently present an analytical barrier.

It is envisioned that the residual strength predicting procedure should, as a minimum, account for the following in its fracture criterion (i.e., in step (6), Figure 5):

- . Slow, stable tear
- . Crack tip plasticity
- . Possibility of either skin or reinforcement fracture
- . Crack buckling
- . Other local (crack vicinity) stress/strain influences (such as crack bulging due to pressurization).

The fracture criterion should be independent of specimen geometry (i.e., width, length, and thickness). In this form a direct comparison can be made between laboratory size specimens (i.e., specimens with cost, material, and machine capacity restraints) and full scale structural behavior.

In summary, a criterion (or criteria) which would provide a rigorously established value of critical stress, strain, deflection, etc., related to crack size would be highly desirable for inclusion in the residual strength prediction technique. The criterion should be applicable to all materials and crack geometries, and to both simple and complex structural elements. Also, it should recognize the parameters indicated in Table I, those in Section 3.2.1, and those mentioned in this section.

## IV REVIEW OF CURRENTLY AVAILABLE RESIDUAL STRENGTH PREDICTION TECHNIQUES

### 4.1 NOTCH STRENGTH OR CRACK STRENGTH ANALYSIS METHOD

#### 4.1.1 Historical Development of Notch (Crack) Strength Analysis (NSA-CSA) Method

In 1952 Kuhn and Hardrath (Reference 11) suggested that the converted Neuber stress concentration factor (Reference 12) could be used to determine an "effective" stress. The Neuber factor  $K_N$  is a modified theoretical factor which accounts for material notch sensitivity by introducing an additional material constant,  $\rho'$ . In this sense, Neuber's  $K_N$  converts a theoretical stress concentration factor into a practical one. The evaluation of a "Neuber constant" (i.e.,  $\rho'$ ) by Kuhn and Hardrath and again by Kuhn and Figge (Reference 13) showed the applicability of the converted Neuber stress concentration factor to prediction of fracture strength of steel and aluminum alloys. However, its applicability was limited to elastic values of "effective" stress. In 1953 Hardrath and Ohman (Reference 14) generalized the "secant modulus" formula of Stowell and incorporated it as part of the analysis to account for fracture in the plastic range.

The Crack Strength Analysis (CSA) method introduced the idealization of representing through the thickness cracks by elliptical holes and included a correction for finite boundaries similar to that proposed by Dixon (References 15 and 16). A single constant was also introduced which included the "Neuber constant" and the ratio of secant to elastic moduli. Two forms of the CSA analysis have been suggested (Reference 17): a so-called "basic" form and a "modified" form. The difference between the two forms is that the "modified" form accounts for material notch strengthening while the "basic" form does not. Thus, a minimum of two tests using cracked specimens is required to establish constants for use in the "modified" form as opposed to one such test for the "basic" form.

The notch (crack) strength analysis method has been used to evaluate the fracture strength of materials since 1962. Its accuracy (often using the simple "basic" form) in predicting fracture stress for unreinforced specimens (buckling restrained) has been shown to be as good as linear elastic fracture mechanics (LEFM) for materials which do not exhibit extensive slow tear or excessive crack tip plasticity (see e.g., References 18 and 19). The application of the NSA or CSA method to residual strength prediction for reinforced structural geometries is unknown. One can assume that for those structures which have small initial crack size (crack length short with respect to reinforcement spacing), limited plasticity, and which are skin fracture critical, good correlation should occur between actual and predicted residual strength. As pointed out by Kuhn (Reference 17) the task of "sorting" fracture analysis for simple panels left no time to devote to the problem of fracture of complex specimens. This of course is the objective of this program.



#### 4.1.2 Theory of NSA and CSA Method

The fundamental principle upon which the NSA and CSA methods are based is that of stress concentration. From an engineering viewpoint, stress concentration is a familiar and reasonable approach to use to determine remaining strength. As in any stress concentration approach, a stressed body containing a discontinuity (in this case an elliptical cavity) can be analyzed to determine a theoretical stress concentration factor ( $K_t$ ) (see Figure 7).

In this case the specimen of Figure 7 will exhibit a uniform gross area tensile stress remote from the elliptical notch of

$$\sigma_g = \frac{P}{WB} .$$

The stress  $\sigma_g$  is uniform across the width (W) and through the thickness (B). The condition in the notched area is nonuniform and contains steep gradients in the vicinity of the notch root as shown in Figure 7.

The average net area stress  $\sigma_N$  along the notch centerline is given by

$$\sigma_N = \frac{P}{(W-2a)B} .$$

The theoretical stress concentration (at the root of the notch) is defined as

$$K_t = \frac{\sigma_{\max}}{\sigma_N} \quad (1)$$

Using results from the two dimensional theory of elasticity, one can obtain a value for  $\sigma_{\max}$ , and the results will be meaningful as long as  $\sigma_{\max} < F_{ty}$ . For some particularly simple geometries and materials (namely isotropic),  $K_t$  can be obtained in a closed form. It may also be approximated using numerical methods for a wide range of geometries and materials of practical interest.

Neuber (Reference 12) converted the theoretical factor to a "practical" factor  $K_N$ . In equation form  $K_t$  is related to  $K_N$  by

$$K_N = 1 + \frac{K_t - 1}{1 + \frac{\pi}{\pi - \omega_e} \sqrt{\frac{\rho'}{\rho}}} \quad (2)$$

where  $\omega_e$  = effective flank angle (defined in Figure 7)  
 $\rho$  = notch root radius

and the factor  $\rho'$  is Neuber's constant. The value of  $\rho'$  is treated as a material constant which can vary from zero (ideally brittle material) to infinity for ideally notch insensitive materials. Equation (2) is only valid in the elastic range. Therefore, when  $\sigma_{\max}$  (Eq. 1) is in the plastic range it becomes an "effective"  $\sigma_{\max}$  which is not "real" in a measurable sense. The Neuber "practical" stress concentration factor,  $K_N$  was used in conjunction with a failure criterion proposed by Kuhn (References 11 and 12) using systematically determined Neuber constants,  $\rho'$ .

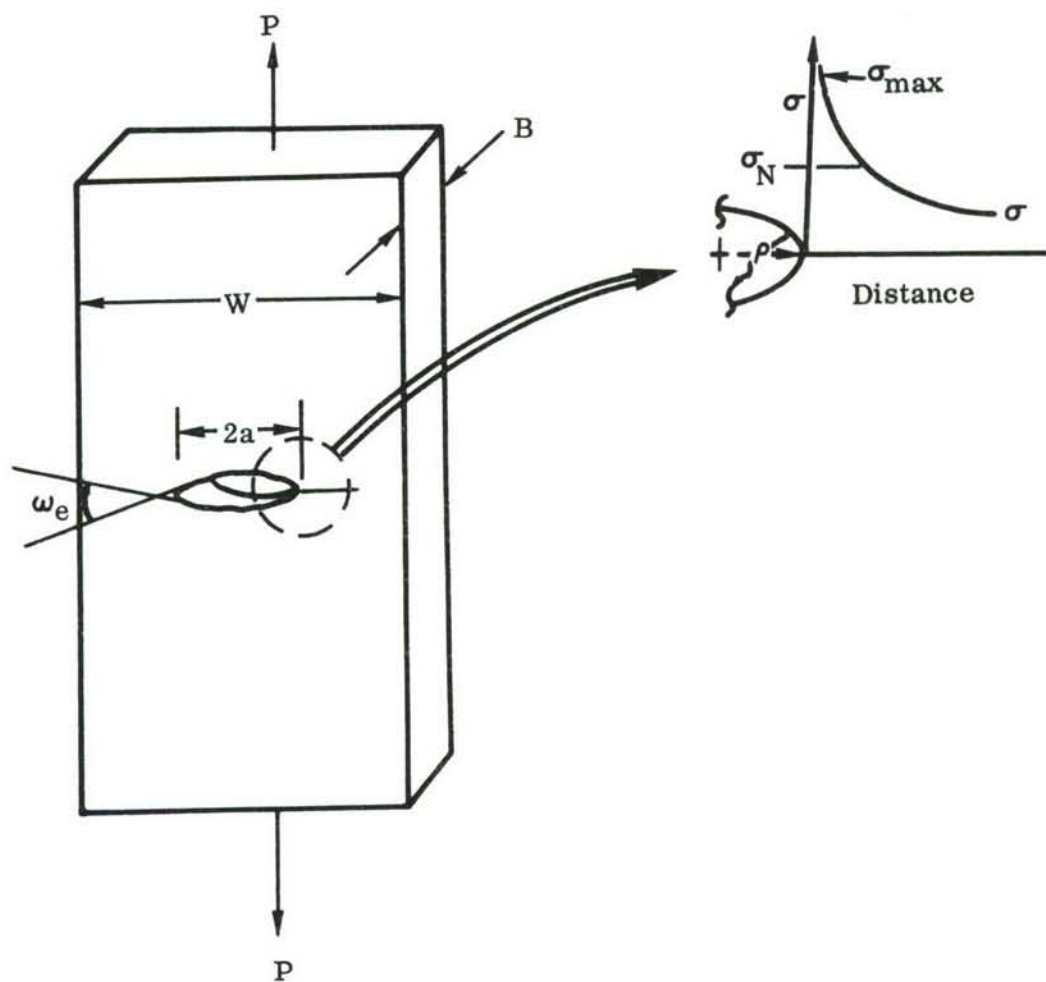


FIGURE 7 SPECIMEN WITH THROUGH-THE-THICKNESS FLAW



To overcome the limitation of being restricted to elastic situations, the Neuber factor was modified to include plasticity as follows:

$$K_p = 1 + (K_N - 1) \frac{E_n}{E_s} \quad (3)$$

where  $E_n$  = secant modulus of elasticity determined at the point where  $\sigma_{\max}$  is "measured."

$E_s$  = secant modulus of elasticity for an average stress far removed from the notch.

If the failure criterion is defined as  $\sigma_{\max} = F_{tu}$ , and if, as in most cases, the net section stress  $\sigma_N < F_{ty}$ , then  $E_n$  in Eq. 3 will be taken as the secant modulus at the point of maximum stress (i.e.,  $E_n = E_u$ ) and  $E_s = E$ , the value of Young's modulus. Equation 3 can then be written as

$$K_u = 1 + (K_N - 1) \frac{E_u}{E} \quad (4)$$

In the absence of available stress-strain data Kuhn (Reference 13) and Hardrath (Reference 14) estimated the ratio of secant to Young's moduli in Equation (4) from material elongation (e) data as follows:

$$\frac{E_u}{E} \approx \frac{1}{1 + \frac{.8eE}{F_{tu}}} \quad (5)$$

where

$$e = \frac{\text{Elongation in Standard Gage Length}}{\text{Original Gage Length}} .$$

Kuhn (Reference 17) recommends caution in using Equation (5) and states that actual stress-strain data from the material of interest should be used to establish  $E_u/E$  whenever it is available.

Some materials exhibit notch strengthening ( $\sigma_N > F_{tu}$ ), and the uniaxial stress-strain curve therefore lacks meaning for these materials using the NSA method. The treatment of plasticity for notch strengthening materials is not possible using the NSA method unless major modifications would be made, and this does not seem to have been done as yet.

In some specimen geometries the situation of net section fracture stresses greater than yield strength occurs. This is normally caused by the presence of small crack aspect ratios  $\left( \frac{\text{Crack Length}}{\text{Specimen Width}} \right)$ . Kuhn (Reference 17) has fitted available data in the  $\sigma_N > F_{ty}$  range with the expression

$$K_u = 1 + (K_N - 1) \frac{E_u}{(E E_N)^{\frac{1}{2}}} \quad (6)$$

where  $E_N$  is the secant modulus at  $\sigma_N$ .

For the particular geometry of Figure 7 the theoretical stress concentration factor (when the crack is in the form of an elliptical cavity) is given by

$$K_t = 1 + 2 \lambda_w \left( \frac{a}{\rho} \right)^{\frac{1}{2}}. \quad (7)$$

The factor  $\lambda_w$  is taken from the photoelastic results for stress concentration due to the presence of a crack proposed by Dixon (Reference 16) for specimens of finite geometry. The value of the quantity,  $\lambda_w$ , can vary from unity for small crack aspect ratios to zero for large crack aspect ratios. In the CSA method, it is used in a different manner. As the effective flank angle ( $\omega_e$ ) of the elliptical cavity decreases when the cavity approaches a crack, in the limit  $\omega_e \rightarrow 0$ , and Equation (2) reduces to (using Equation 7):

$$K_N = 1 + \frac{2 \lambda_w \left( \frac{a}{\rho} \right)^{\frac{1}{2}}}{1 + (\rho/\mu)^{\frac{1}{2}}} \quad (8)$$

However, when  $\omega_e \rightarrow 0$ ,  $\rho \rightarrow 0$  (that is, as the ellipse becomes a crack) and thus, Equation (8) becomes

$$K_N \approx 1 + 2 \lambda_w \left( \frac{a}{\rho'} \right)^{\frac{1}{2}}. \quad (9)$$

For situations in which  $\sigma_N < F_{ty}$ , substitution of Eq. (9) into Eq. (4) yields

$$K_u = 1 + 2 \lambda_w \left( \frac{a}{\rho'} \right)^{\frac{1}{2}} \frac{E_u}{E} \quad (10)$$

Kuhn (Reference 3) combined the "material constants"  $\frac{1}{\sqrt{\rho'}}$  and  $\frac{E_u}{E}$  into the factor  $C_m$  and also included the constant 2 so that, by definition,

$$C_m = \frac{2}{\sqrt{\rho'}} \frac{E_u}{E}. \quad (11)$$

The units of  $C_m$  are in(inches)<sup>-1/2</sup> and are consistent with stress concentration theory. The "constant"  $C_m$  will vary with temperature, thickness, and other environmental factors. Equation (10) can then be rewritten as

$$K_u = 1 + C_m \lambda_w \sqrt{a} \quad (\sigma_N < F_{ty}) \quad (12)$$

and the net section stress at failure becomes, using the failure criterion  $\sigma_{\max} = F_{tu}$ ,

$$\left. \begin{aligned} \sigma_N &= \frac{F_{tu}}{K_u} \\ \text{or} \quad \sigma_N &= \frac{F_{tu}}{1 + C_m \lambda_w \sqrt{a}} \end{aligned} \right\} (\sigma_N < F_{ty}) \quad (13)$$

For the case of "notch strengthening", equation (13) was generalized by Kuhn (Reference 17) to

$$\left. \begin{aligned} \sigma_N &= \frac{F_{tu}'}{K_u'} \\ \sigma_N &= \frac{F_{tu}'}{1 + C_m' \lambda_w \sqrt{a}} \end{aligned} \right\} \quad (14)$$

In this case the local (near crack tip) tensile stress,  $F_{tu}'$ , and "material constant,"  $C_m'$  must be determined indirectly from two fracture test specimens of radically different crack aspect ratios. If it is known that "notch strengthening" is not active ( $F_{tu}' = F_{tu}$ ) one of the two crack specimen tests can be replaced by a conventional tensile test coupon to obtain stress-strain data. In this case, of course, Equation (14) reduces to Equation (13). Kuhn (Reference 17) recommends that the constant  $C_m$  should not be determined from experimental values of  $K_u$  since  $K_u$  is very sensitive to errors when  $\sigma_N > F_{ty}$ . (From Equation 6 it can be seen that  $K_u$  is influenced by  $E_u$ ,  $\sigma_N$ , and  $\rho'$  when  $\sigma_N > F_{ty}$ ). Values of  $C_m$  and  $C_m'$  are given in Reference 20 for a wide range of materials.

In summary, the basic crack strength analysis (CSA) given in Equation (13) and the "modified" CSA method given by Equation (14) form the basis of the predictive methods of material fracture strength determination.

#### 4.1.3 Computational Procedure

As with any method of fracture analysis a "material constant" (in this case,  $C_m$  or  $C_m'$ ) must first be obtained from fracture tests of either one or more cracked specimens before any computations can be performed. This implies (from Equation (11)) that:

- a. Neuber's constant ( $\rho'$ ) must be known
- b. Both secant and Young's moduli are known.

Also, during specimen testing, the following must be observed:

- a. Crack buckling is suppressed
- b. Cracks of different aspect ratios are fractured
- c. Specimen length to width ratios are greater than 2:1
- d. Environmental and loading effects are properly introduced (e.g., temperature, load rate, etc.).

Once the above conditions are met a value of  $C_m$  or  $C_m'$  will be obtained and one may proceed with calculations of fracture stress as follows:

Calculate  $\lambda_w$  from the Dixon (Reference 15) relationships for crack aspect ratios of interest. For example, the finite width correction for the center cracked tension (CCT) geometry is

$$\lambda_w = \frac{\sqrt{1 - \frac{2a}{W}}}{\sqrt{1 + \frac{2a}{W}}} \quad (15)$$

The correction for edge cracked geometry is given in References 16, 17, or 20.

Calculate  $K_u$  from Equation (12).

Calculate  $\sigma_N$  from Equation (13) or (14) (depending on presence of notch strengthening).

Calculate gross area fracture strength  $\sigma_g$  from

$$\sigma_g = \sigma_N \frac{(W - 2a)}{W} \quad (16)$$



#### 4.1.4 Capability, Limitations and Possible Potential for the NSA (CSA) Method in Structural Residual Strength Determination

Since the NSA (CSA) method was primarily developed as a tool for material fracture strength determination (in the presence of a crack), its direct application to residual strength prediction for the general case of cracked structure appears remote. For those structures which are skin fracture critical and normally fail in an elastic manner, the NSA (CSA) method should provide suitable solutions. However, it is difficult to anticipate these conditions in service. Undue penalties and/or unconservatism can result if the NSA (CSA) method is applied to arbitrary structure due to the multitude of affecting parameters not included in the analysis (see e.g., Table I of Section III). For these reasons it is difficult to see a potential for the extension of this method into prediction of residual strength for typical aircraft structure. This is particularly true in light of the lack of corroborating data for these types of structural arrangements.

#### 4.2 EFFECTIVE WIDTH ANALYSIS METHOD

##### 4.2.1 Historical Development of Effective Width Analysis Method

In 1959, Crichlow presented what is referred to as an effective width method of residual strength prediction (Reference 21). Several residual strength problems were analyzed including cracked flat and curved unreinforced and reinforced panels under simple tension loading. In Reference 21 non-linear load-deflection characteristics of the attachments and material plastic yielding are treated using redundant analysis methods.

Crichlow and Wells in 1966 (Reference 22) analyzed both flat and curved reinforced panels. Also at that time they adopted the Kuhn (References 11, 13, 17, 18, and 20) notch strength approach for flat panel fracture prediction (see Equations 13 and 14). In References 23 and 24 Crichlow indicated that since both the effective width and NSA (CSA) methods contained material constants, and final design of fatigue sensitive areas is always based on experimental substantiation of the fracture strength for any given structure, the choice of methods (equations) was a matter of convenience and personal preference.

Thus, the effective width technique offered a means to empirically evaluate fracture strength and residual strength as long as material constants were determined. Correction factors were introduced to account for curvature, buckling, and several other parameters noted in Table I, Section III.

##### 4.2.2 Theory of Effective Width Method

The effective width technique for both residual strength and fracture strength determination is based on equilibrium of forces. Remote from the crack area the stress  $\sigma_g$  is uniform through the thickness and across the width and assumes the value  $\sigma_g = \sigma_c$  (the subscript c denoting critical condition) at the onset of fracture (see Figure 8). In the net section (see insert to Figure 8) the stress is not uniform and of course no load can be

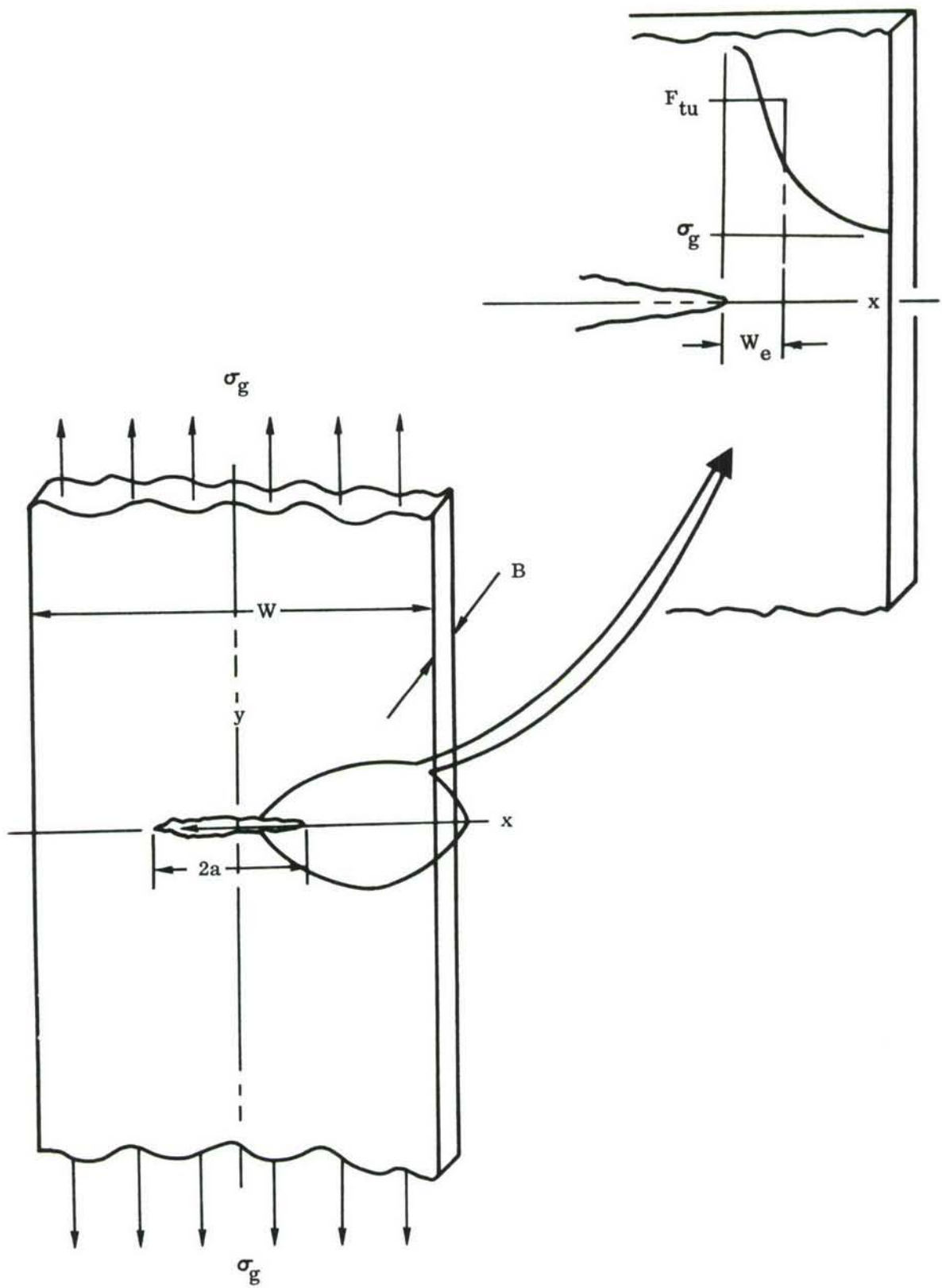


FIGURE 8 GEOMETRY FOR EFFECTIVE WIDTH ANALYSIS METHOD

carried across the cracked area. In the effective width concept that load which would be carried by the crack (if it were not there) is carried by the material adjacent to the crack tips. This load is defined as

$$P_{\text{CUT LOAD}} = 2 \sigma_g a B \quad (17)$$

In Equation (17),  $a$  is the crack half-length at fracture, i.e., it includes any slow tear which may have taken place. In particular the true stress distribution is approximated as being replaced by an effective width of material ( $W_e$ , Figure 8) stressed in the material ultimate strength. The remaining material is then considered stressed to  $\sigma_g$ . By equilibrium of forces,

$$\sigma_g = F_{tu} \frac{1}{1 + a/W_e} \quad (18)$$

From Equation (18), the fracture strength,  $\sigma_g$ , can be determined provided  $W_e$  can be evaluated.  $W_e$ , the material constant in the effective width method, is established experimentally from

$$W_e = \frac{a}{\left( \frac{F_{tu}}{\sigma_g} \right) - 1} \quad (19)$$

Obviously, Equations (18) and (19) express the identical relationship between the variables involved. This means that in order to make a prediction of the gross strength  $\sigma_g$  of a cracked structure, one must have available test data for an equivalent crack configuration from a simple panel fracture test. As with the data of Kuhn (Reference 17) finite boundaries were found to influence the values of  $W_e$  determined from Equation (19). To account for this behavior Crichlow (Reference 21) incorporated a correction for finite boundaries (from a best fit of the data) which contained two coefficients  $W_o$ , the effective width for an infinitely wide panel and  $W_1$ , a characteristic length established from best fits of fracture test data for various panel widths. The correction takes the form

$$W_e = W_o \tanh \left( \frac{W-2a}{W_1} \right) \quad (20)$$

where  $W$  and  $2a$  are defined in Figure 8. Observe that for  $W \rightarrow \infty$ ,

$\tanh \left( \frac{W-2a}{W_1} \right) \rightarrow 1$ , and  $W_e \rightarrow W_o$ . Substituting Expression (19) for  $W_o$ , one finds

$$W_e = \frac{a}{\left( \frac{F_{tu}}{\sigma_g} \right) - 1} \tanh \left( \frac{W-2a}{W_1} \right) \quad (21)$$



Equations (20 and (21) indicate that two material constants ( $W_o$  or  $\sigma_g$  and  $W_1$ ) must be determined from fracture tests on precracked panels in order to determine the effective width  $W_e$  of a finite width specimen. Substituting Equation (20) into Equation (18) yields the general formula of the effective width method for fracture strength of flat, unstiffened panels

$$\sigma_g = \sigma_c = \frac{F_{tu}}{1 + \frac{a}{W_o \tanh\left(\frac{W-2a}{W_1}\right)}} \quad (22)$$

As pointed out above, the crack lengths in this case are those at fracture, i.e., they include the increment due to slow tear (if present) for the material of interest.

In the effective width method originally proposed in Reference 21 and redefined in References 23 and 24, Crichlow established equilibrium equations based on the cut load being balanced by the reserve load remaining in the uncracked, adjacent structure for fail-safe operation. The equations were dependent on panel type and included a reduction in panel strength from material ultimate strength behavior. As defined, each panel type requires prior knowledge of the effective width ( $W_e$ ) which is a function of material type and test specimen geometry. To determine residual strength these equilibrium equations are then solved for residual strength,  $\sigma_c$ .

<u>PANEL TYPE</u>	<u>EQUILIBRIUM EQUATIONS</u>
Flat, unstiffened (Also see Equations 17 and 18)	$(2 \sigma_c a_c B) = (2 W_e B (F_{tu} - \sigma_c))$ (Cut Load) = (Residual Strength of Skin)
Flat, Stiffened	$(2 \sigma_c a_c B) = (2 W_e B + \Sigma A_e) (F_{tu} - \sigma_c)$ (Cut Load) = (Residual Strength of Skin and Stiffener)
Curved, Stiffened and internally pressurized	$(2 P_c a_c \text{ Radius}) = (2 W_e B + F_{tu} \Sigma A_e) \times \text{frame}$ $\left( F_{tu_{\text{skin}}} - \frac{P_c \text{ Radius}}{B} \right)$ (Cut Load) = (Residual Strength of Unbroken Elements)
	( $P_c$ = Critical Internal Pressure)
Planked or Spliced	$(\sigma_c W_m B_m) = \left( 2 W_e B_{\text{skin}} (F_{tu} - \sigma_c) \right)$ (Cut Load) = (Residual Strength of Adjacent Panels)

The subscript "m" denotes mid-panel conditions and the subscript "c" denotes critical conditions.

#### 4.2.3 Computational Procedure

Examples of the detailed procedures involved in using the effective width residual strength method are given in References 21 through 24 and will not be covered in this report. It will suffice to briefly outline the basic procedure. Any details must be examined in light of individual requirements for the particular type of structure of interest.

The basic procedure consists of the following steps:

Categorize the structure into flat stiffened, curved stiffened, etc.

Determine the associated material fracture strength from Equation (22) where the material constants  $W_0$  and  $W_1$  are found from simple panel fracture data - or - use the NSA or CSA method to determine fracture strength (e.g., see Reference 17).

Using the appropriate equilibrium equation (Reference 21) calculate the residual strength for the structure of interest (with a fixed crack geometry).

#### 4.2.4 Capability, Limitations and Possible Potential for the Effective Width Method in Structural Residual Strength Determination

Crichlow (Reference 21) originally proposed the effective width method as a structural analysis tool to predict residual strength. In this respect it is unique among the techniques reviewed. Correlation was made with residual strength data and an attempt was made to account for plastic material behavior.

Many of the parameters which affect structural residual strength as well as material fracture strength were accounted for in the proposed analysis (see e.g., Table I, Section III). Admittedly, most of the parameters were treated empirically, however this was acceptable practice at the time of its development. With the availability of newer structural analysis techniques (e.g., finite element methodology) and high speed computers, more accurate predictions can be made of local stress states with more complex loading arrangements. For example, the influence of skin attachment to substructure is known to have a definite influence on residual strength. These influences would be difficult to include in the equilibrium equations proposed in Reference 21 without extensive work. Hence other methods appear to offer greater potential for future applications.



#### 4.3 LINEAR ELASTIC FRACTURE MECHANICS METHODS

##### 4.3.1 Theory and Historical Development of Fracture Mechanics Methods

The basic theory and history behind fracture mechanics will not be discussed in detail here since many recent state-of-the-art-surveys have presented comprehensive reviews of linear elastic fracture mechanics as a material failure criterion (see e.g. References 5, 19, 25). Briefly, however, it should be noted that Griffith (References 26 and 27) was the first to provide a satisfactory solution to the problem of brittle fracture. He deduced an expression for the fracture stress of a brittle material containing a flaw. In an extension of Griffith's work, Irwin (Reference 28) found that a flawed material appeared to possess a critical strain energy release rate  $G_c$  such that, when the loading caused the associated value of  $G$  to reach  $G_c$ , the crack started to propagate. Irwin also showed that  $G$  could be related to  $K$ , the stress intensity factor, which is a measure of the local stress environment at the crack tip. Thus, the problem could be reduced to the determination of  $K$  for a case of interest and a subsequent comparison with a critical value of  $K$ , namely  $K_{Ic}$ . The approach is termed linear elastic fracture mechanics because even though a modest amount of plasticity is permitted, it is treated as a localized condition, and the problem is really one in elasticity. Hence, a number of elasticians have contributed solutions for  $K$  for a variety of loadings and geometries. The present report is concerned with the general tendency to use a fracture mechanics approach to analyze structure in combination with a critical stress intensity criterion. This necessitates some review in order to evaluate its potential.

In general the linear elastic fracture mechanics (LEFM) approach to structural analysis of fracture critical structure has taken several approaches. One is to provide closed form solutions for stress intensities of typical crack geometries and another is to employ finite element analyses to obtain crack tip stress intensities. In the former case, several solutions are available for riveted and integrally stiffened structural arrangements with through crack geometries in uniaxial tension (see e.g., References 29, 30, and 31). The second procedure has been reported in a series of documents, the latest being References 2 and 32 for representative aircraft structure. The value of crack tip stress intensity for the reinforced panel (found by either method) is compared to a critical value of stress intensity ( $K_{Ic}$ ) obtained by test of an unreinforced specimen. Thus a critical stress at failure is obtained and the possibility of crack arrest (at the reinforcements) can be evaluated.

##### 4.3.2 Capability, Limitations and Possible Potential for the Linear Elastic Fracture Mechanics Method in Structural Residual Strength Determination

For both the closed form and finite element approaches, knowledge of the so-called plane stress fracture toughness ( $K_{Ic}$ ) is required for the material



and thickness of interest. This presents a major difficulty since appropriate test procedures are not available in standardized form. Elastic fracture is assumed or else corrections are included in the stress intensity formulation to account for plasticity at the crack tip. Structural parameters such as crack buckling, nonlinear reinforcement behavior, unsymmetrical cracking, etc., are not included. In the closed form solutions those which apply to mechanically attached stiffeners assume rigid rivet or attachment behavior where it is known in reality (see e.g. Reference 2) that rivet shear loading in the presence of a skin crack causes rivet yielding. Subsequent load transfer becomes important to the fracture process, particularly when establishing whether the situation is a skin or stiffener critical structure. Although it may be possible using finite element procedures to obtain refined values of elastic stress intensity for a given problem, the values will lack meaning if plasticity at the crack tip or nonlinear behavior in adjacent structure becomes significant.

In comparing the virtues of closed form vis a vis finite element approaches, the former has the distinct advantage that questions of proper grid point spacing and associated inaccuracies do not arise. On the other hand numerical techniques, and particularly finite element approaches are widely applicable. Hence a much broader spectrum of potential problems can be considered.

The potential of current state-of-the-art, linear elastic fracture mechanics as a predictive method for plane stress fracture analysis should be considered good for those materials which exhibit little slow tear. If these conditions are not met (which is usually the case with common aircraft structural materials) then either modifications or extensions to existing techniques, or development of improved techniques is required. The use of finite element procedures as a tool in residual strength prediction will be discussed further in Section VI.

#### 4.4. SUMMARY

##### 4.4.1 Applicability of Existing Methods

In view of the discussion presented in this section, it should be apparent that all of the presently existing methods fall considerably short of the "ideal" method discussed in Section III. One of the stated properties of the "ideal" method is its applicability to a wide class of structural, residual strength problems. In contrast, the existing techniques for residual or fracture strength prediction are all confined to restrictive areas of application. The notch strength analysis method is the most limited, being applicable only to unreinforced structure. The effective width technique can be applied to more types of structural arrangements (e.g., unreinforced curved panels, reinforced flat panels, and reinforced curved panels) than the notch strength method. However, the application of the method requires the establishment of the numerical values of empirical constants for the particular crack geometry. More significantly, the predictions of residual strength made by the effective width technique are (as currently presented, see e.g., Reference 23) based on measurement of reinforcement efficiency. The efficiency is a function of means of attachment, thickness of skin and width of reinforcement spacing and must be experimentally validated.



Rather than specifically treating reinforcement geometry, the effective width technique recognizes the stiffener moment of inertia, stiffener area and stiffener centroidal distance from the skin plane as being important.

The linear elastic fracture mechanics methods have the general characteristic that the theoretical base is considerably more rigorous than the other two methods discussed. The use of finite element techniques as illustrated, for example, in Reference 2, allows a wide range of structural parameters to be adequately treated (within the context of linear elastic fracture mechanics). Actual reinforcement shapes and attachment details can be recognized. In the LEFM approach, plasticity can be accounted for in several ways, although in applications of LEFM to the prediction of the residual strength of thin skin structures (e.g., References 2 and 32), plasticity has not as yet, been treated. The potential for including plasticity in a meaningful way exists. Hayes (Reference 5) shows how the Dugdale (Reference 33) plastic zone model can be treated in a convenient way. He also indicates how materials displaying Prandtl-Reuss plasticity can be treated, following a procedure given by Swedlow (Reference 34). In Section VI of this report, these plastic zone models will be discussed in considerable detail.

This technique begins to approach the desired characteristics of the "ideal" method with regard to structural parameters as listed in Table I (Section III).

#### 4.4.2 Treatment of Material Parameters

The currently available methods of residual strength prediction are perhaps farther removed from the requirements of the "ideal" method in the treatment of material parameters than in any other area. The current methods are particularly deficient in the treatment of plasticity in cracked structures. For materials in which plasticity is of a limited nature (i.e., for brittle or semi-brittle materials which have a propensity toward plane strain failures) residual strength predictions based on the existing methods may be satisfactory. However, when extensive plasticity or slow crack extension prior to fracture exists, all the existing methods break down. The notch strength method attempts to handle plasticity by modifying the Neuber factor as shown in Equation (3). The modification is based on values of the secant modulus. The effective width technique does not specifically recognize plasticity. Whatever plasticity exists in a given case shows up by virtue of the values of the constants  $W_0$  or  $\sigma_g$  and  $W_1$  found by using Equations (20) or (21) in conjunction with test results. Obviously, any subtleties in the plastic behavior are completely masked over in both the NSA, CSA, and effective width approaches.

Plasticity in a cracked structure is not limited to the crack tip vicinity. Reinforcement yielding is also a distinct possibility, although it has not been considered to date.

The remaining material parameters listed in Table I are largely untouched by existing methods. Slow tear, or stable crack extension, is an important consideration in plane stress and mixed mode fracture. Distinct possibilities exist for including this in predictive techniques in the future (see Section 5.5.1 and Section VI). To some extent, slow tear behavior has been considered in Reference 32.

## V DEMONSTRATION OF CAPABILITIES FOR RESIDUAL STRENGTH PREDICTION

To indicate the complexity of the requirements for structural residual strength prediction the problem has been separated into three distinct areas:

- (1) unreinforced structure (plain sheets)
- (2) simple reinforced structure (e.g., flat panels with geometrically simple stiffeners - straps or Z sections - attached by means of a single line of rivets or bonded)
- (3) complex reinforced structure (substantial substructure, curved panels, multiple rivet lines, etc.).

The bulk of experimental work conducted to date has been performed on simple, unreinforced panels. Principally, the aim has been to verify a fracture criterion or criteria. The test results are then utilized to establish certain empirical factors required in the analyses (as described in Section IV).

The "ideal" method would necessarily include the ability to analyze all three geometric complexities listed above within its framework. No method currently available will provide solutions to all three areas of increasing complexity.

The purpose of this program is to increase the confidence in and improve the accuracy of plane stress residual strength predictions for structural elements, as noted in Section III. By examining the predictions of residual strength by the various methods and subsequently correlating them with existing data for simple structural elements, an indication of the accuracy of each method can be ascertained. Each structural category listed above and method will be examined in turn from the standpoint of agreement between predictions and test results.

Prior to the analytical/experimental correlation activity, an examination of fracture and residual strength data for repeatability will be undertaken. This will reveal to what extent any particular method under consideration must comply with experimental results to achieve a desired degree of accuracy. An examination of those parameters which tend to introduce errors into residual strength prediction due to their effect on measured strength (e.g., strain rate, crack tip buckling, specimen dependency, etc.) will be presented. Possible means of incorporating these effects into a developed method will also be discussed.



## 5.1 SIMPLE UNREINFORCED PANELS

### 5.1.1 Fracture Strength Repeatability

Several investigators have, during the course of their fracture strength studies, examined the correlation between predicted strengths (usually based on their failure criterion) and measured values. Kuhn (Reference 18) compared the Notch Strength Analysis (NSA) and linear elastic fracture mechanics (LEFM-modified to account for crack tip plasticity) predictions with an independent set of fracture data. In spite of limitations present in both methods, the correlations between measured and predicted values were within  $\pm 15\%$  for aluminum alloy data for both methods.

Liu (Reference 35), examining a quantity of aluminum, steel, and titanium fracture toughness data (both  $K_{Ic}$  and  $K_{Ic}$ ) from several sources and several specimen types, concluded that a two parameter log-normal distribution function would provide a satisfactory fit for both plane strain and plane stress data. In essence, his results imply that statistical distribution functions commonly used to fit material property data (e.g.,  $F_{tu}$ ,  $F_{ty}$ , etc.) are also applicable for fitting toughness data.

There is a tendency for greater variation in the measured values of plane stress fracture toughness than in values of plane strain fracture toughness. Partial responsibility for these variations can be placed on the lack of standards for fracture testing of materials which fail in modes other than plane strain. Also, experimental difficulties such as inability to determine the extent of slow tear accurately tend to increase variability in data.

An independent source of fracture data (Vlieger--Reference 32) has been examined to determine the extent of variability of measured stresses and crack lengths. These data are unique in that both unreinforced and reinforced panels were fabricated from the same lot of material and subsequently fracture tested. Vlieger then used the unreinforced panel fracture strength data to predict the fracture stress for simple reinforced panels using his residual strength model.

Figure 9 schematically indicates the stress or load versus crack growth relationship for a simple center cracked tension specimen. For an initial crack size,  $2a_0$ , no increase in crack length is observed in a rising load test until point A is reached. At the associated crack initiation stress,  $\sigma_i$  the crack extension process proceeds with small increase in load or stress. The initiation stress is difficult to determine in a rising load test since both the load and crack must be observed at the same time. Often this process is photographically recorded and presents difficulty in interpreting data. The plastic zone at the crack tip tends to mask the small crack extension which takes place at point A.

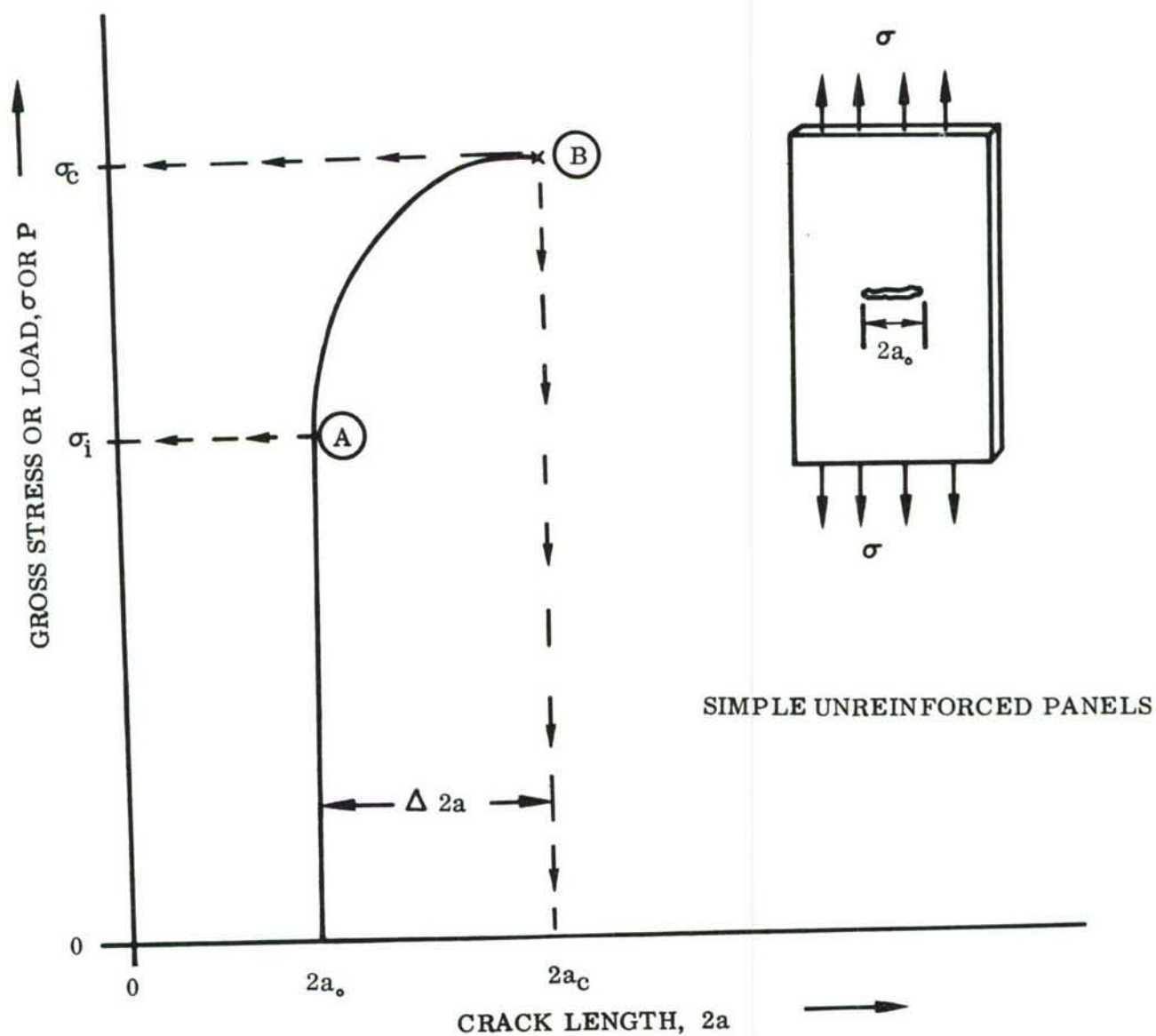


FIGURE 9 SCHEMATIC OF THE FRACTURE PROCESS IN PLANE STRESS WITH ACCOMPANYING SLOW TEAR



Under the increasing load or stress (Figure 9) slow crack extension (slow tear) takes place along the path AB. A corresponding increment of crack extension,  $\Delta 2a$  (the slow tear) occurs along the path AB and critical (fracture conditions prevail as  $2a \rightarrow 2a_c$  and  $\sigma \rightarrow \sigma_c$  at point B. Along the path AB crack acceleration takes place, and even with high speed motion pictures the critical crack size,  $2a_c$  is difficult to obtain with accuracy. Compliance methods in conjunction with photographic recording can reduce some of the error in interpreting initiation of slow tear. However, the corresponding fracture load or stress can be determined quite readily from the load cell indicator since it is normally the maximum stress in the fracture process for a rising load fracture test.

To indicate the variability in fracture data, the unreinforced panel data of Reference 32 have been compared on the basis of stress to initiate slow crack growth ( $\sigma_i$ ) and critical fracture stress ( $\sigma_c$ ). In order to remove some of the difficulty in interpreting crack length, particularly for the critical case, the data of Reference 32 is analyzed on initial crack size,  $2a_o$ .

Figure 10(a) shows these data from a 7075-T6 aluminum alloy for initial slow tear and Figure 10(b) for critical conditions in 12-inch wide center cracked tension specimens. As Vlieger's data were taken under controlled and well established procedures, and the crack extension variability has been removed by using the initial crack length, these data (Figure 10) provide an indication of initiation and fracture stress variations.

The spread in initiation stress at beginning of slow tear,  $\sigma_i$  (Figure 10(a)) can be seen to encompass a  $\pm 10\%$  variation from an average curve drawn through the data. This spread is caused by the previously discussed inability to accurately determine the initiation point of slow tear (Figure 9, point A), and in particular the associated load or stress. Using the stress at fracture as a parameter (for these data the stress at maximum load) the variation between duplicate specimens is reduced considerably as shown in Figure 10(b). In fact the largest variation in stress at fracture, for duplicate tests at a fixed initial crack size is 2.5 ksi. The corresponding stress at initiation of slow tear (Figure 10(a)) is double this value.

For comparative purposes McCabe (Reference 36), reporting on a plane strain fracture toughness test series round robin, indicates that for a given material all values of  $K_{Ic}$  (using a tentative standard test method) were within  $\pm 10\%$  of a grand mean  $K_{Ic}$  value.

#### 5.1.2 Impact of Material Fracture Variability on Selected Criterion and Analysis Method

If a variation of 10% or less can be anticipated in measured values of  $K_{Ic}$  (Reference 36) and 5% for fracture stress of a semi-brittle material (Reference 32), it follows that the selected criterion will probably contain fracture data within a 5% to 10% scatter band. This is not thought to be an unreasonable spread when one considers lot to lot variations in the usual material properties such as  $F_{tu}$ ,  $F_{ty}$ , etc. Keeping this anticipated variation in mind, the goal for accuracy of both the failure criterion or criteria which will be employed and the analysis method should be within the same domain of accuracy, i.e.,  $\pm 10\%$ .



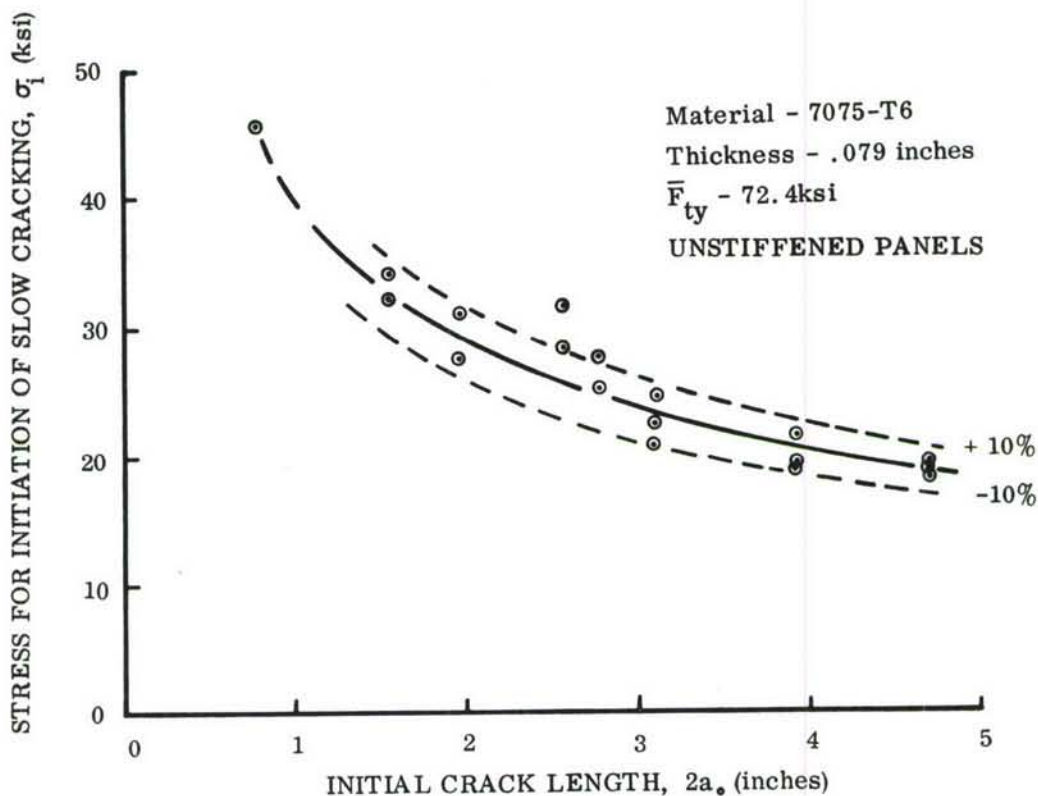


FIGURE 10(a) REFERENCE 32 FRACTURE DATA - STRESS AT INITIATION OF SLOW TEAR VERSUS INITIAL CRACK SIZE

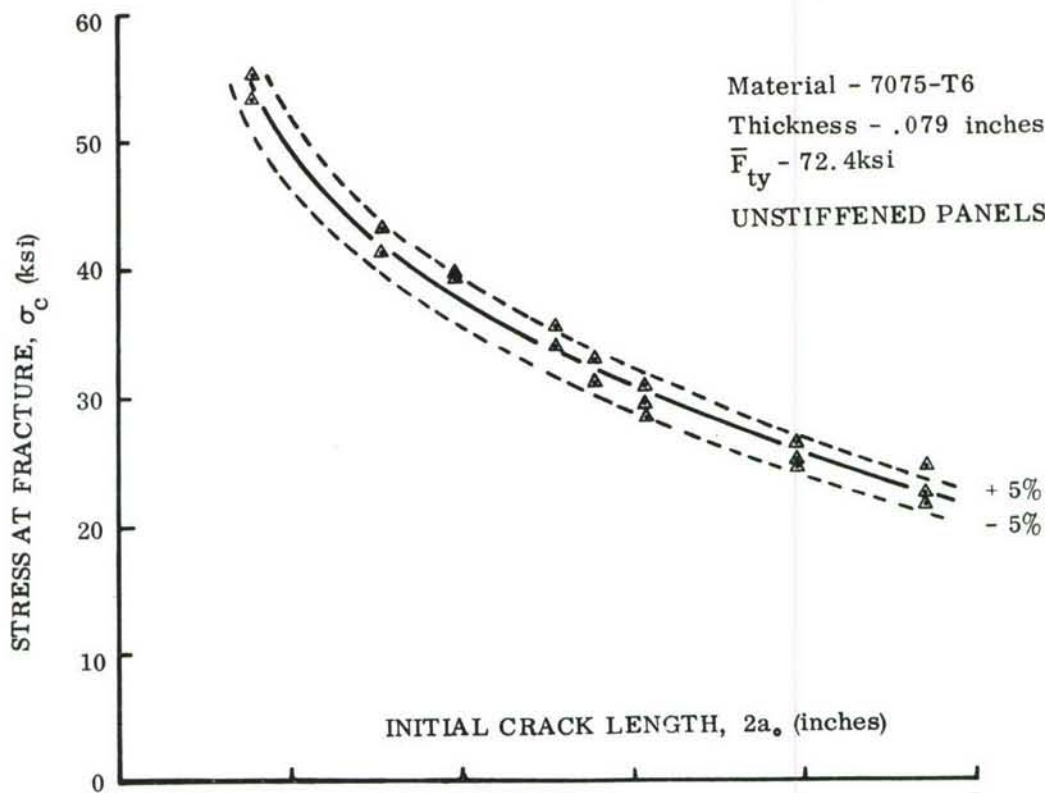


FIGURE 10(b) REFERENCE 32 FRACTURE DATA - CRITICAL STRESS VERSUS INITIAL CRACK SIZE

In this regard it is important to remember that the plotting of these data was based on original crack size. Except for a rare case most of the materials fracturing in plane stress will exhibit varying amounts of slow tear. Although using the original crack size will provide greater accuracy, for many aircraft applications it becomes necessary to have knowledge of both the initial and critical crack sizes. For these cases the crack growth resistance curve (see section 5.5.1) appears promising.

It follows from the discussion of experimental accuracy that the developed method of analysis should strive for a similar degree of accuracy. This point becomes clearer when the various parameters which can affect the fracture process are considered (i.e., Table I)

In summary the developed analysis method should, within reason, be able to match the experimental results within 10%. For those materials which exhibit large amounts of slow tear the crack growth resistance concept appears most promising to determine critical crack size.

In the next sub-section the simple reinforced panel geometries (i.e., the next step in increasing panel complexity) of Reference 32 will be examined for experimental repeatability.

## 5.2 SIMPLE REINFORCED PANELS

### 5.2.1 Residual Strength Repeatability

In a simple, cracked, reinforced panel (skin with attached reinforcement) the fracture process shown in Figure 9 is essentially unchanged with this exception: the amount of slow tear and the magnitude of the crack tip stress environment can be altered by the position of the reinforcements relative to the crack. To illustrate this behavior Figure 11 schematically shows the crack growth versus gross stress or load for two possible crack configurations in simple reinforced panels. (Note that the dashed curve is displaced to the right for reasons of clarity. As shown  $a_1 = a_2$  and the vertical portions of the curves coincide.) Neglecting the reinforcement planform and the method of attachment for the moment, the crack at a reinforcement (Figure 11, case number 1, curve ABC), and between reinforcements, case number 2 (DEF) are both possible in service.

Consider first case number 1, the crack at a reinforcement. Starting with a crack of half length  $a_1$ , the crack will (as in the unreinforced panel case, Figure 9) remain stable up to some load or stress A at which time slow crack extension commences. In case 1 the initiation stress will be influenced by the reinforcement at the panel centerline. Slow tear will commence and take place at higher stresses than for the unreinforced case, and the magnitudes will be directly dependent on the load transfer to the intact stringer bridging the crack. For case 2 (Figure 11) slow tear will occur at the same stress as for the unreinforced panel case. That is, the stress at A, Figure 9 is equal to the stress at D, Figure 11 for panels of the same thickness and material and having equal crack lengths. Assuming that the initial crack sizes are equal (i.e.,  $a_1 = a_2$ ) it will be noticed that the stress at D is lower than at A due to the absence of the panel centerline stringer. The stress at A and D (Figure 11) can also be affected by inplane panel buckling which will be discussed in section 5.5.2. The bridging

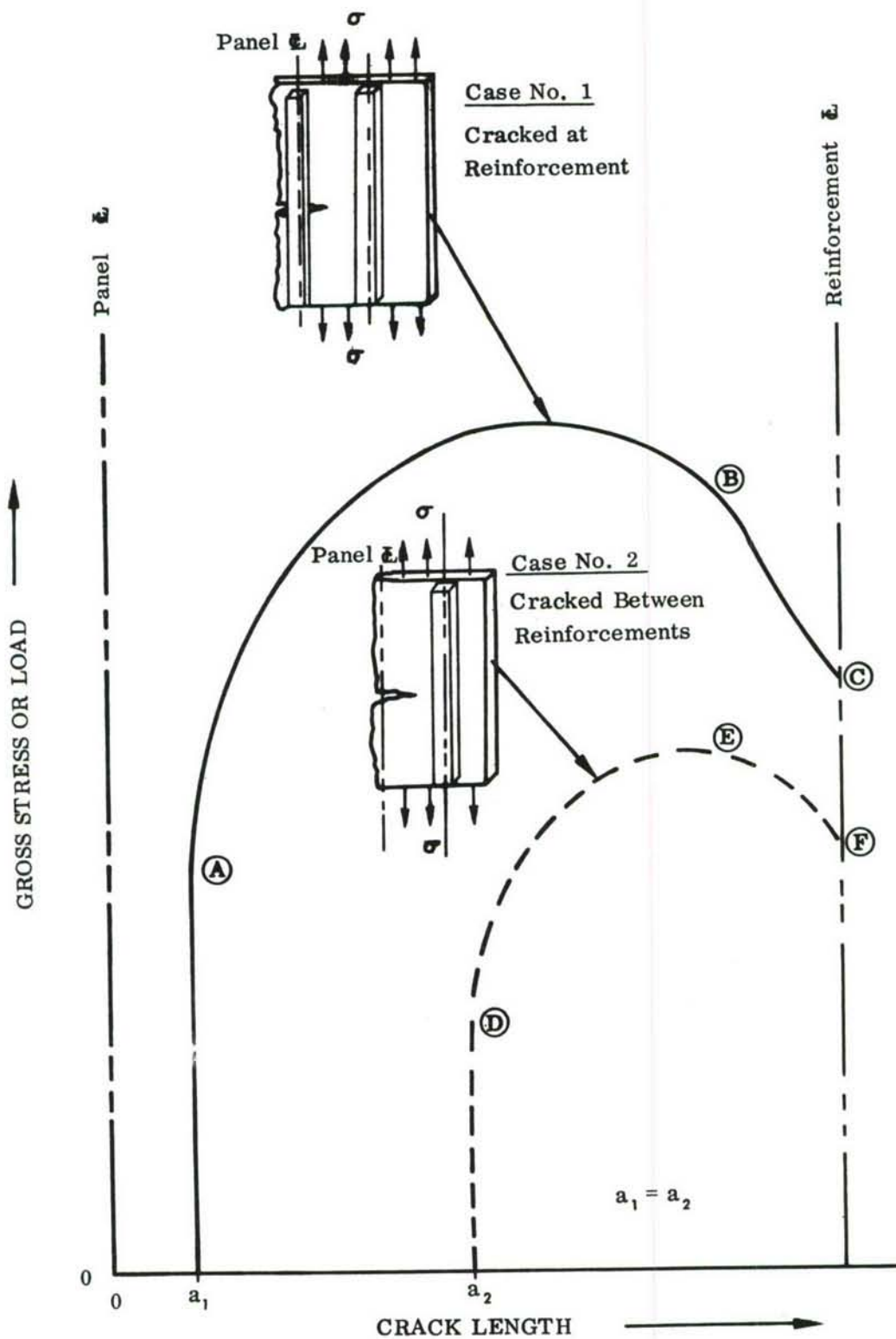


FIGURE 11. SCHEMATIC OF FRACTURE PROCESS FOR SIMPLE REINFORCED PANELS



action will minimize such buckling in case number 1 as long as the reinforcement remains intact. Other factors which will affect the crack initiation stress are crack size and position of the crack tip in relation to the nearest reinforcement, as well as environment, loading rate, etc. (see section 5.5). For the simple cases of Figure 11 an increase in load or stress will cause increasing slow tear up to some maximum stress followed by an instability and crack extension under decreasing stress conditions (i.e., crack extension could be maintained at lower loads), as indicated by points B and E. Once the crack reaches the vicinity of the outer reinforcement, the reinforcement will pick up the stress caused by the redistribution due to the presence of the crack. The degree to which this redistribution is accepted by the reinforcement depends on many factors such as method of attachment, contact area, stiffness of the reinforcement, etc. (again neglecting environmental factors).

The stress difference between case 1, point C and case 2, point F is caused by the panel centerline stringer picking up some of the overall panel load in case 1. Once this stringer fails, dynamic (short duration) stresses of unknown magnitude will occur in the panel and normally cause overloads to the remaining structure. In such cases the efficiency of the near reinforcement in containing the crack is evaluated by the familiar fail safe test of fuselage shells punctured under load. It becomes obvious that the role of the reinforcement becomes quite important in residual strength and both a skin and reinforcement critical criterion may be required in residual strength analysis development.

Vlieger (Reference 32) examined two types of riveted reinforcement (flat strap and Z stiffened) with crack geometries situated between straps and between and under the Z sections for flat panels in tension loading. The repeatability of these data was compared in a manner similar to the unreinforced panel data (Figure 10). These data contain reinforcement influences on the slow crack growth initiation stress for the crack at Z section panels (case 1), and critical fracture stress for the crack between reinforcement (case 2) panels. To make a fair comparison with the unreinforced panel data the initiation stress at the start of slow tear was used for both the riveted, flat strap and riveted Z stiffened panels. Figure 12 shows the stiffened panel data and the dashed curves indicate the  $\pm 10\%$  data spread of Figure 10(a) for the unstiffened panels. It is obvious that the majority of the stiffened panel data fall within the scatter band of the unreinforced panels. It is encouraging to note that the reinforced panel data is so repeatable at replicated initial crack lengths. In fact, the variability is markedly less than the unstiffened panel data. The same narrow scatter is found in the critical fracture stress (residual strength) of the reinforced panels of Reference 32. Replicated tests of reinforced panels gave repeatability within 5 ksi.

It should be noted that the material used in Reference 32 (7075-T6) is considered one of the more frangible alloys (e.g., see Reference 37). For such a material, crack growth under rising load conditions takes place with little corresponding acceleration in crack growth at constant load as would occur with a tougher aluminum alloy such as 2024-T3. (Note that all stresses are considerably below  $\bar{F}_{ty}$ .) For this reason the fracture and residual strength data of Reference 32 would be expected to show good repeatability. Since it is desired to set some limits on the accuracy of the residual strength analysis method to be developed it would appear that a  $\pm 10\%$  accuracy may

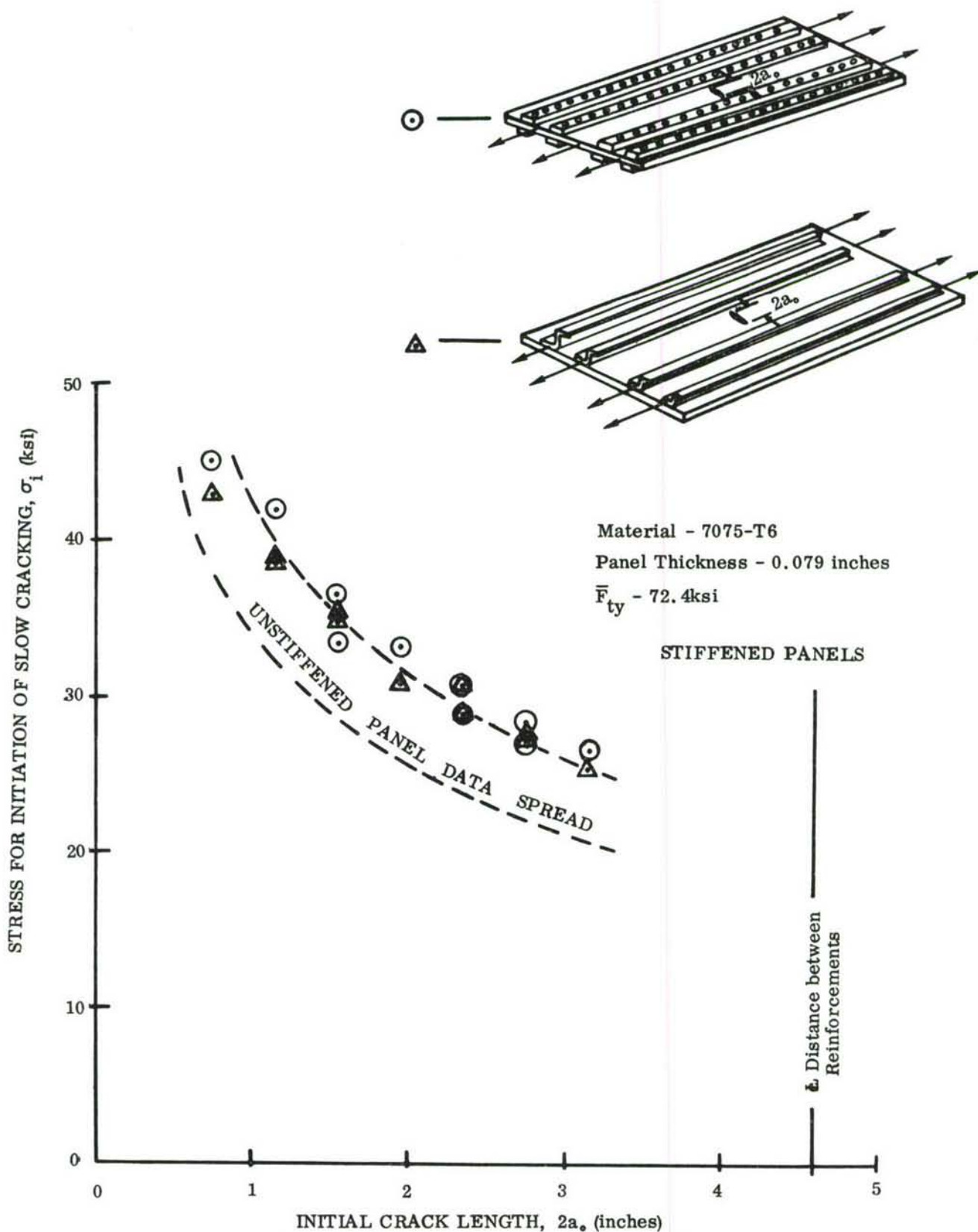


FIGURE 12 REFERENCE 32 FRACTURE DATA-STRESS AT INITIATION OF SLOW TEAR vs INITIAL CRACK SIZE



be acceptable based on residual strength data discussed above. As a preliminary assessment, residual strength predictions will be made in the next subsection using the methods described in Section IV.

### 5.3 RESIDUAL STRENGTH PREDICTIONS FOR SIMPLE REINFORCED PANELS

The method of Crichlow (Reference 24), which for short crack lengths (in relation to reinforcement spacing) is currently analogous to Kuhn's method (see Reference 17), has been employed in section 5.3.2 to analyze residual strength data presented by Vlieger (Reference 32) on simple reinforced, 7075-T6 panels. Also, comparisons have been made in section 5.3.1 using LEFM. In particular, the closed form solution of Poe (Reference 31) has been used. The failure criteria utilized were the critical Neuber notch factor  $\rho'$  for the Kuhn method, whereas the Poe method used the  $K_c$  approach of LEFM.

It will be noticed that the basic assumptions of each method require that the actual panel geometry be somewhat idealized. This is due to the simplified nature of the methods. For the purposes of the present evaluation study, however, it is believed that a fair comparison can be made.

#### 5.3.1 Poe's Method with $K_c$ of LEFM as a Failure Criterion

5.3.1.1. Assumptions In using Poe's method the following is assumed:

- . in-plane loading only
- . rigid rivets
- . rivet force transverse to applied stress neglected
- . stiffener possesses axial stiffness only.

The fact that Poe's method neglects the bending stiffness of the reinforcement means that it should rigorously be applied only to reinforcements which are symmetrically placed about the sheet midplane (that is, to situations in which no bending takes place, and hence the neglect of bending stiffness is inconsequential). However, Poe's method can also be applied without significant error to cases in which the stiffener axial stiffness greatly predominates over the stiffener bending stiffness. For example, a configuration involving stiffeners which are flat rectangular straps is one for which the neglect of bending stiffness is not a serious omission. When stiffeners are considered which have the typical structural shapes (e.g., hats, Z's, channels, etc.), the use of Poe's method is not advisable since bending stiffness may then constitute a significant parameter in the problem.



Notwithstanding the above, the Poe approach will be used to analyze Z stiffened stringers as indicated below.

5.3.1.2. Procedure The percent stiffening (nondimensional stiffness) for Vlieger's Z stiffened panels is, using a relationship from Poe (Reference 31)

$$\text{Percent Stiffening} = \frac{100}{1 + \left[ \frac{sBE}{wt_s E_s} \right]} \quad (23)$$

where  $t_s$  is the stringer or reinforcement thickness,  $w$  is the effective stringer width, and  $E_s$  is reinforcement modulus.

The thickness of the riveted skin,  $B$ , the reinforcement spacing,  $s$ , and the modulus of skin ( $E$ ) and stringer ( $E_s$ ) are given in Reference 32. Using these data, Equation (23) becomes,

$$\text{Percent Stiffening} = \frac{100}{1 + \left[ \frac{2.3'' (0.079'') 10^7 \text{ psi}}{0.87'' (0.063'') 10^7 \text{ psi}} \right]} \approx 23\%$$

For this percentage stiffening, the ratio of panel stress intensity with reinforcement to stress intensity without reinforcement,  $\lambda$ , is given below for the crack geometries of cases 1 and 2 of Figure 11.

Ratio of Half-Crack Length to Z Stringer Spacing, $a/s$	Case 1 $\lambda_1$	Case 2* $\lambda_2$
0.1	0.965	0.99
0.2	0.92	0.98
0.3	0.85	0.965
0.4	0.84	0.945
0.5	0.83	0.91
0.6	0.82	0.87
0.7	0.80	0.85
0.8	0.78	0.825
0.9	0.755	0.80
1.0 Cracked from Stringer to Stringer Centerline	0.70	0.79
1.2	0.62	0.765
1.4	0.61	0.74
1.5	0.61	0.71

\* In Reference 31, symmetry is assumed for both crack and reinforcements about the panel centerline. Also, simple reinforcement geometry (i.e., flat straps) are assumed to exist. In the Reference 32, Z stiffened data, these conditions are not met, particularly in Case 2 where the centerline stringer is missing. Therefore the use of the Reference 31 analysis is questionable in this case, and good correlation is not expected. However, some indication of anticipated residual strength trends should be indicated, with predicted results being higher than measured strengths.

From Reference 38 an average value of plane stress fracture toughness for 0.079 inch thick 7075-T6 aluminum is given as

$$\bar{K}_c = 70 \text{ ksi} \sqrt{\text{inch}}$$

The following fracture criterion is employed to predict residual strength for the Case 1 and Case 2 panels.

$$\bar{K}_c = \sigma_{c_{1,2}} \sqrt{\pi a_c} \lambda_{1,2} \quad (24)$$

Solving Equation 24 for average critical gross area panel residual strength ( $\bar{\sigma}_c$ )

$$\bar{\sigma}_{c_{1,2}} = \frac{\bar{K}_c}{\sqrt{\pi a_c} \lambda_{1,2}}$$

For assumed values of critical crack length,  $a_c$ , the computed curves are shown in Figures 13(a) and 13(b) for the two crack cases indicated. Note that some cracks ran to, and some ran between, the rivet holes in the nearest stringer after the fracture initiated. For both panel types (Cases 1 and 2), the prediction is higher at the longer crack lengths than the actual failure stresses. This is expected due to the assumptions listed in section 5.3.1.1 (inherent in the Poe analysis) which lead to higher predicted stresses for Z section stiffened panels than actually observed. It would be expected that the data would fall below the predictions due to reinforcement eccentricity and subsequent superimposed panel bending which are not a part of the Reference 31 analysis.

In light of the basic assumptions cited in section 5.3.1.1, and the anticipated restrictions mentioned previously, the correlations of Figure 13 are considered quite good. The experimental results for the Case 1 panels show the same trends as the Poe analysis and confirm the analytical trend predicted by Vlieger in his report (Reference 32).

One can thus conclude that even though the assumptions of the Poe analysis (zero bending, rigid attachments, etc.) were violated, good correlation (within 10%) was obtained. However, the predictions were on the high side, and would lead to optimistic values of residual strength. Considering the material and its fracture characteristics, a more advanced method of analysis is warranted to include those factors not considered in closed form solutions such as Reference 31.

### 5.3.2 Kuhn Method with NSA as a Failure Criterion

Since the ratio of initial crack length to reinforcement spacing for the Reference 32 data is  $\leq 0.7$ , and since the Crichlow analysis permits crack lengths as large as the reinforcement spacing (see e.g., References 21 and 24) to be considered, it becomes a matter of choice (for the shorter crack lengths)

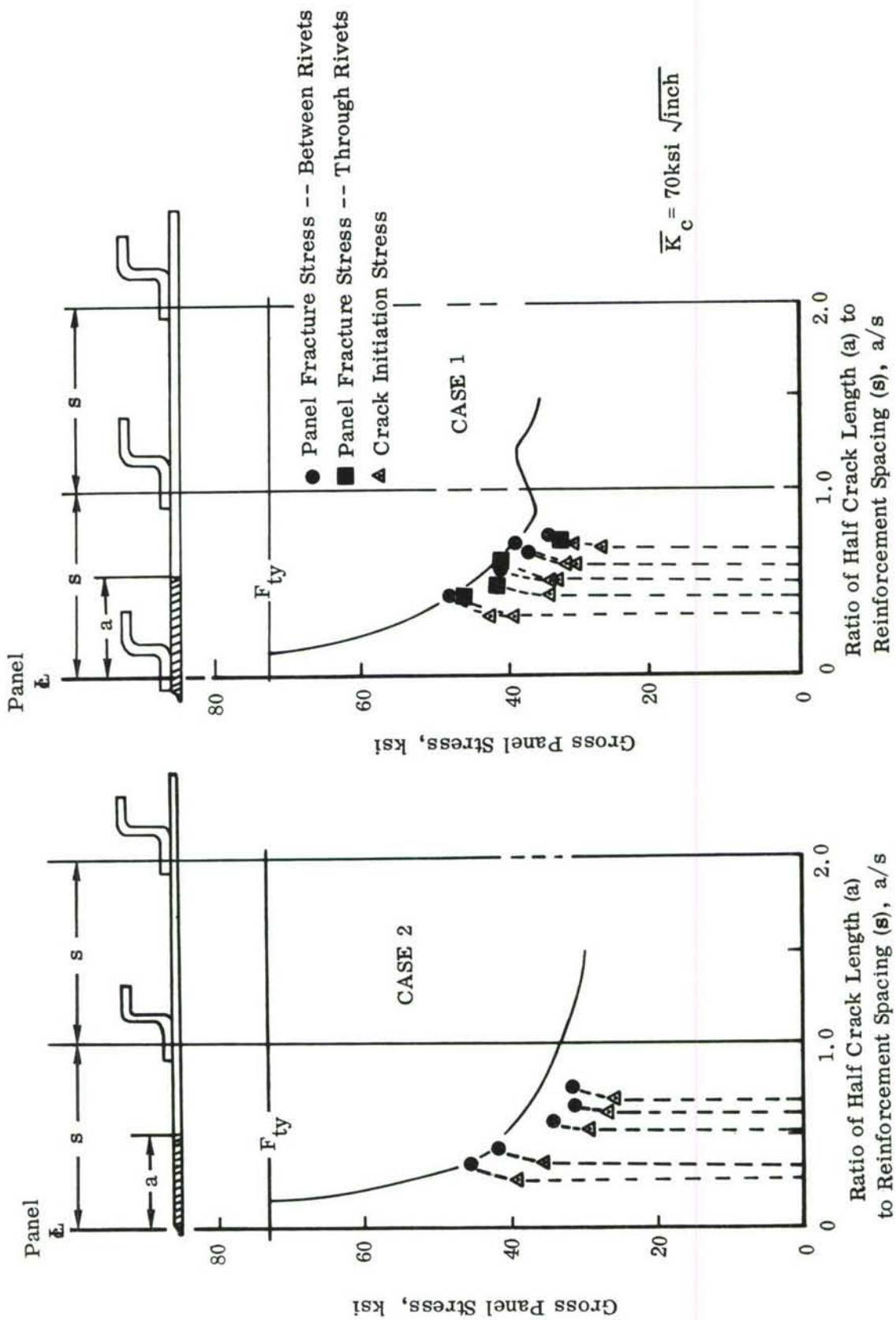


FIGURE 13(b) RESIDUAL STRENGTH FOR REF. 32 DATA USING REF. 31 METHOD OF ANALYSIS AND  $K_c$  FRACTURE CRITERION

FIGURE 13(a) RESIDUAL STRENGTH FOR REF. 32 DATA USING REF. 31 METHOD OF ANALYSIS AND  $K_c$  FRACTURE CRITERION



as to whether an effective width or a notch strength analysis should be used to predict residual strength. The NSA method (see Section 4.1) has been selected here for demonstration purposes. In using the NSA method for residual strength prediction, it should be kept in mind that its basic foundation is in the prediction of fracture strength for unreinforced panels.

#### 5.3.2.1. Assumptions

The critical crack length ( $a_c$ ) is less than the stringer or reinforcement spacing. (The data of Reference 32 is within this range, see e.g., Figure 13.)

Other assumptions as indicated in section 4.1.1.

#### 5.3.2.2. Procedure

From References 17 or 24, the residual strength  $\bar{\sigma}_g$  of a reinforced panel is,

$$\bar{\sigma}_g = \bar{\sigma}_c = \frac{F_{tu} \left[ 1 - \left( \frac{2a_o}{W} \right) \right]}{1 + C_m \left( \frac{1 - \frac{2a_o}{W}}{1 + \frac{2a_o}{W}} \right) \sqrt{a_o}} \quad [a_o < s] \quad (25)$$

observe that Equation (25) follows from Equations (11), (13), (15), and (16).

In Equation (25), the following material property data apply (from Reference 32):

$F_{tu}$ , ultimate strength = 78.6 ksi (case 1)

$F_{tu}$ , ultimate strength = 79.3 ksi (case 2)

$C_m \approx 1.4\sqrt{\text{inch}}$  (from Reference 17, at room temperature)

For the Z stiffened panels of Reference 32 it becomes a difficult task to select a value of panel width to use in Equation (25) for computational purposes.

The Kuhn equation can be rewritten for this case assuming infinite panel width as an approximation. Then Equation (25) becomes

$$\sigma_c = \frac{F_{tu}}{1 + 1.4\sqrt{a_o}}$$

for Vlieger's case 2 panels.

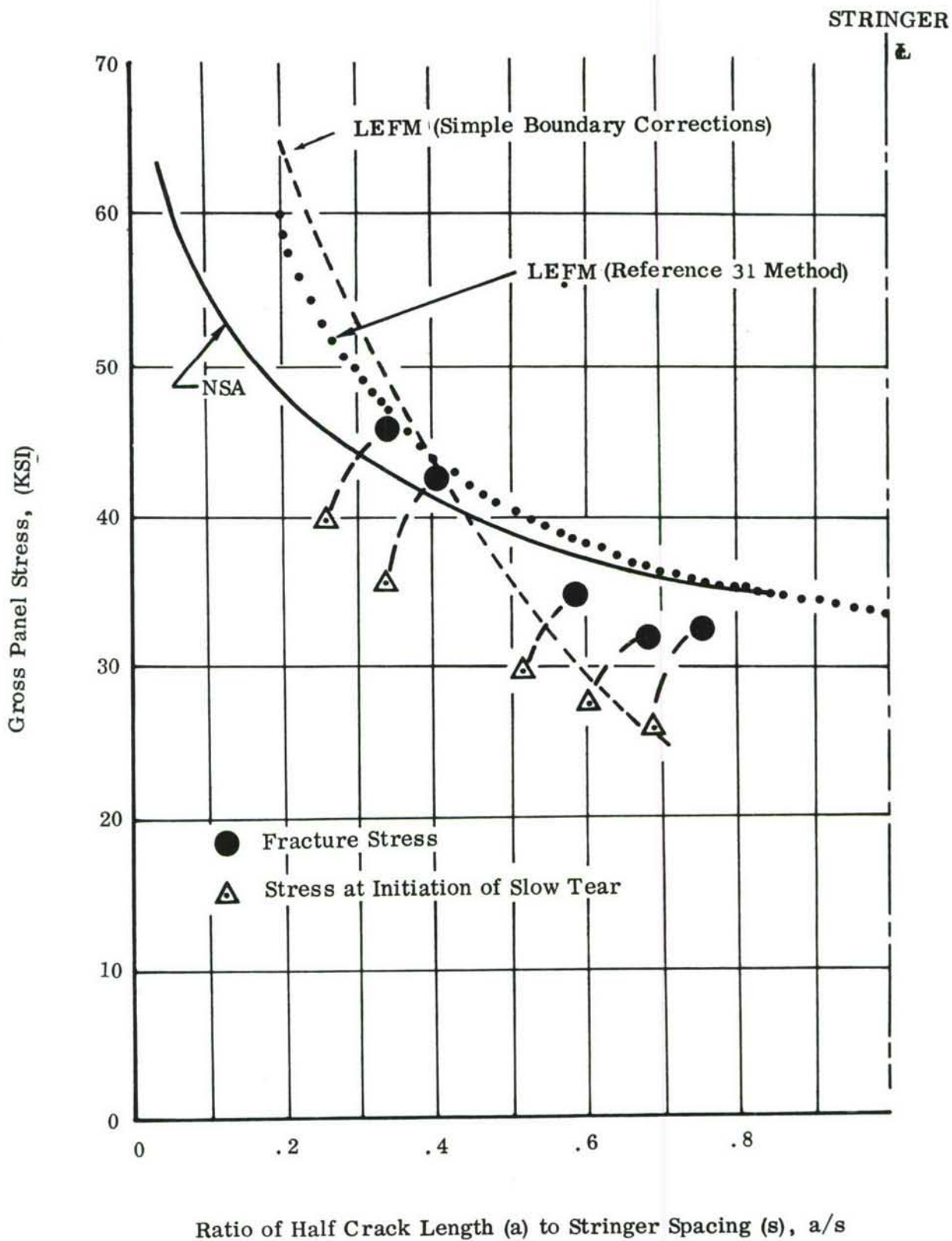


FIGURE 14 KUHN ANALYSIS METHOD USING NSA FRACTURE CRITERION COMPARED TO LEFM METHODS AND  $K_c$  CRITERION - CASE 2 PANELS

The predicted curve is shown as the solid curve in Figure 14 for the case 2 panels. Also shown is the section 5.3.1 prediction (dotted curve) obtained using LEFM. For comparative purposes, the "classical" LEFM curve (dashed) is shown assuming an effective panel width of twice the reinforcement spacing (i.e., double the width between Z stringers for case 2 panels). Computations were carried out using a nominal  $\bar{K}_c$  of 70 ksi  $\sqrt{\text{inch}}$  and finite width corrections ( $\lambda$ ) from Reference 39 for center cracked tension panels. Thus the "classical" LEFM predictions were made according to

$$\bar{\sigma}_c = \frac{\bar{K}_c}{\sqrt{\pi a_c} \lambda} \quad (26)$$

The computed NSA curve (solid) of Figure 14 would generally provide an optimistic value of fracture stress whereas LEFM underpredicts fracture stress for longer crack lengths.

It is obvious that the NSA curve has the proper trend. Unfortunately this analysis can only treat cases where critical crack size is much less than the stringer spacing. Thus a gap exists in the residual strength curve between a/s ratios of  $\sim .8$  and 1. As noted previously the "classical" LEFM (with simple boundary corrections) method does not correlate well. However its use with the Poe analysis is considered good, although all methods tend to overpredict residual strength.

#### 5.4 RESIDUAL STRENGTH PREDICTIONS FOR PANELS OF COMPLEX GEOMETRY

The current state-of-the-art of residual strength prediction for complex structure has been summarized in a recent series of research reports (for example see References 2, 40, 41, and 42). It must be noted that the failure criterion is normally fracture mechanics oriented and the analysis method involves finite element techniques, particularly for the more complex structure (such as skin, frame, and longeron and various combinations) and the associated complex loading conditions. Closed form solutions such as presented in References 29 through 31 will have little success in predicting the residual strength of complex stiffened panels.

The degree of accuracy for the prediction of residual strength can be quite good for skin materials which exhibit small amounts of slow tear and are skin fracture critical (Reference 2). Once extensive amounts of crack tip plasticity, reinforcement and/or attachment yielding, and other factors (to be discussed in Section 5.5) occur, the current methods tend to break down. Suggestions as to possible ways of treating these effects are discussed in Section VI.



## 5.5 PARAMETRIC INFLUENCES AND THEIR EFFECT ON RESIDUAL STRENGTH PREDICTION

In Section 3.2.1 some of the parameters were described which will affect the residual strength prediction by altering the failure criterion or criteria. Some of these parameters can be controlled in the testing required for establishing a criterion (e.g., buckling can be controlled by suppression plates). Most of the parameters are not readily amenable to analytical treatment (e.g., strain rate, temperature, etc.) and must be treated in an empirical or semi-empirical manner.

Many of these parameters have a direct effect on the failure criterion, and it is planned to treat them as an influence on the crack growth resistance curve, slow tear or perhaps some newer criterion such as  $J_{critical}$ .

### 5.5.1 Crack Growth Resistance Concept and Its Use as a Failure Criterion

The resistance curve ( $R$  or  $K_R$ ) concept was first introduced in 1960 (Reference 43) and has received increased attention recently as a means to:

- predict the extent of slow crack growth prior to fracture
- characterize plane stress toughness
- bridge the gap between brittle and semi-brittle fracture and fracture with large plasticity at the crack tip.

Several reports and papers have been published and a symposium has been sponsored on the experimental determination of the resistance curve for both metallic and nonmetallic materials (see References 6, 37, and 44 through 48). Since the experimental methods for obtaining the resistance curve have been well documented, and the theory behind its development has been described in detail elsewhere (see Reference 43 and 49), it will suffice here to indicate its usage in an overall residual strength prediction method.

The resistance curve is essentially a measure of the resistance a material offers to crack extension. It is a function of thickness and currently thought to be independent of initial crack size and specimen geometry. To indicate the general trend and specimen independency, the data for 7075-T6 sheet material from References, 6, 37, and 47 are presented as common  $K_R$  curve in Figure 15. At first glance the spread in the data for one specimen geometry (center cracked tension) appears excessive. These differences could have been caused by material lot differences since all the data from Reference 6 were taken from the same lot of material and indicate closer agreement between different specimen types (CCT and CLWL) than data for a similar specimen type (CCT) but from different material lots.

It may be advisable to place lower bounds on the  $K_R$  curve for each material to avoid regions where the percentage error in  $K_R$  is excessive if this concept is to be used in a residual strength prediction method. However, recent activity in proposed standards for determining  $K_R$  curves may remove some of the data scatter in developing such curves.

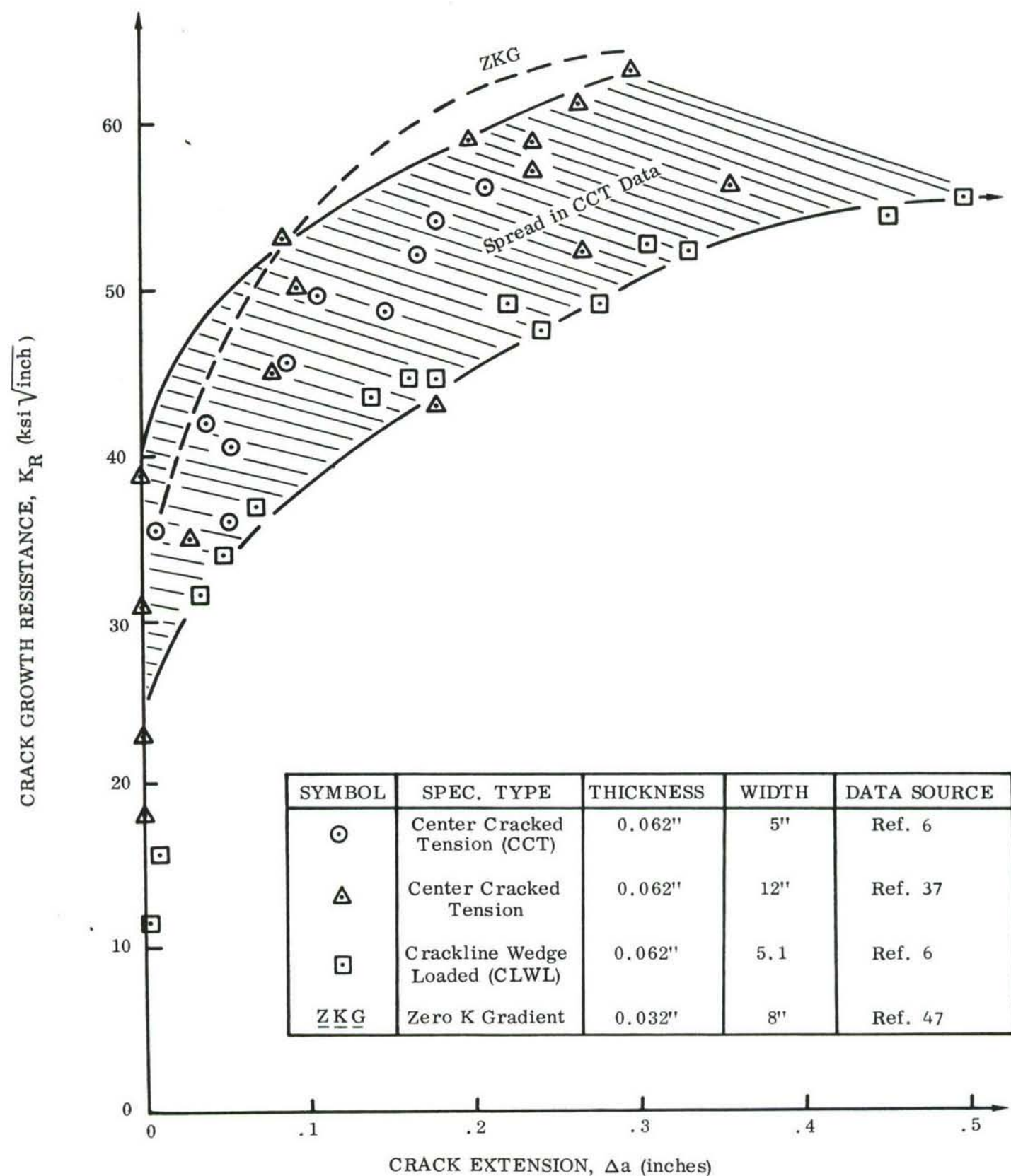


FIGURE 15 COMPARISON OF  $K_R$  CURVES FOR VARIOUS SPECIMEN TYPES



For materials and structures which exhibit a significant amount of slow stable tear (those for which the R curve is a viable failure concept) two criteria must be satisfied. These two criteria specify that

$$K_I \geq K_R$$

$$\frac{\partial K_I}{\partial a} \geq \frac{\partial K_R}{\partial a}$$

for instability conditions. Geometrically speaking, these two criteria state that fracture instability occurs when the  $K_R$  and  $K_I$  curves become tangent to one another. Thus for crack growth instability (fast or rapid fracture) to occur, the increase in  $K_I$  with "a" must equal or exceed the corresponding increase in material resistance to tear,  $K_R$ . Slow stable tear will occur up to this instability point.

Creager and Liu (Reference 50) have applied this criterion to simple, flat strap reinforced, flat panels (attached with a single row of rivets) using a modified form of the stress intensity ( $K_I$ ) analysis of Reference 30. The predictions of failure load were within 10% of the measured values. The analysis was conducted using  $K_R$  data from another source and the predictions are considered good in light of the influence of the reinforcements on the slow tear process, as indicated in Figure 11.

Other factors have been shown to effect the  $K_R$  curve. For example, Wang (Reference 48) has shown a 30% decrease in  $K_R$  values at -65°F from those obtained at room temperature for 7075 and 7079 (T6) sheet. This is not an unexpected trend. However, it must be considered in using the resistance curve in any residual strength failure criterion.

### 5.5.2 Crack Tip Buckling

The inplane buckling of a center cracked, tension loaded panel has been studied by many investigators (e.g., see References 13, 51, 52 through 55). All have indicated large reductions in critical fracture stress as a result of buckling. A good review of the various problems associated with the measurement and prediction of plane stress crack buckling is contained in Reference 54. As noted in Reference 54, in-plane crack buckling is a large deflection problem and must be a function of how much deflection occurs.

The usual equation for the prediction of critical buckling stress has the form

$$\sigma_{bc} = kE \left( \frac{B}{2a} \right)^2 \quad (27)$$



where  $B$  is sheet thickness and  $2a$  is the crack length. For each case  $k$  varies for the particular model employed. Thus some estimate of critical buckling stress can be made for simple unreinforced panels. For reinforced panels the problem becomes more difficult due to the interaction of reinforcements with local crack tip stress fields.

No simple solution appears available to introduce this effect in an analytical residual strength scheme. A semi-empirical solution, such as Equation 27, may be an expedient to evaluate the possibility of crack buckling on a go/no go basis. Whether buckling can be included in the  $R$  curve procedure is speculative, and current methods of thin section fracture eliminate it from the test data by using buckling restraints. Also, they do not include it in the analytical procedure. Clearly this effect requires additional study from an analytical standpoint.

### 5.5.3 Strain Rate

Of all the parameters which affect residual strength, the effect of strain or load rate is the one that has had the least attention. Broek (Reference 56) found little effect of strain rate on stress at initiation of slow tear for aluminum alloys within the range of typical aircraft loading spectra. However, Newman (Reference 57) indicated that strain rate sensitive materials will have decreasing plastic zone sizes for increasing stress rates. This implies that a variation in plastic zone models with strain rate is warranted and advisable for those materials which exhibit strain rate dependency. It is believed that these differences in fracture stress can be explored, evaluated, and incorporated into the  $R$  curve. The effect of this dependency was indicated in Figure 6(b) where the ordinate could have been  $K_R$  as well as stress/load.

The use of stress-strain data at rates encompassing the material operating range is warranted in the developed analysis procedure, and the data itself becomes a part of the material property input as shown in Step 4 of Figure 5.

### 5.5.4 Specimen Dependency and Anisotropic Behavior

For the use of a critical stress intensity ( $K_c$ ) approach it becomes evident that specimen geometry is an important factor. This is particularly true of center cracked tension (CCT) loaded panels. Much research has been devoted to setting limits on specimen widths (see References 37, 51, and 55) to obtain values of fracture stress independent of specimen width. In most cases it has been found that exceedingly large (wide) CCT panels are required for fracture strength determination of materials which exhibit large amounts of slow crack extension and crack tip plasticity (Reference 48).

It is believed that the Resistance curve can resolve these influences and make it possible to test smaller panels in a decreasing stress intensity or stress field (e.g., crack line wedge loaded and zero  $K$  gradient (tapered beam) specimens). With these specimens it is possible to remain within stable crack extension for long crack lengths prior to instability (see Figure 15), and thus be able to develop the entire  $K_R$  curve up to plateau values of stress intensity.



In-service conditions can lead to cracks which are oriented in directions inclined to the material rolling direction. It is known that a material's plane strain fracture toughness ( $K_{IC}$ ) varies with the inclination of the crack axis with respect to the principal rolling directions. Reduction in fracture stress has also been observed in thin section fracture. It has been found that with the crack oriented normal to the rolling direction, the highest fracture stress is achieved.

One cannot anticipate under in-service conditions that the crack will be aligned in the optimum toughness direction. Therefore, it has been previously proposed (Reference 58) that the crack oriented parallel to the rolling direction, since it represents the most unfavorable service condition, would provide a lower bound value of  $K_C$ .

What is required is a systematic study of the influence of both upper and lower bound values on residual strength prediction. It is postulated that this can be accomplished through the  $K_R$  curve. Thus for a given structural element if the principal stress direction is normal to the rolling direction, and remains so in service, one will avoid an undue penalty by using lower bound values.

In summary, many of the parameters which will affect the failure criterion and/or analysis method can be included in the resistance curve, or as will be discussed in Section VI, through a critical J concept.

#### 5.5.5 Value of Continued Development of Existing Methods

From the comparisons of analytical and experimental results for the data of Reference 32 it would appear that any of the predictive techniques would fulfill the required accuracy ( $\pm 10\%$ ) of the desired method. It must be remembered that these data were obtained on a high strength aluminum alloy (7075) which exhibits negligible slow tear prior to fracture and moderate toughness. For these reasons any residual strength method which is based on elastic fracture theory will produce satisfactory accuracy. If data on panels of simple geometry with a tougher alloy (e.g., 2024) had been available in a consistent form, with both reinforced and unreinforced data from the same lot, the existing methods would not provide adequate predictions. The elastic solutions would then predict lower residual strengths for both simple and reinforced panel geometries. The need for inclusion of plasticity in any fracture strength scheme is indicated by the continued modifications to the NSA method.

From the available evidence it would appear to be prudent to discount any additional developmental work on the NSA (CSA) and effective width methods. They are too empirically based and inflexible to meet the requirements of the "ideal" method. LEFM, on the other hand, does appear to be capable of significant generalization. Residual strength predictions for plane stress situations can be made provided plasticity and slow tear, as a minimum, are included in the solution. Section VI discusses the planned development, starting with LEFM as a basis of departure.

## VI PLANNED DEVELOPMENT OF RESIDUAL STRENGTH PREDICTION TECHNIQUE

Throughout the evaluation of residual strength methodology, the need for a general method, capable of giving accurate predictions of residual strength for a wide variety of situations encountered in aircraft structures, has been cited as being of paramount importance. Methodology used to date has been very narrow in terms of applicability, restrictive in the number of parameters considered, and often very superficial in the manner in which the influencing parameters are functionally related to residual strength. As a result, the presently available methods often give residual strength predictions which deviate significantly from actuality.

In launching the development of a new method for residual strength prediction, the defects of the present methods of course have a bearing on the direction of the contemplated activity. The major shortcomings of the past, namely:

- . Restrictive applicability
- . Insufficient treatment of plasticity
- . Inadequate treatment of slow tear

will be addressed and accounted for in the development of the new method.

Two virtues of existing methods which are well worth retaining are the ease with which they can be applied and the relatively inexpensive costs involved in making the predictions. It appears that the new method will, of necessity, require slightly more effort for successful application. Nevertheless, by exercising careful control, the additional capability and the more satisfactory treatment of the pertinent parameters will more than compensate any loss in simplicity.

### 6.1 CANDIDATE ANALYSIS METHODS

After studying a number of candidate parameters for characterizing the crack tip environment, it appears that the most suitable choice for use in the to be developed residual strength method is the J integral introduced by Rice (Reference 59). This quantity can be regarded as the most general single parameter measure of the crack tip environment currently available for the following reasons:

- (1) It can be related to crack opening displacement (see section 6.1.2) and,
- (2) In the elastic range, it reduces to G, the crack extension force, and can be related to K, the stress intensity factor.



Two notable features of J are its path independence and its incorporation of plasticity effects. Both of these attributes will be discussed below.

The J integral is defined as

$$J = \int_{\Gamma} \left\{ W(\epsilon) dy - \vec{T} \cdot \frac{\partial \vec{u}}{\partial x} ds \right\} \quad (28)$$

where W, the strain energy density, is

$$W = \int [\sigma_x d\epsilon_x + \tau_{xy} d\gamma_{xy} + \tau_{xz} d\gamma_{xz} + \sigma_y d\epsilon_y + \tau_{yz} d\gamma_{yz} + \sigma_z d\epsilon_z] \quad (29)$$

For generalized plane stress conditions:

$$W = \int [\sigma_x d\epsilon_x + \tau_{xy} d\gamma_{xy} + \sigma_y d\epsilon_y] \quad (30)$$

The contour integral J is evaluated along the curve  $\Gamma$  which is, in principle, any curve surrounding the crack tip. The positive direction of s in traversing  $\Gamma$  is counterclockwise.

Since the value of J is independent of the particular  $\Gamma$  contour selected, one has complete freedom in the  $\Gamma$  contour actually used. It appears that the path independency is maintained regardless of whether the material obeys linear elastic - nonlinear elastic - deformation theory plastic - or Prandtl-Reuss plastic constitutive relations (see Reference 5).

For ease in evaluation of J, the curve  $\Gamma$  can be taken to be a rectangular path (see Figure 16). Then dy will be nonzero only for those portions of  $\Gamma$  which parallel the Y axis. Thus since W need be evaluated only for those portions of  $\Gamma$  for which dy is nonzero, the computation of J is simplified.

In Equation (28), the second integral involves the scalar product of the tractive stress vector  $\vec{T}$  and the vector whose components are the rates of change of displacement with respect to x. Resolving into components, one has

$$\frac{\partial \vec{u}}{\partial x} = \frac{\partial u}{\partial x} \hat{i} + \frac{\partial v}{\partial x} \hat{j} \quad (31)$$

where u and v are the displacements in the x and y directions, respectively and  $\hat{i}$  and  $\hat{j}$  are the corresponding unit vectors. Also

$$\vec{T} = T_x \hat{i} + T_y \hat{j} = T_1 \hat{i} + T_2 \hat{j} \quad (32)$$

where  $T_1$  and  $T_2$  are related to the tractive stress components through the outward normal by  $T_i = \sigma_{ij} n_j$ . To establish the precise form of  $T_i$  at all points along a

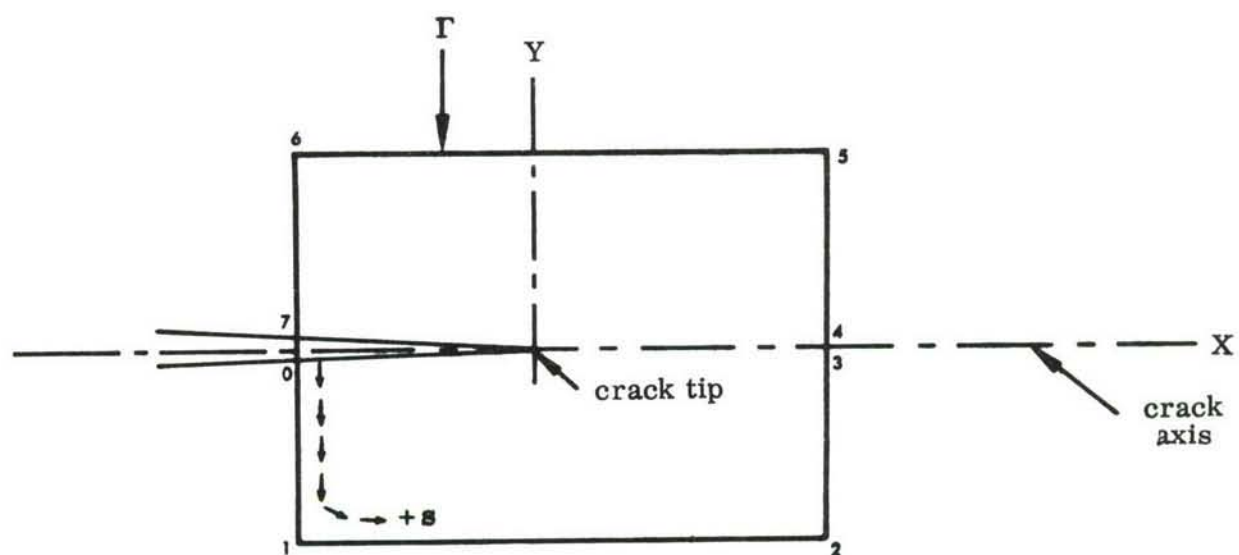


FIGURE 16 RECTANGULAR PATH FOR J CALCULATION

rectangular  $\Gamma$  contour, consider again the crack and the surrounding  $\Gamma$  contour shown in Figure 16. An outward-pointing unit normal vector  $\hat{n}$  will have components  $n_1$  and  $n_2$  (in the  $x$  and  $y$  directions respectively) as listed in Column (3) of Table II for the five segments of the  $\Gamma$  curve indicated. Applying  $T_i = \sigma_{ij}n_j$ , the values of  $T_i$  are given in Column (4) of Table II.

The formation of the  $\vec{T}$  and  $\frac{\partial u}{\partial x}$  vectors is shown in Columns (5) and (6), respectively, and the scalar product is calculated in Column (7). The relationship between  $ds$  and either  $dx$  or  $dy$  is indicated in Column (8) and the net contribution of each segment to the  $J$  integral is indicated in Column (9) of Table II.

In the case of uniaxial loading, by virtue of the symmetry which exists with respect to the crack plane, one can write

$$J = 2 \int_{(x,y)_6}^{(x,y)_7} \left[ W - \sigma_x \left( \frac{\partial u}{\partial x} \right) - \tau_{xy} \left( \frac{\partial v}{\partial x} \right) \right] dy + 2 \int_{(x,y)_5}^{(x,y)_6} \left[ \tau_{xy} \left( \frac{\partial u}{\partial x} \right) + \sigma_y \left( \frac{\partial v}{\partial x} \right) \right] dx$$

$$+ 2 \int_{(x,y)_4}^{(x,y)_5} \left[ W - \sigma_x \left( \frac{\partial u}{\partial x} \right) - \tau_{xy} \left( \frac{\partial v}{\partial x} \right) \right] dy \quad (33)$$

#### 6.1.1 Treatment of Structures Made of Prandtl-Reuss Materials

The  $J$  integral can be evaluated by performing the integrations indicated in Equation (33). The strain energy density  $W$  appearing in Equation (33) is, for plane stress conditions, given by Equation (30). In order to carry out the integration indicated in Equation (30), one needs a relationship between stresses and strains which realistically models the behavior actually exhibited by plastically deforming materials. For many materials, the Prandtl-Reuss equations provide a satisfactory relationship. They are, for the case of plane stress

$$\begin{bmatrix} d\epsilon_x \\ d\epsilon_y \\ d\epsilon_z \\ d\gamma_{xy} \end{bmatrix} = \begin{bmatrix} \frac{1}{E} & -\frac{\nu}{E} & 0 & \frac{3\sigma'_x}{2\bar{\sigma}} \\ -\frac{\nu}{E} & \frac{1}{E} & 0 & \frac{3\sigma'_y}{2\bar{\sigma}} \\ -\frac{\nu}{E} & -\frac{\nu}{E} & 0 & \frac{3\sigma'_z}{2\bar{\sigma}} \\ 0 & 0 & \frac{2(1+\nu)}{E} & \frac{3\tau_{xy}}{\bar{\sigma}} \end{bmatrix} \begin{bmatrix} d\sigma_x \\ d\sigma_y \\ d\tau_{xy} \\ d\bar{\epsilon}_p \end{bmatrix} \quad (34)$$



TABLE II TERMS USED IN J INTEGRAL DETERMINATION

(1)	(2)	(3)	(4)	(5)	(6)	(7)	(8)	(9)
SEGMENT OF Γ CURVE	TRACTION STRESS COMPONENTS	COMPONENTS OF OUTWARD UNIT NORMAL	$T_i = \sigma_{ij} n_j$	$\vec{T} = T_1 \hat{i} + T_2 \hat{j}$	$\frac{\partial \vec{u}}{\partial x}$	$-\vec{T} \cdot \frac{\partial \vec{u}}{\partial x}$	ds	CONTRIBUTION TO J INTEGRAL FROM SEGMENT
0-1	$\sigma_x = \sigma_{11}$ $\tau_{xy} = \sigma_{12}$	$n_1 = -1$ $n_2 = 0$	$T_1 = -\sigma_x$ $T_2 = -\tau_{xy}$	$-\left[ \sigma_x \hat{i} + \tau_{xy} \hat{j} \right]$	$\begin{pmatrix} \partial u / \partial x \\ \partial v / \partial x \end{pmatrix} \hat{i} + \begin{pmatrix} \partial u / \partial x \\ \partial v / \partial x \end{pmatrix} \hat{j}$	$-\left[ \sigma_x (\partial u / \partial x) + \tau_{xy} (\partial v / \partial x) \right]$	-dy	$\int_{(x,y)_0}^{(x,y)_1} \left[ W - \sigma_x \left( \frac{\partial u}{\partial x} \right) - \tau_{xy} \left( \frac{\partial v}{\partial x} \right) \right] dy$
1-2	$\sigma_y = \sigma_{22}$ $\tau_{xy} = \sigma_{12}$	$n_1 = 0$ $n_2 = -1$	$T_1 = -\tau_{xy}$ $T_2 = -\sigma_y$	$-\left[ \tau_{xy} \hat{i} + \sigma_y \hat{j} \right]$	$\begin{pmatrix} \partial u / \partial x \\ \partial v / \partial x \end{pmatrix} \hat{i} + \begin{pmatrix} \partial u / \partial x \\ \partial v / \partial x \end{pmatrix} \hat{j}$	$-\left[ \tau_{xy} (\partial u / \partial x) + \sigma_y (\partial v / \partial x) \right]$	dx	$\int_{(x,y)_1}^{(x,y)_2} \left[ \tau_{xy} \left( \frac{\partial u}{\partial x} \right) + \sigma_y \left( \frac{\partial v}{\partial x} \right) \right] dx$
2-5	$\sigma_x = \sigma_{11}$ $\tau_{xy} = \sigma_{12}$	$n_1 = 1$ $n_2 = 0$	$T_1 = \sigma_x$ $T_2 = \tau_{xy}$	$\sigma_x \hat{i} + \tau_{xy} \hat{j}$	$\begin{pmatrix} \partial u / \partial x \\ \partial v / \partial x \end{pmatrix} \hat{i} + \begin{pmatrix} \partial u / \partial x \\ \partial v / \partial x \end{pmatrix} \hat{j}$	$\sigma_x (\partial u / \partial x) + \tau_{xy} (\partial v / \partial x)$	dy	$\int_{(x,y)_2}^{(x,y)_5} \left[ W - \sigma_x \left( \frac{\partial u}{\partial x} \right) - \tau_{xy} \left( \frac{\partial v}{\partial x} \right) \right] dy$
5-6	$\sigma_y = \sigma_{22}$ $\tau_{xy} = \sigma_{12}$	$n_1 = 0$ $n_2 = 1$	$T_1 = \tau_{xy}$ $T_2 = \sigma_y$	$\tau_{xy} \hat{i} + \sigma_y \hat{j}$	$\begin{pmatrix} \partial u / \partial x \\ \partial v / \partial x \end{pmatrix} \hat{i} + \begin{pmatrix} \partial u / \partial x \\ \partial v / \partial x \end{pmatrix} \hat{j}$	$\tau_{xy} (\partial u / \partial x) + \sigma_y (\partial v / \partial x)$	-dx	$\int_{(x,y)_5}^{(x,y)_6} \left[ \tau_{xy} \left( \frac{\partial u}{\partial x} \right) + \sigma_y \left( \frac{\partial v}{\partial x} \right) \right] dx$
6-7	$\sigma_x = \sigma_{11}$ $\tau_{xy} = \sigma_{12}$	$n_1 = -1$ $n_2 = 0$	$T_1 = -\sigma_x$ $T_2 = -\tau_{xy}$	$-\left[ \sigma_x \hat{i} + \tau_{xy} \hat{j} \right]$	$\begin{pmatrix} \partial u / \partial x \\ \partial v / \partial x \end{pmatrix} \hat{i} + \begin{pmatrix} \partial u / \partial x \\ \partial v / \partial x \end{pmatrix} \hat{j}$	$-\left[ \sigma_x (\partial u / \partial x) + \tau_{xy} (\partial v / \partial x) \right]$	-dy	$\int_{(x,y)_6}^{(x,y)_7} \left[ W - \sigma_x \left( \frac{\partial u}{\partial x} \right) - \tau_{xy} \left( \frac{\partial v}{\partial x} \right) \right] dy$

where

$$\begin{aligned}
 \sigma_x' &= \frac{1}{3} (2\sigma_x - \sigma_y) \\
 \sigma_y' &= \frac{1}{3} (2\sigma_y - \sigma_x) \\
 \sigma_z' &= -\frac{1}{3} (\sigma_x + \sigma_y) \\
 \bar{\sigma} &= \left[ \sigma_x^2 - \sigma_x \sigma_y + \sigma_y^2 + 3\tau_{xy}^2 \right]^{\frac{1}{2}}
 \end{aligned} \tag{35}$$

The primed quantities in Equations (35) are sometimes referred to as the deviatoric stress components in the plasticity literature. The barred quantities (i.e.,  $\bar{\sigma}$  and  $\bar{\epsilon}_p$ ) are the equivalent stress and the equivalent plastic strain.

Substituting Equations (34) into Equation (30), one obtains

$$W = \frac{1}{2E} \left[ \sigma_x + \sigma_y \right]^2 + \frac{1+\nu}{E} \left[ \tau_{xy}^2 - \sigma_x \sigma_y \right] + \int \bar{\sigma} d\bar{\epsilon}_p \tag{36}$$

In studying Equation (36), observe that  $W$  will have a unique value only if unloading (at every point of the body being considered) is not permitted. To illustrate this point, consider a body that is initially unloaded and unstrained. Then

$$\sigma_x = \sigma_y = \tau_{xy} = \bar{\sigma} = \bar{\epsilon}_p = 0 .$$

If loading is applied and increased to the point where the onset of plastic action is imminent, in general  $\sigma_x$ ,  $\sigma_y$ ,  $\tau_{xy}$ , and  $\bar{\sigma}$  will be nonzero.

However, the integral in Equation (36) will still be zero since  $\bar{\epsilon}_p$  has remained at its initial zero value. If the body were unloaded at this point,  $W$  would be a unique function of stress, regardless of loading history.

If, instead of unloading at the onset of plastic action the body is loaded into the plastic range, the integral in Equation (36) makes a contribution to the value of  $W$ . When the body is subsequently unloaded, the values of  $\sigma_x$ ,  $\sigma_y$ ,  $\tau_{xy}$ , and  $\bar{\sigma}$  all return to their initial zero values, but the plastic strain  $\bar{\epsilon}_p$ , being unrecoverable, retains its peak value. Thus the integral

$\int_0^{\bar{\epsilon}} \bar{\sigma} d\bar{\epsilon}$  makes a nonzero contribution to  $W$  when the body is back in its

initial unloaded state. If loading into the plastic range followed by unloading is permitted  $W$  becomes multivalued. It follows that  $J$  is also multivalued for this occurrence.

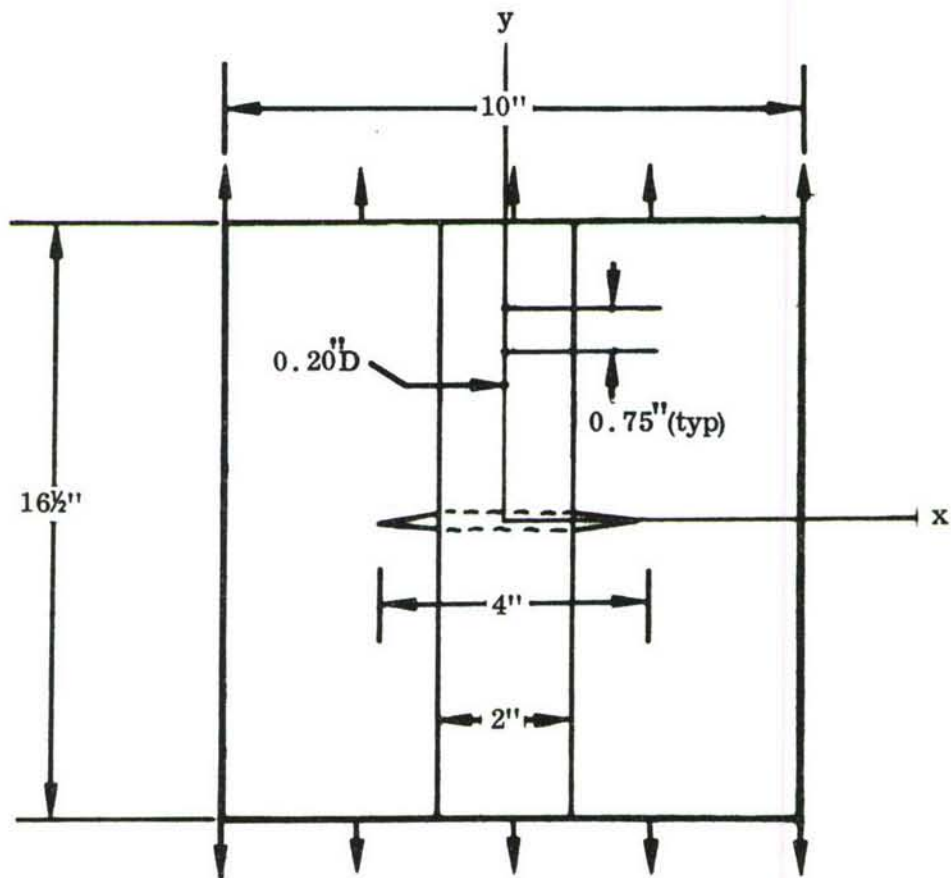
The statements made in the preceding paragraph would appear to seriously limit the use of  $J$  as a fracture criterion since the case of loading into the plastic range followed by unloading (i.e., the case for which  $J$  is multivalued) occurs when crack extension takes place. On the basis of a number of examples, Hayes (Reference 5) deduced that monotonic loading conditions prevail throughout a cracked body under steadily increasing load applied to the boundaries, provided that crack extension does not occur. Thus, valid  $J$  calculations can be performed for this case. The case of crack extension will be discussed in section 6.2.1.

**6.1.1.1. Example Problem** To illustrate the steps involved in numerically evaluating the  $J$  integral for a Prandtl-Reuss material, consider the cracked, strap-stiffened sheet shown in Figure 17. The finite element idealization (representing one quarter of the problem of Figure 17) is shown in Figure 18 and consists of 421 grid points, 397 panels representing the sheet, 11 panels representing the rivets, and 22 panels representing the strap. Since the case of a stringer in the form of a flat strap has been found by Isida (Reference 60) to be one in which the stiffener bending stiffness is negligible compared to the stiffener axial stiffness, both strap and sheet were represented by membrane elements. The  $\Gamma$  contour along which  $J$  is to be calculated is indicated in Figure 18.

The strap, sheet, and rivet material will be regarded as being capable of experiencing a considerable amount of plastic deformation during the loading process. To be explicit, the material from which the strap, sheet, and rivets are made will be assumed to exhibit the stress-strain curve of Figure 19 when loaded uniaxially. Under the conditions shown in Figure 17, of course, all material points are not in a state of uniaxial stress. However, an equivalent stress  $\bar{\sigma}$  can be calculated for every point of Figure 17 by combining the components of the actual stress state (i.e.,  $\sigma_x$ ,  $\sigma_y$ ,  $\tau_{xy}$ ) as indicated in the last of Equations (35). The assumption is made that, just as Figure 19 relates a uniaxial stress to a uniaxial strain it may also be used to relate the equivalent stress  $\bar{\sigma}$  to an equivalent strain  $\bar{\epsilon}$ .

The NASTRAN finite element program was used to analyze the structure of Figure 17. This program was chosen because it has an operational elastic-plastic capability and is relatively efficient.





Note: Strap, sheet  
and rivets all assumed  
to be aluminum

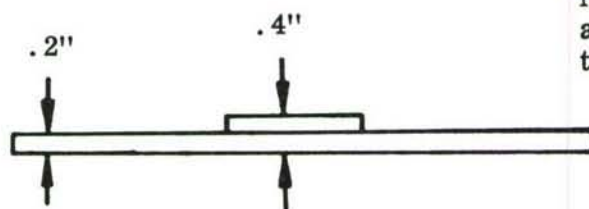


FIGURE 17 CRACKED STIFFENED SHEET

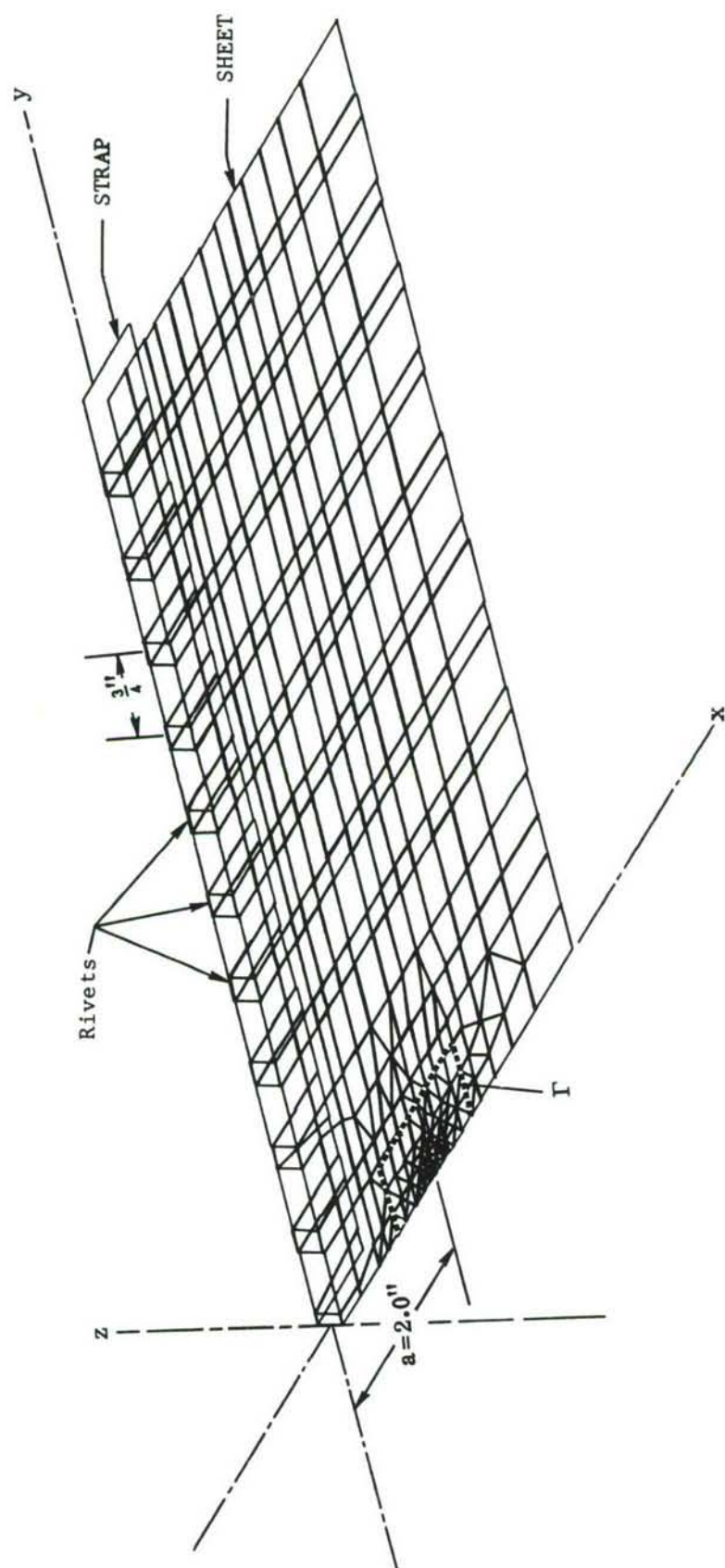


FIGURE 18. GRID SYSTEM AND  $\Gamma$  CONTOUR FOR J CALCULATION

UNDEFORMED SHAPE

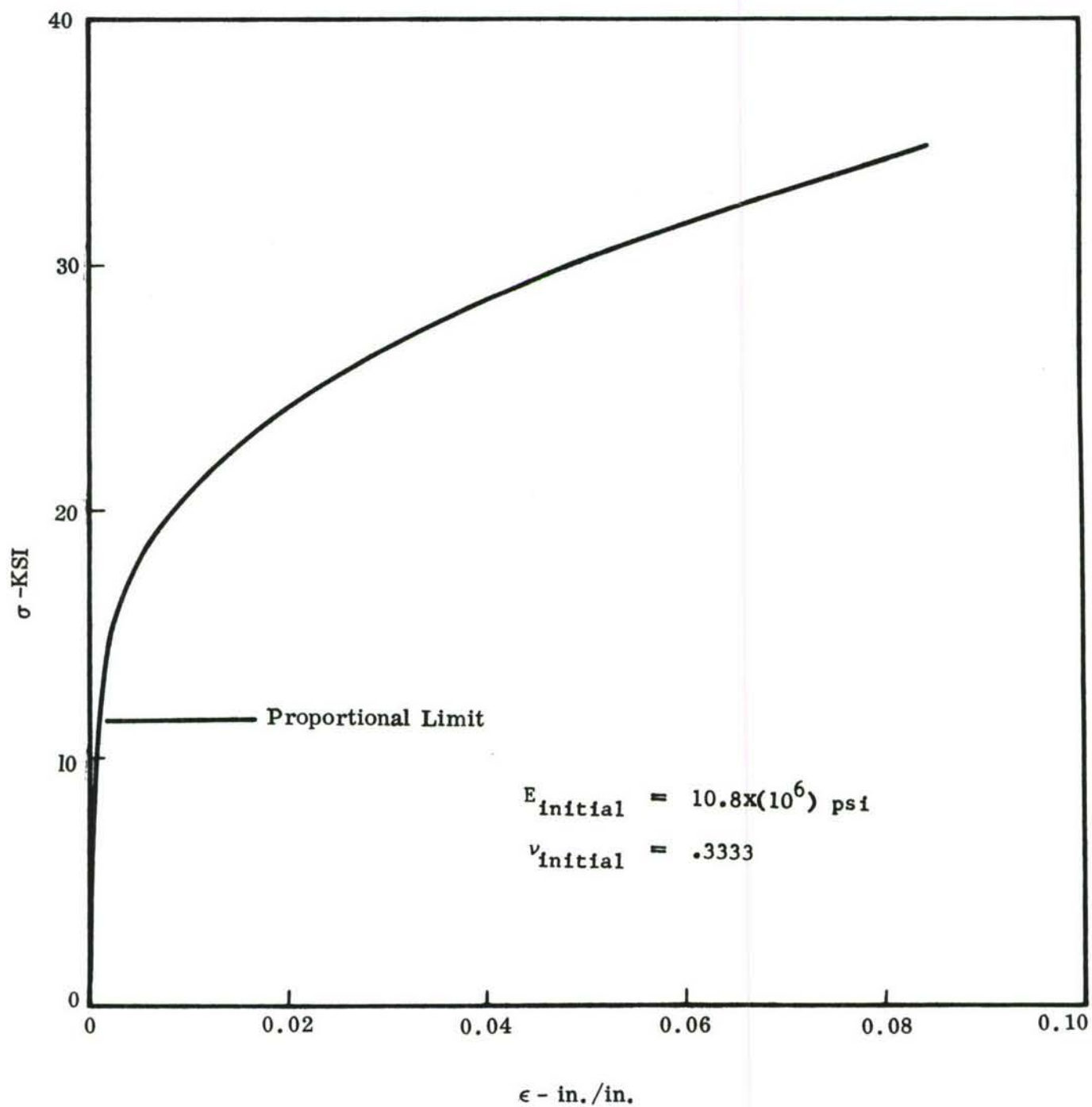


FIGURE 19 UNIAXIAL STRESS-STRAIN CURVE



The procedure employed by NASTRAN to solve elastic-plastic problems is, in effect, a piecewise linear scheme which involves an incremental application of the applied load. The problem actually solved utilized the stress increments listed in Table III. Essentially, 9 elastic problems were solved and appropriately combined to yield the desired elastic-plastic solution. On the basis of an earlier elastic solution to the problem, the first stress increment was selected equal to 2100 psi so that the stress in the most highly stressed finite element was just above the proportional limit stress of 11,500 psi.

TABLE III  
STRESS INCREMENTS - ELASTIC-PLASTIC ANALYSIS

<u>Increment Number</u>	<u>Stress Increment (psi)</u>	<u>Accumulated Stress (psi)</u>
1	2100	2100
2	300	2400
3	400	2800
4	500	3300
5	600	3900
6	700	4600
7	800	5400
8	900	6300
9	1000	7300

A summary of the steps in the NASTRAN computational procedure is as follows:

1. Using the initial elastic properties, determine the displacements and stresses resulting from stress increment #1 (2100 psi) by performing an elastic analysis.
2. At all points in the structure, form  $\bar{\sigma}$  according to the last of Equations (35).
3. From Figure 19 (actually from its tabular equivalent which consists of 201 points, resulting in a 200 segment multilinear approximation to Figure 19) determine  $\bar{\epsilon}$  at all points in the structure.
4. By linear extrapolation of the strain data, estimate the value of  $\bar{\epsilon}$  at every point of the structure corresponding to the accumulated stress of stress increments #1 and #2.

5. Enter the tabular equivalent of Figure 19 with the  $\bar{\epsilon}$  estimate generated in step (4) and determine the estimated equivalent stress resulting from the application of stress increments #1 and #2 at all points in the structure.
6. From the actual  $\bar{\sigma}$  and  $\bar{\epsilon}$  data for stress increment #1 and the estimated  $\bar{\sigma}$  and  $\bar{\epsilon}$  data for stress increment #2, estimate the tangent modulus at all points.
7. Using the tangent moduli found in step (6), form a new structural stiffness matrix.
8. Applying only stress increment #2 (i.e., 300 psi) use the result of step (7) to perform a linear finite element analysis, resulting in displacements and stresses corresponding to increment #2.
9. Superimpose the stresses from steps (1) and (8) and form a new  $\bar{\sigma}$  value at all points in the structure.
10. Repeat steps (3) through (9) until all 9 stress increments of Table III have been applied.

By following the steps indicated above, the NASTRAN procedure produces stresses and displacements which incorporate the elastic-plastic nature of the material. The Prandtl-Reuss relations (Equations (34)) are solved for finite stress increments instead of for infinitesimal increments. As a result, numerical errors are introduced which can become quite large. Nevertheless, if the load increments are sufficiently small (those listed in Table III are thought to be in this category), acceptably accurate results should be obtained.

The NASTRAN procedure indicated above required 20.43 minutes of CPU time and 4.00 minutes of I/O time on an IBM 370/165 computer to execute the nine increment elastic-plastic problem indicated in Table III. This is substantially longer than the time required to perform nine elastic runs. A significant amount of time is apparently used in going to and from the  $\bar{\sigma}$  vs  $\bar{\epsilon}$  table and in forming and assembling the updated stiffness matrices at each increment of loading.

In calculating  $J$ , the  $\Gamma$  contour and the nodes shown in Figure 20 were employed. When the plastic zone does not penetrate the integration boundary (i.e., when  $\bar{\epsilon}_p = 0$ ), Equations (33) and (36) result in (using the grid points shown in Figure 20 to indicate integration limits),

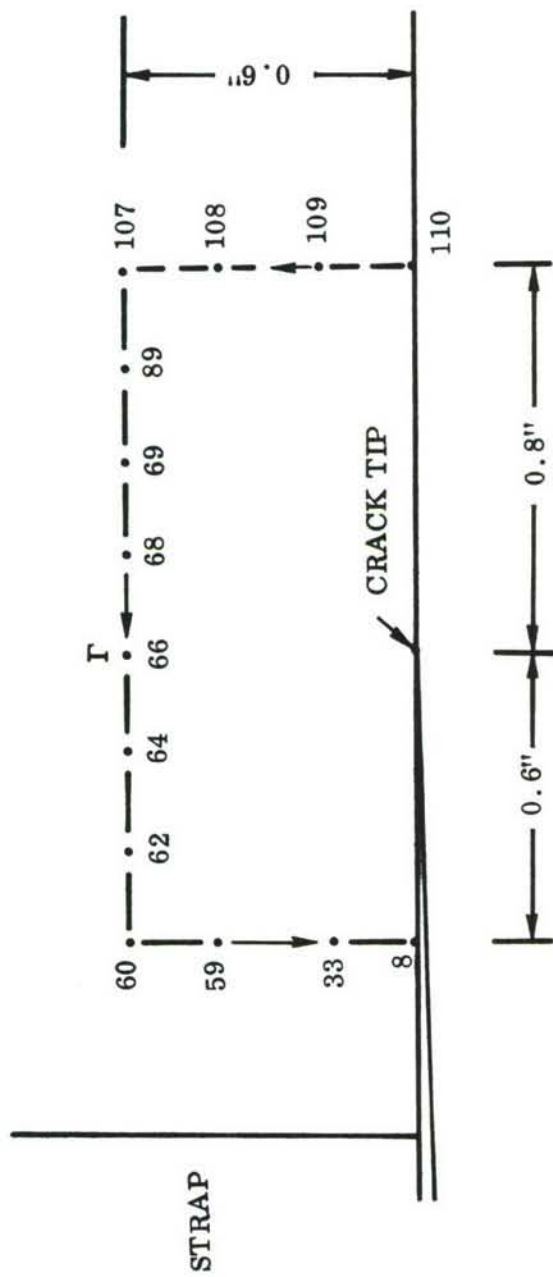


FIGURE 20 NODES INVOLVED IN J CALCULATION



$$\begin{aligned}
J = & 2 \int_{110}^{107} \left[ \frac{1}{2E} (\sigma_x + \sigma_y)^2 + \frac{1+\nu}{E} (\tau_{xy}^2 - \sigma_x \sigma_y) - \sigma_x \left( \frac{\partial u}{\partial x} \right) - \tau_{xy} \left( \frac{\partial v}{\partial x} \right) \right] dy \\
& + 2 \int_{107}^{60} \left[ \tau_{xy} \left( \frac{\partial u}{\partial x} \right) + \sigma_y \left( \frac{\partial v}{\partial x} \right) \right] dx \\
& + 2 \int_{60}^{8} \left[ \frac{1}{2E} (\sigma_x + \sigma_y)^2 + \frac{1+\nu}{E} (\tau_{xy}^2 - \sigma_x \sigma_y) - \sigma_x \left( \frac{\partial u}{\partial x} \right) - \tau_{xy} \left( \frac{\partial v}{\partial x} \right) \right] dy
\end{aligned} \tag{37}$$

To facilitate the post-processing of the NASTRAN-generated data required to calculate  $J$ , a RAX program was written which numerically integrates Equation (37).

The RAX program requires as input the NASTRAN-produced  $\sigma_x$ ,  $\sigma_y$ , and  $\tau_{xy}$  values in the 24 elements contiguous to the  $\Gamma$  contour and the  $u$  and  $v$  displacements at 22 grid points on and adjacent to the  $\Gamma$  contour for each of the nine load increments. Thus, in order to calculate  $J$  a total of 1044 pieces of input data were required. The RAX program calculates  $J$  by averaging the stresses, forming central difference approximations for the displacement derivatives, forming the integrals indicated in Equation (37) and then summing the results.

To accommodate cases in which the plastic zone has penetrated the vertical portions of the  $\Gamma$  contour, the RAX program calculates the prints out  $\bar{\sigma}$  in the following segments of Figure 20: 110-109, 109-108, 108-107, 60-59, 59-33, and 33-8. When  $\bar{\sigma}$  in these segments exceeds the proportional limit stress  $F_{tp}$  (in this case, from Figure 19,  $F_{tp} = 11.5$  ksi), one can consult the stress-strain curve to determine  $\bar{\epsilon}$ , and then determine the contribution of  $\int \bar{\sigma} d\bar{\epsilon}_p$  to the strain energy (Equation (36)) and to the value of  $J$  (Equation (28)). The values of  $\bar{\sigma}$  along the vertical  $\Gamma$  segments were less than 11.5 ksi for the loads shown in Table III and hence  $\int \bar{\sigma} d\bar{\epsilon}_p$  had no contribution.

The results of the present computations are shown in Figure 21.

It is interesting to note that the loads of Table III do not cause a significant departure from the linear relationship of  $\sqrt{J}$  with applied stress which is found using purely elastic constitutive relations (see Figure 22). This behavior was also observed by Hayes (Reference 5) for unstiffened cracked sheets with applied stress to yield stress ratios equal to or less than 0.7.

Obviously, the stresses of Table III were chosen for illustrative purposes only. In a typical residual strength application, one would probably be interested in significantly higher applied stress levels. The procedure indicated will yield valid  $J$  information regardless of applied stress level.

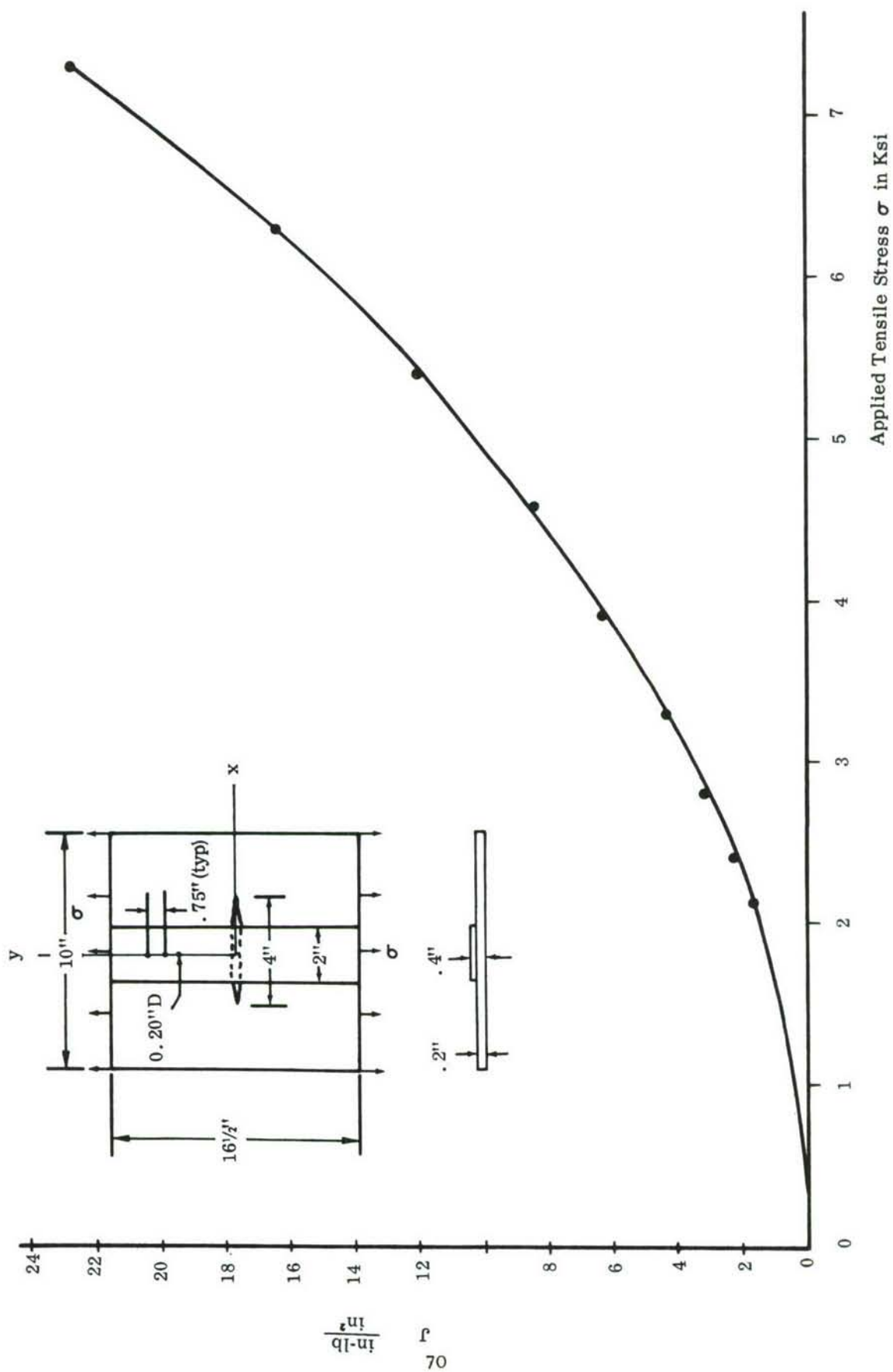


FIGURE 21 J VS. APPLIED STRESS FOR A STRAP-STIFFENED SHEET CONTAINING A CRACK WITH  $a \approx 2$  INCHES

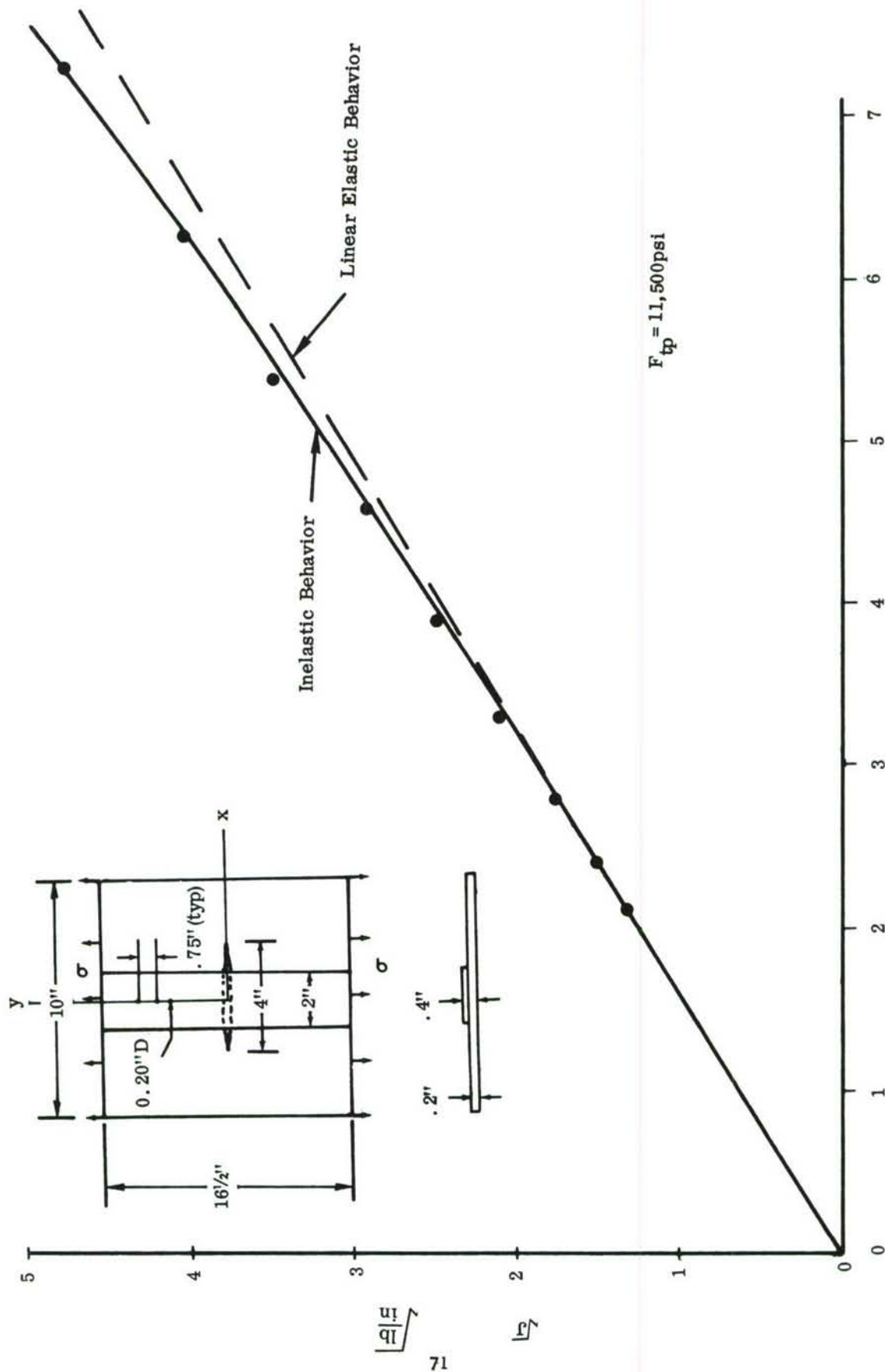


FIGURE 22 NEAR-LINEAR RELATIONSHIP BETWEEN  $\sqrt{J}$  AND APPLIED STRESS FOR CRACKED STIFFENED SHEET



The plastic zones determined using the piecewise linear elastic-plastic procedure are obtained without the necessity of a priori assumptions as to shape. Figure 23 shows the plastic zones corresponding to applied stress levels of 3300 psi, 5400 psi, and 7300 psi. These zones were obtained from the NASTRAN results by identifying those finite elements for which  $\bar{\sigma}$  exceeds  $F_{tp} = 11,500$  psi.

Note that at the highest applied stress level indicated in Figure 23 (viz. 7300 psi), the strap material in the immediate vicinity of the crack experiences a stress of 12,500 psi, and thus load redistribution takes place. The J values given herein thus account for reinforcement yielding.

It should be noted that although no a priori assumptions with regard to plastic zone size and shape are necessary in using the method indicated above this luxury produces lengthy computer runs. If an initial estimate could be made of the plastic zone size, computer runs would be subsequently executed with only the material within the preselected zone being allowed to exhibit elastic-plastic behavior. The material outside the preselected zone would remain elastic for all increments of applied stress, and the corresponding element stiffness matrices would be invariant throughout the loading process. This would reduce computer execution times. In the course of the residual strength method to be developed, this technique will be employed.

Another possibility for treating elastic-plastic behavior more efficiently is when the plastic zone shape for a material can be specified in advance. In particular, when the Dugdale wedge-shaped plastic zone (Reference 33) is a suitable approximation, the technique indicated in the next section is appropriate.

#### 6.1.2 Treatment of Structures Made of Materials Displaying Dugdale-Type Plastic Zones

In the work to be conducted in subsequent Phases, it is anticipated that some of the materials to be treated will display Dugdale-type wedge-shaped plastic zones prior to fracture. The simplicity of the Dugdale approach, the economy associated with its use, and the instances in which Dugdale solutions yield results substantially in agreement with tests are well known features of the Dugdale model.

In the description of a Dugdale problem "a" is a fictitious half-crack length which is related to the real (i.e., the physically existing) half-crack length c by means of "a" = c + plastic zone length. After determining several elastic stress intensity factors for the crack of artificial half-length "a", the solution for the real crack of half-length c is obtained by superposition. The superposition is performed in such a way that stresses remain finite throughout the body. The superposition involves (1) the applied load acting on a structure having an artificial crack of length 2a and (2) a stress equal to the yield stress acting over the length ("a"-c) at each end of the artificial crack (i.e., over the plastic zones). When the solution is completed, the magnitude of applied load necessary to produce a plastic zone of length "a"-c is obtained for a structure having a real crack of half-length c.

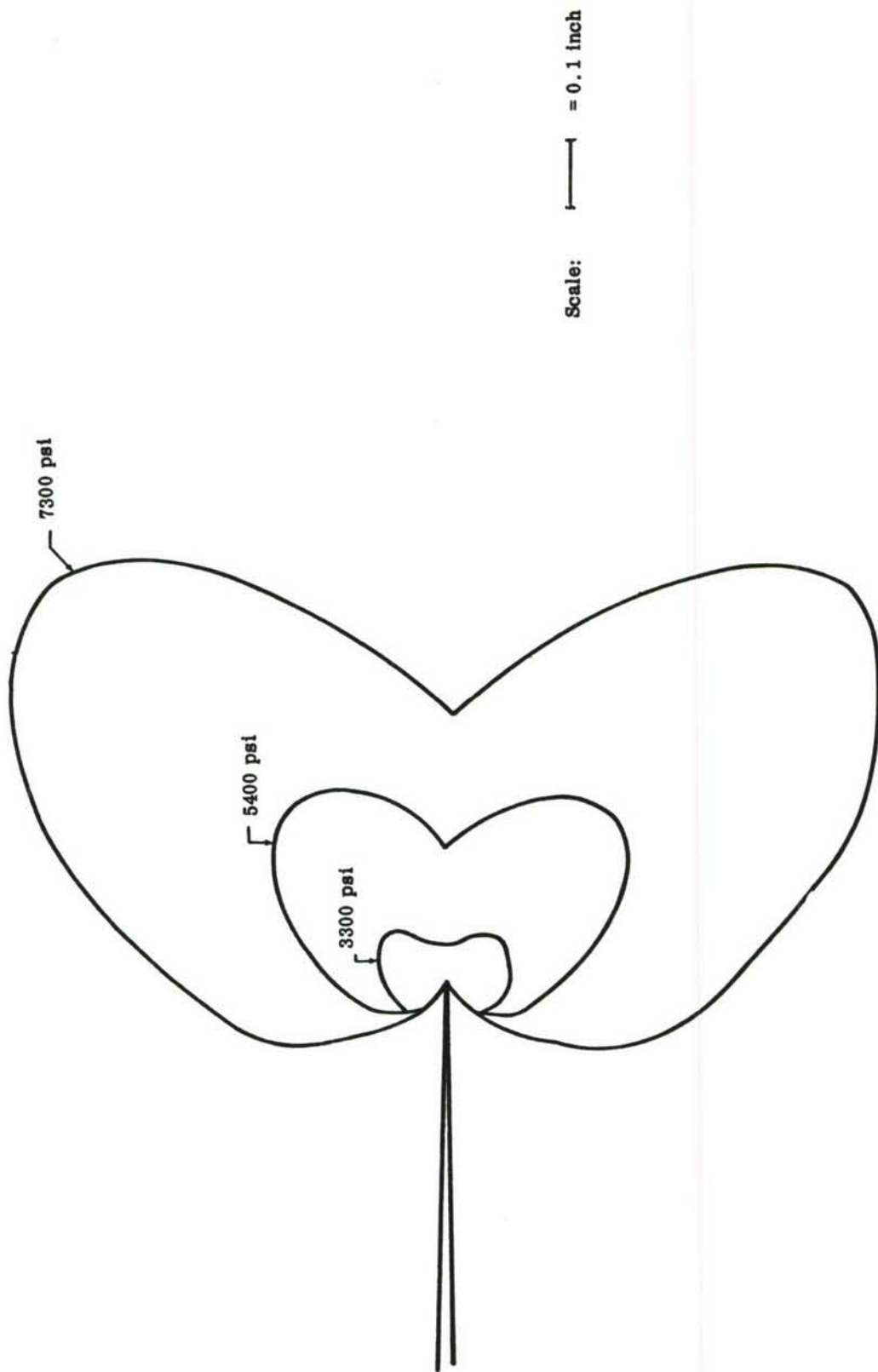


FIGURE 23 PLASTIC ZONES ARISING DUE TO APPLIED STRESS OF 3300, 5400, AND 7300 psi

Notice that the manner of solution involved in the Dugdale approach is such that nonzero crack opening displacements  $\delta$  are predicted in the region between the end of the physical crack and the end of the artificial crack. This, of course, is not possible and is merely a consequence of the simplifications made.

The crack opening displacements  $\delta$  can be related to  $J$  as shown by Rice (Reference 7). Suppose that in Figure 16 the  $\Gamma$  contour used is adjusted such that points 6 and 7 coincide and also points 0 and 1 coincide. Also, suppose points 2, 3, 4, and 5 are displaced to the left and coalesced so that they all are at the origin. If the  $x$  coordinate of points 0, 1, 6, and 7 is selected so that it corresponds to the end of the physically existing crack, the situation is as shown in Figure 24.

Although the  $\Gamma$  contour of Figure 24 is inclined with respect to the  $x$ -axis, the dimensions of the plastic zone are such that the previously derived expressions for a rectangular contour can be used with negligible error. Hence, from column (9) of Table II the expression for  $J$  corresponding to the  $\Gamma$  contour shown in Figure 24 is

$$J = \int_{(x,y)_1}^{(x,y)_2} [\tau_{xy} \left( \frac{\partial u}{\partial x} \right) + \sigma_y \left( \frac{\partial v}{\partial x} \right)] dx + \int_{(x,y)_5}^{(x,y)_6} [\tau_{xy} \left( \frac{\partial u}{\partial x} \right) + \sigma_y \left( \frac{\partial v}{\partial x} \right)] dx \quad (38)$$

In the Dugdale formulation, the stress state existing in the plastic zone is simplified to the point where  $\sigma_y$  is the only nonzero stress component.

Then Equation (38) becomes

$$\begin{aligned} J &= \int_{(x,y)_1}^{(x,y)_2} \sigma_y \left( \frac{\partial v}{\partial x} \right) dx + \int_{(x,y)_5}^{(x,y)_6} \sigma_y \left( \frac{\partial v}{\partial x} \right) dx \\ &= \int_c^a \sigma_y \frac{\partial}{\partial x} (v^-) dx + \int_a^c \sigma_y \frac{\partial}{\partial x} (v^+) dx \\ &= - \int_c^a \left[ \sigma_y \frac{\partial (v^+)}{\partial x} - \sigma_y \frac{\partial (v^-)}{\partial x} \right] dx = - \int_c^a \sigma_y \frac{\partial (v^+ - v^-)}{\partial x} dx \\ &= - \int_c^a \sigma_y \frac{\partial \delta}{\partial x} dx \end{aligned}$$

where  $v^+$  and  $v^-$  are the displacements at the upper and lower crack surfaces, respectively, and  $\delta$ , the crack opening displacement, is given by

$$\delta = v^+ - v^- .$$



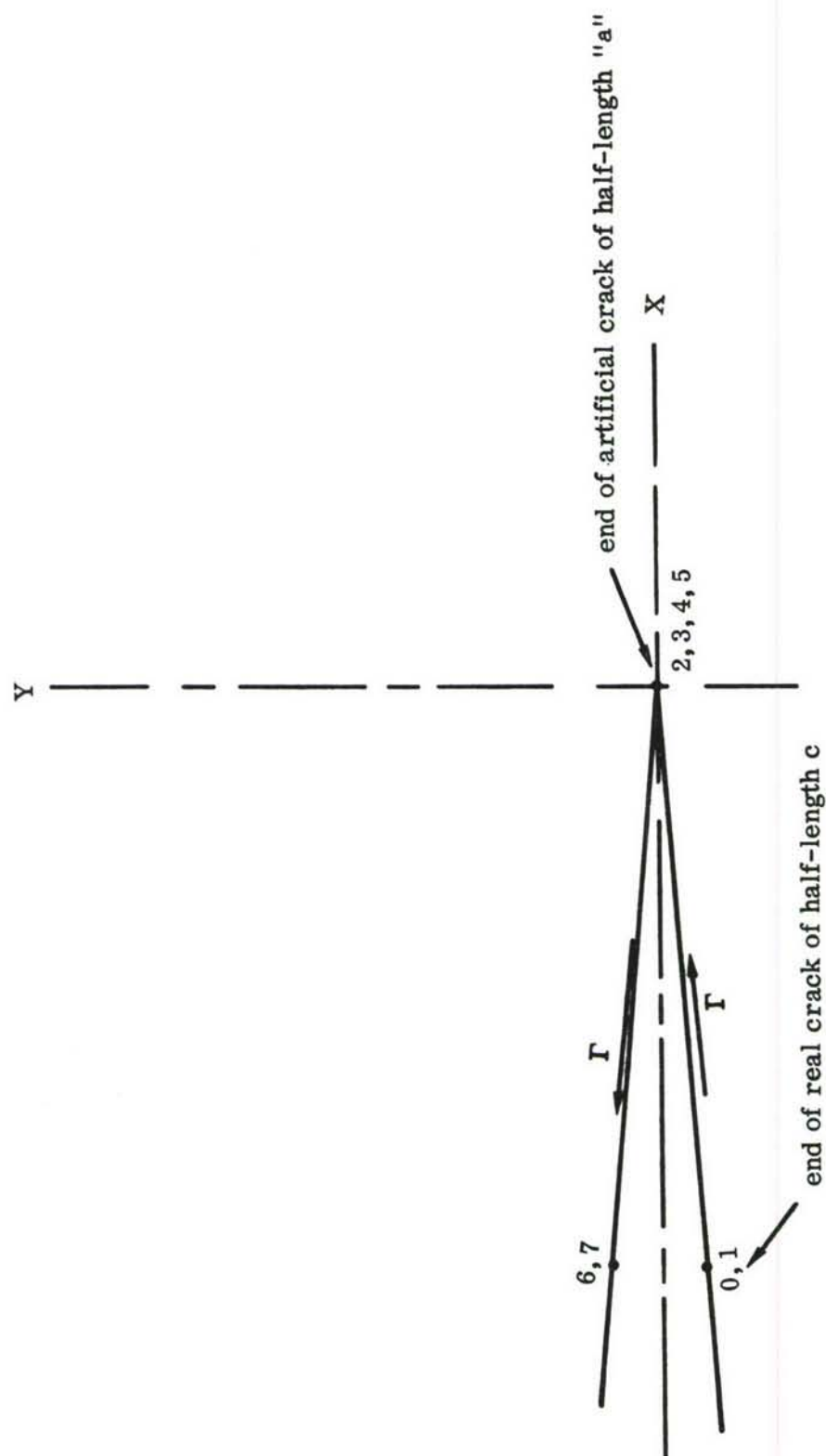


FIGURE 24  $\Gamma$  CONTOUR USED IN J CALCULATION FOR DUGDALE-TYPE MATERIALS

Since  $\sigma_y (=F_{ty})$  is constant in the plastic zone,

$$J = \sigma_y \delta_c = F_{ty} \delta_c \quad (39)$$

Equation (39) is the desired relation between crack opening displacement at the physical crack tip  $\delta_c$  and  $J$ . Hence, in order to calculate  $J$ , one need only find  $\delta_c$  and then multiply by  $F_{ty}$ .

#### 6.1.2.1 Example Problem

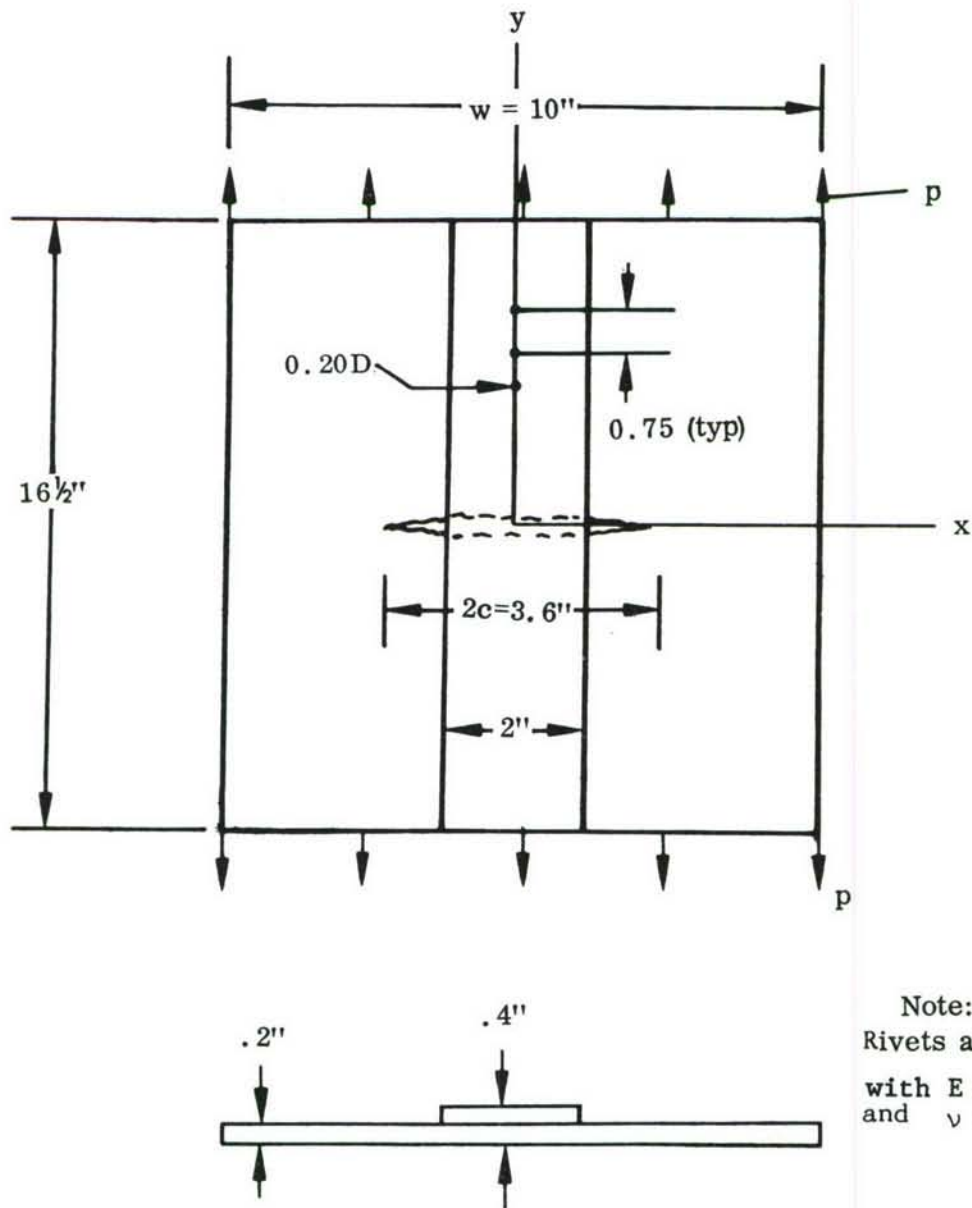
Recently Hayes and Williams (Reference 61) presented a method which allows Dugdale model crack tip plasticity solutions to be obtained in a straightforward manner. The approach uses the Buekner method (Reference 62) which has been shown to give highly accurate results.

In this report, the Reference 61 method will be applied to the cracked, stiffened sheet shown in Figure 25. The physical crack length,  $2c$ , is 3.6 inches as indicated, and the crack aspect ratio  $\frac{2c}{W} = 0.36$ . The method assumes a series of plastic zone lengths and then determines the corresponding value of the remotely applied stress  $p$  necessary to give rise to each of the plastic zone lengths.

The calculations involved in performing the Dugdale solution are summarized in Table IV. Twenty separate problems were considered and subsequently superimposed to arrive at the desired result. Actually, one NASTRAN finite element run (using the idealization of Figure IV and consisting of 20 subcases) was executed. The run required 8.44 minutes of CPU time and 5.65 minutes of I/O time on an IBM 370/165 computer. All 20 subcases were elastic solutions, and, as indicated in Table IV, ten subcases were fully loaded cracks and ten subcases partially loaded cracks. In each of the 20 subcases a stress of 10 ksi was applied over either the entire crack half surface (a) or over only the plastic zone length (a) - c. All cases considered were symmetrical cracks about the panel centerline.

In employing the Buekner method (Reference 62) to perform the elastic calculations the first step is to calculate the strain energy  $U_d$  corresponding to Buekner's "difference state." In equation form

$$U_d = - \frac{1}{2} \int_s T_i^0 u_i ds = - \frac{1}{2} \int_s [T_x^0 u + T_y^0 v] ds \quad (40)$$



Note: Sheet, Strap and Rivets are all made of steel, with  $E = 30 (10^6)$  psi and  $\nu = .3$

FIGURE 25 CRACKED STIFFENED SHEET



TABLE IV. CALCULATIONS FOR DUGDALE PROBLEM

1	2	3	4	5	6	7	8	9	10
Plastic Zone Length Inches	a = c + Plastic Zone	Fully Loaded Crack			Partially Loaded Crack			$\frac{p}{F_{ty}}$	$\delta_c/2$ in.
		$\frac{U_d}{in.-lb.}$ in.	$\frac{\partial U_d}{\partial a} = G$ lb/in.	$V_c * 10^4$ in.	$\frac{U_d}{in.-lb.}$ in.	$\frac{\partial U_d}{\partial a} = G$ lb/in.	$V_c * 10^4$ in.		
.10	1.90	11.214	10.660	2.8294	.0560	0.562	.5599	.230	.4934x10 <sup>-4</sup>
.15	1.95	11.747	12.200	3.5023	.0841	0.944	.5617	.278	.2237x10 <sup>-3</sup>
.20	2.00	12.434	12.610	4.2062	.1504	1.445	.7612	.338	.3586x10 <sup>-3</sup>
.25	2.05	13.008	12.530	4.6792	.2286	1.827	.9284	.381	.4639x10 <sup>-3</sup>
.30	2.10	13.687	13.815	5.1927	.3331	2.565	1.1257	.431	.6040x10 <sup>-3</sup>
.40	2.20	15.196	13.785	6.1296	.6634	3.032	1.5570	.469	.7155x10 <sup>-3</sup>
.60	2.40	17.948	16.477	7.5617	1.3631	5.254	2.2541	.565	1.0959x10 <sup>-3</sup>
.80	2.60	21.787	18.560	9.0379	2.7650	6.923	3.1349	.611	1.2963x10 <sup>-3</sup>
1.00	2.80	25.372	18.280	10.293	4.1326	7.463	3.8873	.640	1.4662x10 <sup>-3</sup>
1.20	3.00	29.099	18.635	11.396	5.7502	8.088	4.5969	.658	1.5756x10 <sup>-3</sup>

where  $U_d$  is the change in energy or energy difference between the uncracked and cracked configurations. In Equation (40),  $T_i^o$  represents stresses that exist in the crack-free body at the locations where the crack will subsequently be introduced, and  $s$  is one half of the (symmetrical) crack surface area per unit thickness. In the case of an uncracked strap stiffened sheet (where both strap and sheet are the same thickness and have the same modulus) subjected to an external tensile stress  $\sigma_y = 10,000$  psi, a uniform stress state is induced. Thus,  $T_x^o = 0$  and  $T_y^o = 10,000$  psi = 10 ksi. The quantities  $u_i$  in Equation (40) are the components of displacement on the crack face due to the tractions  $T_i^o$  applied to the crack faces in a reversed sense acting alone. In the present case Equation (40) reduces to

$$U_d = -\frac{1}{2} \int_s T_y^o v \, ds \quad (41)$$

and the  $v$  displacements can be found from a finite element run where the crack surface is loaded with a uniform stress of  $-T_i^o$  ( $= -10$  ksi), but the panel is otherwise unloaded. Note that this loading causes negative  $v$  displacements. By symmetry, Equation (41) can be written

$$U_d = - \int_0^a T_y^o v \, dx \quad (42)$$

where  $U_d$  has units of, for example,  $\frac{\text{in.-lb.}}{\text{in.}}$  or lb.

Numerical integration of Equation (42) is performed according to

$$U_d \approx -T_y^o \sum_{i=1,2,3,\dots} v_i \Delta x_i = - \sum_{i=1,2,3,\dots} P_i v_i \quad (43)$$

where  $\Delta x_i$  are finite increments associated with the grid points on the crack face.

Values of  $U_d$  corresponding to the elastic solutions for cracks of length  $2a$  are given in column 3 of Table IV for the fully loaded crack. The values of  $U_d$  for the partially loaded crack, loaded over the lengths  $a$ - $c$  and corresponding to the plastic zone, are presented in column 6 of Table IV. The evaluation of Equation (43) using NASTRAN-generated displacement results was accomplished using a simple RAX computer program.

Columns 4 and 7 give values of  $\partial U_d / \partial a$  for the fully loaded and partially loaded cases, respectively. The values were obtained numerically by using central difference formulas, except at  $a = 1.90$  and  $a = 3.00$ , where forward and backward differences were used, respectively. In assessing the results shown in Column 4 of Table IV, note that, while in general  $\partial U_d / \partial a$  ( $= G$ ) increases

with  $a$ , in three instances (at  $a = 2.05$ ,  $a = 2.20$ , and  $a = 2.80$ ) it appears that  $\partial U_d / \partial a$  decreased with  $a$ .

One might think that the anomalous behavior could be resolved by employing more significant figures in the values of  $U_d$  used in forming the numerical derivatives. This was done and little improvement in the values of  $\partial U_d / \partial a$  was noted. The trouble arises because of the idealization used. An idealization consisting of a fine mesh size in the vicinity of the crack tip which gradually becomes more coarse away from the crack tip is suitable for the analysis of a single crack length problem (for example, such an idealization was found quite adequate for the problem discussed in Section 6:1.1.1). In the present case, when one is interested in a series of crack lengths, a more suitable choice appears to be a grid system which employs uniformly spaced nodes over the entire range of interest. This is the type of idealization used by Hayes and Williams in Reference 61. When such a grid is used, the  $\Delta x$  values in Equation (43) are all the same and hence the calculation  $U_d$  by summing a series of terms is a more accurate approximation to the integral of Equation (42) than when large differences in the  $\Delta x$  values exist (as in the present case). This requirement for uniform grid spacing in the region of interest should be adhered to (insofar as practically possible) in any future calculations.

Columns 5 and 8 of Table IV give the  $v$  displacements at the physical crack tip (i.e., at  $x = c$ ). The superposition of the elastic solutions which really embodies the Dugdale approach is performed in Columns 9 and 10. Finiteness of stresses at  $x = c$  is ensured by requiring that the net stress intensity factor due to the remote loading applied in conjunction with the yield stress loading (applied in the plastic zone) vanishes. This occurs when the ratio of applied stress  $p$  to the yield stress  $F_{ty}$  is given by

$$\frac{p}{F_{ty}} = \left[ \frac{\left( \frac{\partial U_d}{\partial a} \right) \text{ column 7}}{\left( \frac{\partial U_d}{\partial a} \right) \text{ column 4}} \right]^{\frac{1}{2}} \quad (44)$$

Values obtained using Equation (44) (listed in Column 9) are the ratios of applied stress to yield stress necessary to produce Dugdale type yield zones of the sizes indicated, assuming an initial crack of  $2c = 3.6$  inches (see Figure 25).

When the externally applied stress ( $p$ ) is applied with the magnitudes given in Column 9 of Table IV, the resulting displacements at the crack tip are given by



$$\frac{\delta}{2} = \frac{p}{(10 \text{ ksi})^*} \left[ \begin{matrix} (v_c) \\ \text{column 5} \end{matrix} \right] - \frac{F_{ty}}{10_{\text{ksi}}} \left[ \begin{matrix} (v_c) \\ \text{column 8} \end{matrix} \right] \quad (45)$$

$$\delta = \frac{2 F_{ty}}{(10_{\text{ksi}})^*} \left[ (\lambda) \left( \begin{matrix} (v_c) \\ \text{column 5} \end{matrix} \right) - \left( \begin{matrix} (v_c) \\ \text{column 8} \end{matrix} \right) \right]$$

and  $\lambda$  are the values given in Column 9 of Table IV. Assuming  $F_{ty} = 54.3 \text{ ksi}$  for the steel of interest (representing a high toughness-low strength steel), the resulting values of  $\frac{\delta_c}{2}$  are given in Column 10 of Table IV.

The information contained in Columns 9 and 10 of Table IV is plotted in Figures 26 and 27 respectively. From these plots one can read off the plastic zone size and crack opening displacement resulting from a given externally applied stress for material exhibiting a Dugdale type plastic zone at the crack tip. Having  $\delta_c$ , one can compute the corresponding J from Equation (39).

#### 6.1.3 Indicated Direction of Analytical Approach - Planned Residual Strength Prediction Technique

The discussion presented in Sections 6.1.1 and 6.1.2 indicates that several alternatives are available in the area of candidate analysis methods. The best candidate analytical parameter to be used to characterize the crack tip environment appears to be the J integral. Plasticity can be accounted for in the following ways, all of which are compatible with the J integral approach:

Plasticity Theory	Need for a priori Plastic Zone Specification		Cost of Computer Solution
	Size	Shape	
Prandtl-Reuss	arbitrary	arbitrary	relatively high
Prandtl-Reuss	pre-selected	arbitrary	moderate
Dugdale	arbitrary	pre-selected	relative in-expensive

---

$(10_{\text{ksi}})^*$  A stress of 10ksi was applied over the crack and plastic zone for convenience. Any stress may be chosen for a given problem.

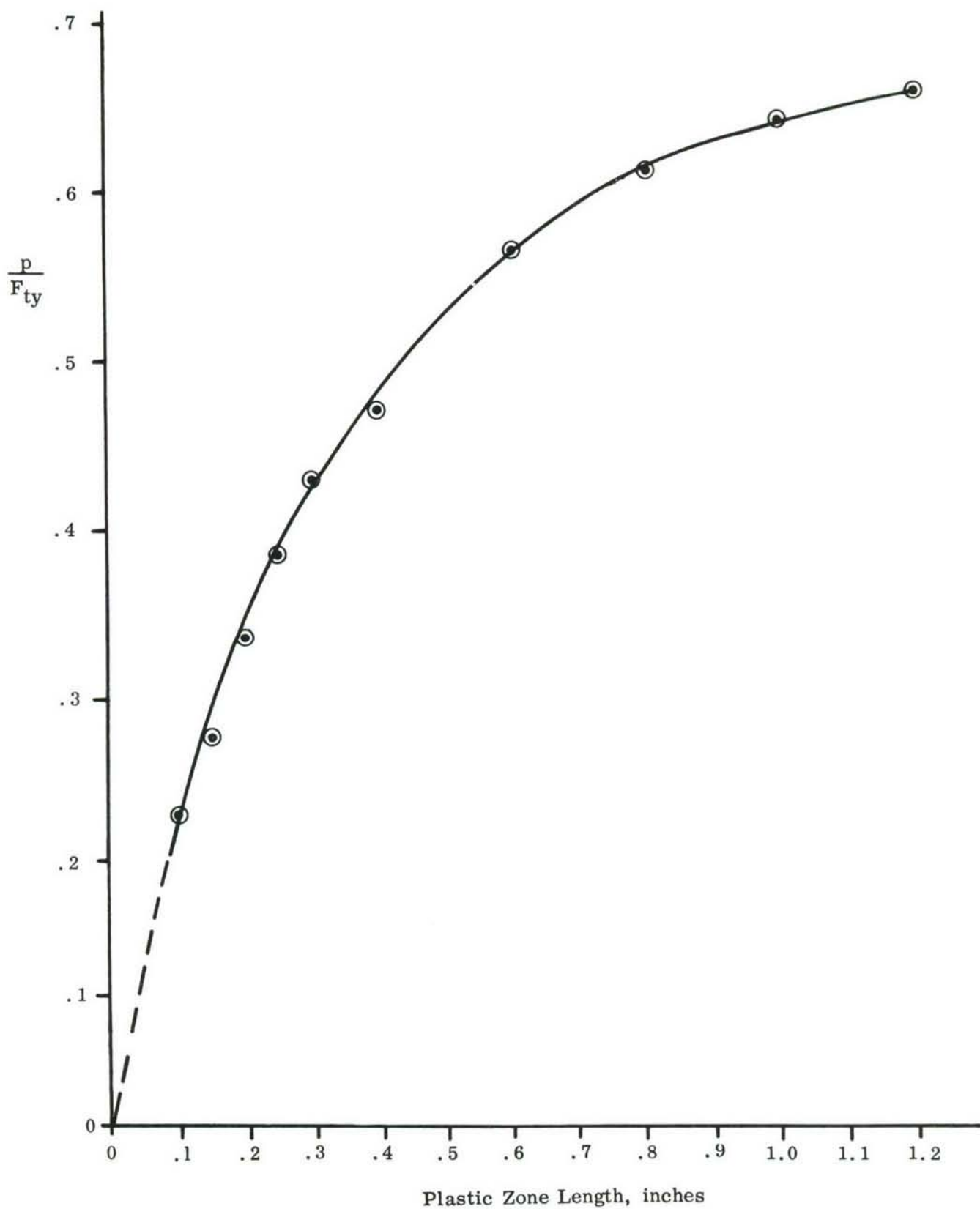


FIGURE 26 APPLIED TENSILE STRESS-PLASTIC ZONE LENGTH RELATIONSHIP

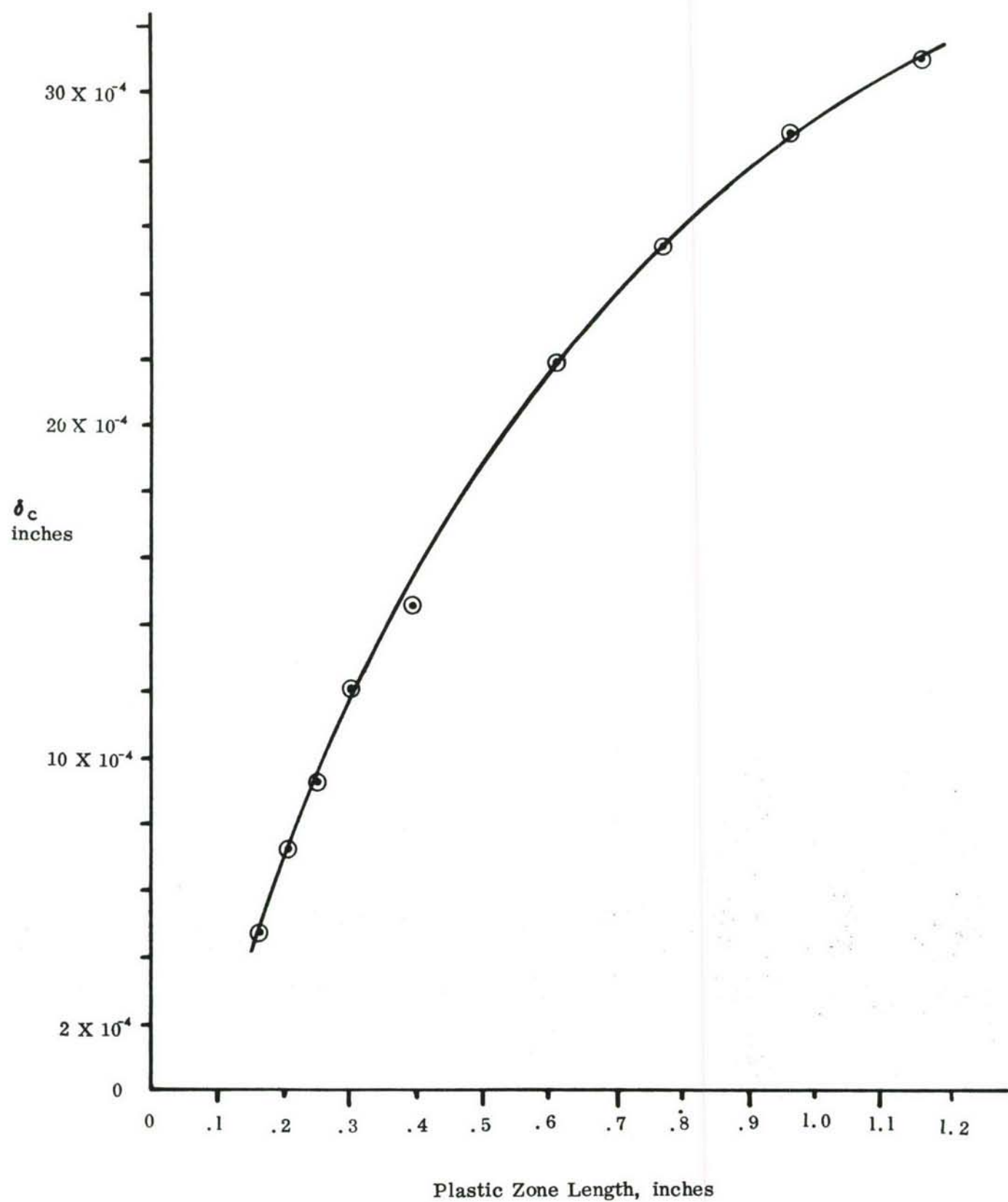


FIGURE 27 CRACK OPENING DISPLACEMENT - PLASTIC ZONE SIZE RELATIONSHIP



As emphasized in Sections 6.1.1 and 6.1.2, complete freedom from a priori plastic zone specification is possible, but the results are quite costly. Preselection of zone size and/or shape can bring costs down as indicated above.

A possibility apparently exists for wider use of the Dugdale model. Hayes (Reference 5) points out by means of examples that even though the Dugdale model may be physically inappropriate for a given material (i.e., the plastic zones displayed by the material may not resemble the wedge shaped zones assumed in the Dugdale formation), J values computed assuming Dugdale behavior may not differ significantly from more rigorously determined J values using the procedure outlined in Section 6.1.1. Perhaps such a correspondence exists for the materials to be considered in other phases of this program. If so, use of the Dugdale model would allow residual strength predictions to be made more economically (and without introduction of undue inaccuracies) than if strict adherence to the Section 6.1.1 procedure is maintained.

It might seem peculiar that the candidate analysis methods all utilize conventional finite elements. The recently developed elements (References 63 and 64) which specifically contain required singularities in assumed strain distribution appear extremely attractive when elastic problems are being treated. Developmental work is currently underway under Air Force Flight Dynamics Laboratory sponsorship (Contract F33615-72-C-1739) aimed at specifically treating singularities as well as permitting material non-linearity in the immediate crack tip vicinity. While this work will be monitored throughout the course of the present investigation, it is felt that plane stress fracture implies large plastic zones, and hence a capability which requires size limited plasticity is not expected to be utilized. If and when the technique is extended to treat large scale plasticity, it is recommended that it be incorporated into the residual strength prediction technique to be developed in this investigation.

## 6.2 CANDIDATE FAILURE CRITERION

As discussed in Section 6.1, the J integral has been selected as the parameter to describe the crack tip environment. The failure criterion to be used in the residual strength prediction technique will be a generalized  $J_{cr}$  criterion. Details of the criterion to be used are given in Section 6.2.1.

The reasons for the selection of J as the "crack environment describer" have been outlined in Section 6.1. It must be acknowledged that although J represents a generalization of previously advanced "environment describers" such as G, K, and C.O.D., parameters which are even more all-encompassing than J are currently under development. In particular, a concept which shows considerable promise is the field energy approach (Reference 65). This approach assumes that the energy per unit area released when a new crack surface is created can be related to  $S/r$ . In this approach r is the

radial distance from the present crack tip (assumed small but nonzero) and  $S$ , the strain energy density factor, represents the intensity of the  $1/r$  energy field. The direction of crack initiation is determined by finding  $\theta$  such that

$$\frac{\partial S}{\partial \theta} = 0.$$

The existence of crack growth depends on whether or not the value of  $S$  equals the critical value  $S_{cr}$ . The "S" approach has the virtue of being directionally sensitive. Thus cases of complex loading and angled cracks can be treated. At present, however, the method appears to be limited to cases involving limited plasticity at the crack tip, and thus, although promising for future use, it will not be used in the method to be developed for plane stress fracture.

#### 6.2.1 Basis for the $J_{cr}$ Failure Criterion

The use of a critical value of  $J$  as a failure criterion has been suggested by Begley and Landes (Reference 8). They point out, however, that any crack extension necessarily implies unloading near the crack tip resulting in multi-valued  $W$  and  $J$  quantities as has been shown in Section 6.1.1. Therefore they ruled out situations which involved significant subcritical crack growth (slow crack growth) and focused attention on the plane strain case.

The aim of this investigation is to treat plane stress fracture. Hence the problems of subcritical crack growth and attendant unloading at the crack tip must be addressed.

As indicated in Section 5.5.1, the crack growth resistance curve (i.e., the  $R$  curve) appears to provide a useful means for describing the amount of slow stable crack growth which each material exhibits for a given initial crack length. The  $R$  curve shows promise of being an intrinsic material property for fixed values of the following parameters:

- . material
- . thickness
- . temperature
- . strain rate
- . environment.

The technique of utilizing an  $R$  curve in conjunction with plots of  $K$  versus crack length for selected values of applied stress or load has been discussed in Reference 66. The procedure utilizes a tangency condition between the  $R$  curve and a  $K$  curve to determine the fracture stress  $\sigma$  and the associated value of critical crack half-length " $a$ ". The technique appears attractive in the manner in which slow tear is accounted for, but the treatment of plasticity appears to be confined to local crack tip yielding.



Although the discussion to this point would tend to give one the impression that plasticity and slow stable crack extension are separate and distinct phenomena, there does exist a subtle relationship between the two. This has been discussed in Reference 67. The existence of large scale yielding implies a significant amount of material "forgiveness." This tends to increase the amount of slow crack growth which can take place prior to fracture. In order to be in a position to account for plasticity and slow tear in as explicit a manner as possible, the "R" curve concept will be generalized to a  $J_{cr}$  curve concept in the to be developed method.

Just as one can generate an R curve from a series of specimens having varying initial crack lengths, one can establish from these same specimens a  $J_{cr}$  versus "a" curve. Although it will require some confirmative testing, it seems plausible that a  $J_{cr}$  versus "a" curve can be viewed in the same manner as an R curve, that is, as an intrinsic material property.

The tangency criterion suggested in Reference 66 could be generalized so that, instead of working with K and R, one now seeks tangency between the  $J_{cr}$  versus "a" curve and analytically determined J versus "a" curves (determined for a series of applied stress values). As in the K versus R curve case, the tangency point will indicate fracture stress and critical crack size at fracture instability.

The manner in which the J curves would be established requires some discussion. Either Dugdale or Prandtl-Reuss plasticity will be assumed (see Sections 6.1.1 and 6.1.2). A series of J versus applied stress curves for a number of assumed crack lengths would be obtained similar to the one shown in Figure 21. By cross plotting the data, a plot of J versus "a" for selected  $\sigma$  values can be developed as indicated by the solid curves of Figure 28. Notice that in the calculation of the points necessary to establish the solid curves of Figure 28 (i.e., the so-called J curves) a series of problems are solved involving prescribed crack lengths. Therefore the problem of crack extension does not enter in the solution of any given problem. It is assumed, however, that the material is homogenous and its behavior (as shown, for example, by Figure 19) is the same for all crack lengths. That is, whatever process caused the crack to appear initially, the material is considered homogenous throughout, regardless of the initial crack length.

In the use of the J curves in predicting fracture (as opposed to the analytical determination of the J curves) the aspect of slow tear (stable crack extension) is very much present. It has been pointed out in Section 6.1.1 that crack extension involves unloading. Rigor dictates that due to the multivalued nature of W and J when unloading exists, the solid curves in Figure 28 should not be used in cases of crack extension. In the course of the development of the residual strength prediction technique, two avenues of approach will be investigated to solve this problem and are discussed below.



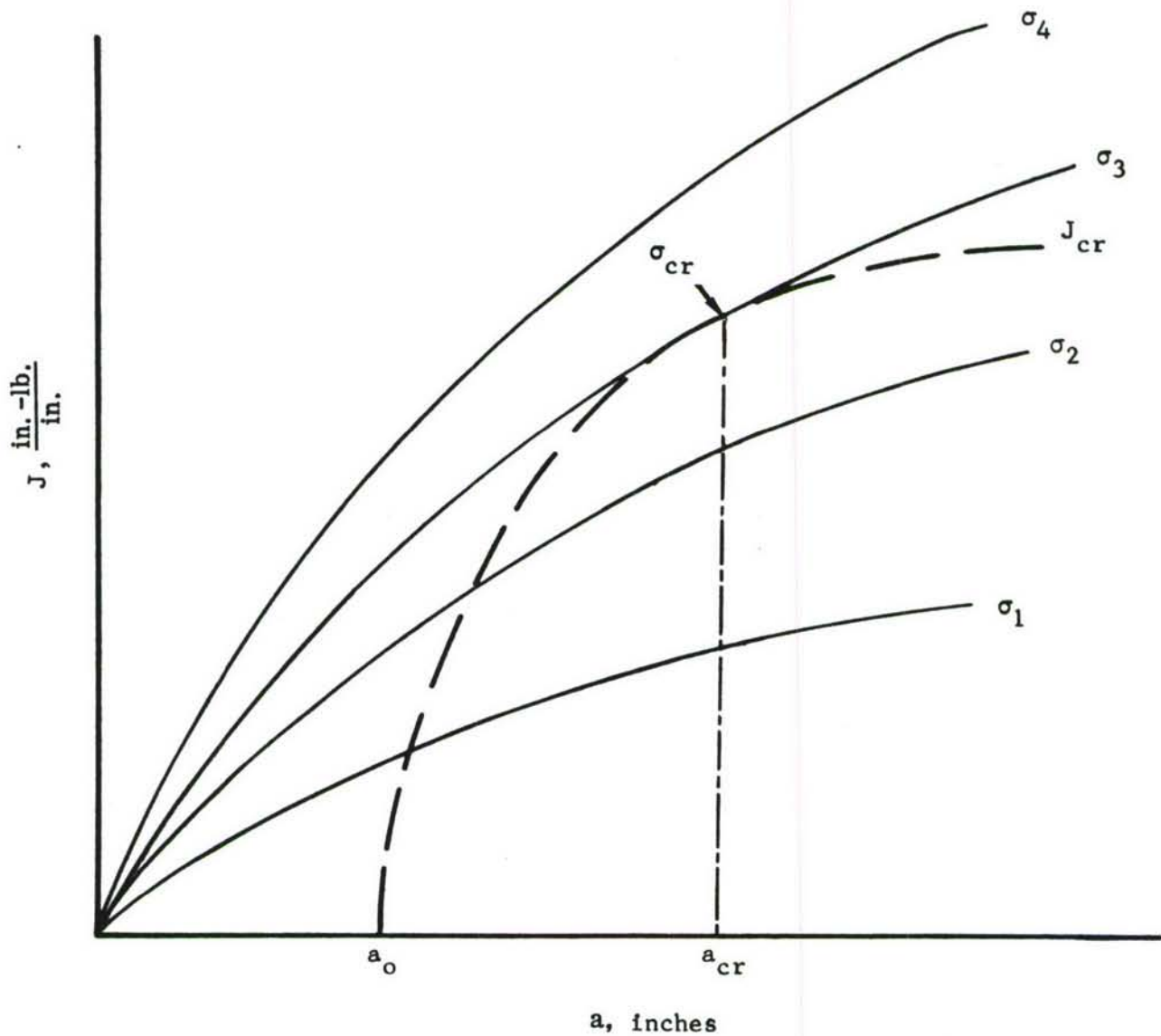


FIGURE 28 RESIDUAL STRENGTH TANGENCY CONDITION SHOWING CRITICAL STRESS  $\sigma_{cr}$  AND CRITICAL CRACK HALF LENGTH  $a_{cr}$  AT FRACTURE INSTABILITY

It may turn out for some materials that the difference between a rigorously correct  $J$  (which accurately incorporates the unloading and redistribution associated with an extending crack) and a  $J$  found in a sequential manner (by considering incremental crack growth and the original stress-strain diagram throughout) is negligible. The error introduced in calculating  $J$  sequentially is a result of the fact that material near the former crack tip which had been loaded plastically, has been work hardened so that this material behaves differently from the material which has not been previously loaded into the plastic range. Ignoring the work hardening associated with prior loading affects primarily the contributions to the  $J$  integral from those portions of the  $\Gamma$  contour in back of the crack tip (i.e., segments 0-1 and 6-7 in Figure 16). Of course it is also recognized that the load redistribution is felt to some extent throughout the entire body. On the basis of a number of computer runs, it has been found that segments 0-1 and 6-7 in Figure 16 have a relatively minor influence on the final value of  $J$ . Hence there is some reason for believing that for some materials a sequential determination of  $J$  for a series of increasing crack lengths may not significantly deviate from the  $J$  actually associated with an extending crack.

If the approximation referred to in the previous paragraph is inappropriate for a given material, it may be feasible to use the basic tangency criterion (Figure 28) to determine residual strength provided that modified  $J$  curves are employed to account for unloading associated with crack extension. It may be possible to empirically establish crack extension factors which could convert the  $J$  curves of Figure 28 (established without specifically treating crack extension) to "actual"  $J$  curves which would include crack extension (and unloading). These modified  $J$  curves would then be used in applying the tangency condition to establish residual strength.

Although the  $J$  and  $J_{cr}$  curves discussed in this section have been restricted to a specific environment, temperature, strain rate, etc., it may be possible at some future date to specify residual strength of a cracked structure for arbitrary strain rate, environment, etc., by interpolating data. Obviously the present state of knowledge is very much deficient in its ability to be able to treat problems of a general nature. The method to be developed will begin to rectify the deficiency, but a complete "ideal" method is clearly out of the question at this stage.

### 6.3 MATERIAL PROPERTY DATA REQUIREMENTS

Based on the anticipated requirements of the residual strength analysis method, determination of the following material properties will be required.

1. Full range stress-strain data
2. Strain rate, stress-strain data
3. Crack growth resistance
4. Slow tear
5. Crack opening displacements
6. Plastic zone geometries
7. Crack tip buckling
8. Others (e.g., Moduli, etc.)

Items 1 and 2 can be obtained from normal stress-strain testing. In some instances testing at temperature will be required. The crack growth resistance data will supply the necessary data for items 3 and 4. The plastic zone (surface) size (item 6) can be readily observed using suitable optical techniques. Normal compliance and strain gage techniques can be employed to determine item 5, and crack tip buckling can be determined by direct comparison with an unbuckled configuration.

Other material properties which are found to be necessary as input for the developed method will be evaluated on an individual basis. From other sections of this report, the shape of the stress-strain curve and plastic zone as well as crack opening displacement become quite important to a J critical approach. Therefore those material properties which affect these items (1, 5, and 6) will require additional study--particularly the "environmental" influences.



## REFERENCES

1. Gran, R. J., et al, "Investigation and Analysis Development of Early Life Aircraft Structural Failures," AFFDL-TR-70-149, March 1971.
2. Swift, T., "Development of the Fail-Safe Design Features of the DC-10," in Damaged Tolerance in Aircraft Structures, ASTM STP 486, American Society for Testing and Materials, 1971.
3. Brown, Jr., W. F., and Srawley, J. E., "Comment on Present Practice," American Society for Testing and Materials, ASTM STP 463.
4. Hahn, G. T. and Rosenfield, A. R., "Sources of Fracture Toughness: The Relation Between  $K_{Ic}$  and the Ordinary Tensile Properties of Metals," Paper presented at ASTM Symposium on Titanium, Los Angeles, April 1967.
5. Hayes, D. J., "Some Applications of Elastic-Plastic Analysis to Fracture Mechanics," Ph.D. Thesis, Department of Mechanical Engineering, Imperial College, University of London, October 1970.
6. Heyer, R. H. and McCabe, D. E., "Crack Growth Resistance in Plane-Stress Fracture Testing," Engineering Fracture Mechanics, Vol. 4, pp. 413-430 (1972).
7. Rice, J. R., in Fracture, H. Liebowitz, Editor, Vol. 2, Academic Press, New York, 1968.
8. Begley, J. A. and Landes, J.D., "The J Integral as a Fracture Criterion," in American Society for Testing and Materials, Fracture Toughness, Proceedings of the 1971 National Symposium on Fracture Mechanics, Part II, ASTM STP 514, 1972.
9. Landes, J. D. and Begley, J. A., "The Effect of Specimen Geometry on  $J_{Ic}$ ," in American Society for Testing and Materials, Fracture Toughness, Proceedings of the 1971 National Symposium on Fracture Mechanics, Part II, ASTM STP 514, 1972.
10. Bucci, R. J., et al, "J Integral Estimation Procedures," in American Society for Testing and Materials, Fracture Toughness Proceedings of the 1971 National Symposium on Fracture Mechanics, Part II, ASTM STP 514, 1972.
11. Kuhn, P., and Hardrath, H. F., "An Engineering Method for Estimating Notch-Size Effect in Fatigue Tests on Steel," NACA TN 2805, 1952.
12. Neuber, H., Theory of Notch Stresses: Principles for Exact Stress Calculation, J. W. Edwards, Publisher, Ann Arbor, Michigan, 1946.

13. Kuhn, P., and Figge, I. E., "Unified Notch-Strength Analysis for Wrought Aluminum Alloys," NASA TN D-1259, 1962.
14. Hardrath, H. F. and Ohman, L., "A Study of Elastic and Plastic Stress Concentration Factors due to Notches and Fillets in Flat Plates," NASA TR 1117, 1953.
15. Dixon, J. R., "Stress Distribution Around a Central Crack in Plate Loaded in Tension; Effect of Finite Width of Plate," Journal of Royal Aeronautical Society, 1960.
16. Dixon, J. R., "Stress Distribution Around Edge Slits in a Plate Loaded in Tension - The Effect of Finite Width of Plate," Journal of Royal Aeronautical Society, 1962.
17. Kuhn, P., "Residual Strength in the Presence of Fatigue Cracks," Paper presented to AGARD, Structures and Materials Panel, 1967. (Also NASA Report - unpublished.)
18. Kuhn, P., "Strength Calculations for Sheet-Metal Parts with Cracks," Materials Research and Standards, Vol. 8, No. 9, September 1968.
19. Wilhem, D. P., "Fracture Mechanics Guidelines for Aircraft Structural Applications," AFFDL-TR-69-111, December 1969.
20. Kuhn, P., "Residual Tensile Strength in the Presence of Through Cracks or Surface Cracks," NASA TN D-5432, March 1970.
21. Crichlow, W. J., "The Ultimate Strength of Damaged Structure-Analysis Methods with Correlating Test Data," in Full Scale Fatigue Testing of Aircraft Structures, F. J. Plantema & J. Schijve editors, Pergamon Press, 1961.
22. Crichlow, W. J. and Wells, R. H., "Crack Propagation and Residual Static Strength of Fatigue-Cracked Titanium and Steel Cylinders," ASTM STP 415, July 1966.
23. Crichlow, W. J., "Stable Crack Propagation-Fail-Safe Design Criteria-Analytical Methods and Test Procedures," Paper No. 69-215 presented at AIAA/AHS VTOL Research, Design and Operations Meeting of AIAA, February 1969.
24. Crichlow, W. J., "The Materials-Structures Interface, A Systems Approach to Airframe Structural Design," Paper presented to AIAA/ASME 10th Structures, Structural Dynamics and Materials Conference, April 1969.
25. Lomack, O. and Vanderveldt, H., "Critical Review of Fracture and Fatigue Analysis," Naval Ship Research and Development Center Report 3655, March 1972.



26. Griffith, A. A., "The Phenomena of Rupture and Flow in Solids," Proc. Royal Society, Series A 221, p. 163, 1921.
27. Griffith, A. A., "The Theory of Rupture," Proceedings of the First International Congress Applied Mechanics, Delft, 1924.
28. Irwin, G. R., "Relation of Stresses Near a Crack to the Crack Extension Force," 9th International Congress Applied Mechanics, Brussels, 1957.
29. Isida, M. and Itagaki, Y., "Stress Concentration of the Tip of the Central Transverse Crack in a Stiffened Plate Subjected to Tension," Proceedings of the Fourth U. S. National Congress of Applied Mechanics, Vol. 2, 1962.
30. Bloom, J. M., "The Effect of a Riveted Stringer on the Stress in a Sheet with a Crack or a Cutout," Office of Naval Research Report No. 20, June 1964, (AD 603693).
31. Poe, Jr., C. C., "The Effect of Riveted and Uniformly Spaced Stringers on the Stress Intensity Factor of a Cracked Sheet," in Proceedings of Air Force Conference on Fatigue and Fracture of Aircraft Structures and Materials, AFFDL TR 70-144, December 1969.
32. Vlieger, H., "Residual Strength of Cracked Stiffened Panels," National Aerospace Laboratory NLR, Netherlands, NLR-TR 71004U, January 1971.
33. Dugdale, D. S., "Yielding of Steel Sheets Containing Slits," J. Mech. Phys. Solids, 1960, Vol. 8, pp. 100 to 104.
34. Swedlow, J. L., "The Thickness Effect and Plastic Flow in Cracked Plates," Office of Aerospace Research, ARL 65-216, Wright-Patterson Air Force Base, Ohio.
35. Liu, A. F., "Statistical Variation in Fracture Toughness Data of Airframe Materials," in Proceedings of the Air Force Conference on Fatigue and Fracture of Aircraft Structures and Materials, AFFDL TR-70-144, Dec. 1969.
36. McCabe, D. E., "Evaluation of the Compact Tension Specimen for Determining Plane Strain Fracture Toughness of High Strength Materials," Journal of Materials, Vol. 7, No. 4, December 1972.
37. Freed, C. N., et al, "Crack Growth Resistance Characteristics of High-Strength Sheet Alloys," Naval Research Laboratory Report, NRL Report 7374, January 1972.
38. Ekvall, J. C., et al, "Engineering Criteria and Analysis Methodology for the Appraisal of Potential Fracture Resistant Primary Aircraft Structure," AFFDL TR-72-80, 1972.
39. Brown, Jr., W. F. and Srawley, J. E., "Plane Strain Crack Toughness Testing of High Strength Metallic Materials," American Society for Testing and Materials STP 410, 1966.



40. AFFDL TR-70-144, Proceedings of the Air Force Conference on Fatigue and Fracture of Aircraft Structures and Materials, 1969.
41. Broek, D., "Concepts in Fail-Safe Design of Aircraft Structures," Battelle Memorial Institute Report dated March 1971.
42. Swift, T., "The Application of Fracture Mechanics to the Design of Damage-Tolerant Stiffened Aircraft Structure," paper presented to American Society for Metals, 1972, WESTEC Conference, March 1972, also Douglas Aircraft Company Paper 5981.
43. Krafft, J. M., et al, "Effect of Dimensions on Fast Fracture Instability of Notched Sheets," in Proceedings of the Crack Propagation Symposium, College of Aeronautics, Vol. 1, Cranfield, England, 1961.
44. Bradshaw, F. J., et al, "The Effect of Section Thickness on the Crack Resistance of Aluminum Alloy L93, with Measurements of Plastic Strain," Royal Aircraft Establishment Report TR 72039, March 1972.
45. Heyer, R. H. and McCabe, D. E., "Plane-Stress Fracture Toughness Testing Using a Crack-Line-Loaded Specimen," Engineering Fracture Mechanics, Vol. 4, 1972.
46. Kendall, D. P., "Crack Growth Resistance in Laminated, Glass-epoxy Sheet," Journal of Materials, JMLSA, Vol. 7, No. 3, September 1972.
47. Ripling, E. J. and Falkenstein, E., "Measuring  $K_R$  Curves for Thin Sheets," in Fracture Toughness Evaluation by R-Curve Methods, American Society for Testing and Materials STP527 (1973).
48. Wang, D. Y., "Plane Stress Fracture Toughness and Fatigue Crack Propagation of Aluminum Alloy Wide Panels," paper presented to Sixth National Symposium on Fracture Mechanics, ASTM, August 1972, also Douglas Aircraft Company Paper 6054.
49. Heyer, R. H., "Crack Growth Resistance Curves (R-Curves) — Literature Review," in Fracture Toughness Evaluation by R-Curve Methods, American Society of Testing and Materials STP527 (1973).
50. Creager, M. and Liu, A. F., "The Effect of Reinforcements on the Slow Stable Tear and Catastrophic Failure of Thin Metal Sheet," AIAA paper No. 71-113, January 1971.
51. Forman, R. G., "Experimental Program to Determine Effect of Crack Buckling and Specimen Dimensions on Fracture Toughness of Thin Sheet Materials," AFFDL TR-65-146, January 1966.
52. Carlson, R. L., et al, "Buckling in Thin Cracked Sheets," in Proceedings of the Air Force Conference on Fatigue and Fracture of Aircraft Structures and Materials, AFFDL TR-70-144, 1969.

53. Dixon, J. R. and Strannigan, J. S., "Stress Distribution and Buckling in Thin Sheets with Central Slits," Fracture 1969, Proceedings of Second International Conference on Fracture, 1969.
54. Zielsdorff, G. F. and Carlson, R. L., "On the Buckling of Thin Tensioned Sheets with Cracks and Slots," paper presented at the Symposium on Fracture and Fatigue, George Washington University, May 3-5, 1972.
55. Walker, E. K., "A Study of the Influence of Geometry on the Strength of Fatigue Cracked Panels," AFFDL TR-66-92, June 1966.
56. Broek, D. and Nederveen, A., "The Influence of the Loading Rate on the Residual Strength of Aluminum Alloy Sheet Specimens," National Aerospace Laboratory, Amsterdam, NLR-TR M. 2154, October 1965.
57. Newman, J. C., "Fracture of Cracked Plates Under Plane Stress," paper presented to the National Symposium on Fracture Mechanics, June 1967.
58. Sullivan, A. M. and Freed, C. W., "The Influence of Geometric Variables on  $K_{IC}$  Values for Two Thin Sheet Aluminum Alloys," Naval Research Laboratory Report 7270, June 1971.
59. Rice, J. R., "A Path Independent Integral and the Approximate Analysis of Strain Concentration by Notches and Cracks," Journal of Applied Mechanics, June 1968, p. 379-386.
60. Isida, M., "Effects of a Stringer on the Stress Intensity Factors for the Tension of a Cracked Wide Plate," Department of Mechanics, Lehigh University, Bethlehem, Pa., Sept. 1965.
61. Hayes, D. J. and Williams, J. G., "A Practical Method for Determining Dugdale Model Solutions for Cracked Bodies of Arbitrary Shapes," International Journal of Fracture Mechanics, Volume 8, No. 3, Sept. 1972, pages 239-256.
62. Buekner, H. F., "Propagation of Cracks and the Energy of Elastic Deformation," Transactions of American Society of Mechanical Engineers, 80E, 1958.
63. Byskov, E., "The Calculation of Stress Intensity Factors Using the Finite Element Method with Cracked Elements," International Journal of Fracture Mechanics, Vol. 6, No. 2, June 1970, pages 159-167.
64. Wilson, W. K., "Crack Tip Finite Elements for Plane Elasticity," Westinghouse Research Laboratories, Scientific Paper 71-1E7-FMPWR-P2, June 1971

65. Sih, G. C., "A Special Theory of Crack Propagation," Methods of Analysis and Solutions to Crack Problems, edited by G. C. Sih, Walters-Noordhoff Publishing, 1972.
66. Creager, M., "A Note on the Use of a Simple Technique for Failure Prediction Using Resistance Curves," in Fracture Toughness Evaluation by R-Curve Methods, American Society for Testing and Materials STP527 (1973).
67. Feddersen, C. E., et al, "An Experimental and Theoretical Investigation of Plane-Stress Fracture of 2024-T351 Aluminum Alloy," NASA CR-1678, September 1970.



Unclassified

Security Classification

**DOCUMENT CONTROL DATA - R & D**

(Security classification of title, body of abstract and indexing annotation must be entered when the overall report is classified)

1. ORIGINATING ACTIVITY (Corporate author) Northrop Corporation Aircraft Division Hawthorne, California 90250		2a. REPORT SECURITY CLASSIFICATION Unclassified	
		2b. GROUP	
3. REPORT TITLE Development and Evaluation of Methods of Plane Stress Fracture Analysis Part I - Review and Evaluation of Structural Residual Strength Prediction Techniques			
4. DESCRIPTIVE NOTES (Type of report and inclusive dates) Final Report (PART I) - July 1972 - February 1973			
5. AUTHOR(S) (First name, middle initial, last name) Ralph M. Verette and David P. Wilhem			
6. REPORT DATE May 1973		7a. TOTAL NO. OF PAGES 110	7b. NO. OF REFS 66
8a. CONTRACT OR GRANT NO. F33615-72-C-1796		9a. ORIGINATOR'S REPORT NUMBER(S) NOR 72-32	
b. PROJECT NO.			
c.		9b. OTHER REPORT NO(S) (Any other numbers that may be assigned this report)	
d.		AFFDL-TR-73-42	
10. DISTRIBUTION STATEMENT This document has been approved for release and sale; its distribution is unlimited.			
11. SUPPLEMENTARY NOTES		12. SPONSORING MILITARY ACTIVITY Air Force Flight Dynamics Laboratory Air Force Systems Command Wright-Patterson AFB, Ohio 45433	
13. ABSTRACT The treatment of residual strength prediction for aircraft structures having through flaws is considered in this report. A discussion of the circumstances which normally give rise to plane stress or mixed mode fracture is presented along with a summary of those elements which would constitute an "ideal" residual strength method. This method would be capable of prescribing the remaining strength possessed by a broad variety of flawed aircraft structures under actual service environments. Currently available predicting techniques fall considerably short of the desired goal, and the strong and weak points of existing methods, as well as comparisons with test results, are presented. A recommended technique is described for residual strength prediction which bridges the gap between the existing methods and the ideal. The recommended approach will account for slow crack growth and plasticity. It appears that the approach will utilize the J integral in combination with a modified form of the crack growth resistance curve in making residual strength predictions.			

DD FORM 1473  
NOV 65

Unclassified

Security Classification

(OVER)

14. KEY WORDS	LINK A		LINK B		LINK C	
	ROLE	WT	ROLE	WT	ROLE	WT
Residual Strength Prediction						
Fracture Strength						
Metallic Fracture						
Finite Element Analysis						
Crack Growth Resistance						
Fracture Criteria						